

Abstract

CROPPER, MICHAEL EVAN. Analytical and Experimental Investigation of the Damping Matrix in Shear Building Models. (Under the direction of Dr. Abhinav Gupta).

In this thesis, we present a study conducted on investigating the nature of damping matrix associated with multi degree of freedom simple shear building models. The various conventional methods of creating damping matrices in structures are summarized and numerical examples are used to illustrate the inconsistencies among them. Numerical examples are also used to illustrate the significance of non-zero off diagonal terms in the transformed damping matrix obtained after pre and post multiplication with mode shape matrix, i.e. the significance of non-classical nature of damping matrix in certain cases. The analytical study is followed by the description of a laboratory experiment that is developed to evaluate the validity of analytical results. The results from experimental studies of simple 2-DOF and 3-DOF shear building models, both with and without supplemental damping devices, are presented to validate the inconsistencies associated with the conventional methods of creating damping matrices in structures. It is also shown that the incorrect formulation of damping matrix results in highly incorrect responses. Several formulations for damping matrices are then proposed and their validity is evaluated by comparison with experimental results.

Analytical and Experimental Investigation of the Damping Matrix in Shear Building Models

by

Michael Evan Cropper

A thesis submitted to the Graduate Faculty of
North Carolina State University
in partial fulfillment of the
requirements for the Degree of
Master of Science

CIVIL, CONSTRUCTION, AND ENVIRONMENTAL ENGINEERING

Raleigh
2006

APPROVED BY:

Chair of Advisory Committee
Abhinav Gupta

Vernon Matzen

John Baugh

Biography

Michael Cropper was born on November 24, 1981 in Charlotte NC. He grew up in Charlotte and received his High School diploma from Charlotte Latin School. He was accepted to North Carolina State University and received a Park Scholarship to study Civil Engineering. He earned a Bachelor of Science degree in Civil Engineering as well as a Spanish Language Minor in May 2004. As a National Science Foundation Graduate Research Fellow, Michael continued his studies and research at NC State in the Civil, Construction, and Environmental Engineering graduate degree program.

Acknowledgements

I would like to thank Dr. Abhinav Gupta for his generous and continuous support throughout my undergraduate and graduate studies. I would also like to thank Dr. Vernon Matzen for his insight and direction with this project. Without their advice and support, as well as that of fellow graduate students Gerald Bridges, Prakash Kripakaran, and Kevin Wilkins, my work on this project would not have been as fulfilling. I would also like to thank Dr. John Baugh for his continued support during my time at NC State.

This research would not have been possible without the support of the National Science Foundation Graduate Research Fellowship Program. The Department of Civil Engineering and North Carolina State University should be acknowledged for their commitment to advanced research.

I would like to share my gratitude for my parents, Tim and Linda, and my sister Beth for their continued encouragement and belief in my goals. I am also very grateful for the support and encouragement of my fiancée Natalie and her family.

Finally I would like to thank my fellow graduate students whom with I shared so many worthwhile moments over the years: Gerald Bridges, Charles Johnson, Jason Patrick, Jason Tucker, and John David Vickery.

Table of Contents

List of Figures.....	v
List of Tables.....	ix
1 Introduction.....	1
1.1 Introduction.....	2
1.2 Objective.....	3
1.3 Organization.....	5
References.....	6
2 Analytical and Experimental Investigation of the Damping Matrix in Shear Building Models (planned for submission to technical journal).....	8
Abstract.....	9
2.1 Introduction.....	9
2.2 Formation of Damping Matrix.....	11
2.3 Laboratory Experiments.....	26
2.4 Proposed Damping Matrix.....	39
2.5 Conclusions and Future Work.....	64
2.6 Acknowledgements.....	65
2.7 References.....	66
3 Summary and Conclusions.....	67
3.1 Summary.....	68
3.2 Conclusions.....	70
3.3 Future Work.....	71
Appendix.....	72
A.1 Laboratory Experiments.....	73
A.2 Shear Structure Experiments – Force Controlled Shake Table.....	75
A.3 Structure with Damper Experiments – Force Controlled Shake Table.....	84
A.4 Structure with Damper Experiments – Displacement Controlled Shake Table.....	96
A.5 Structure with Damper Experiments – Displacement Controlled Shake Table (II).....	102
A.6 Larger Structure – Displacement Controlled Shake Table.....	108
A.7 Direct Solution to the Equation of Motion.....	114

List of Figures

Part II

1.	Simple 2DOF shear building.....	12
2.	Nearly tuned 2-DOF structure, response at DOF 1.....	16
3.	Nearly tuned 2-DOF structure, response at DOF 2.....	16
4.	2DOF structure, response at DOF 1.....	17
5.	2DOF structure, response at DOF 2.....	18
6.	Response at primary system DOF.....	19
7.	Response at secondary system DOF.....	19
8.	Primary-secondary system.....	20
9.	Response at primary system DOF.....	21
10.	Response at secondary system DOF.....	21
11.	2DOF shear model structure.....	26
12.	System identification of SDOF structure.....	28
13.	Response at DOF 1, 2-DOF system.....	29
14.	Response at DOF 2, 2-DOF system.....	30
15.	Response at DOF 1, 3-DOF system.....	31
16.	Response at DOF 2, 3-DOF system.....	31
17.	Response at DOF 3, 3-DOF system.....	32
18.	Simple shock absorber.....	33
19.	2DOF shear structure with damper.....	34
20.	Response at DOF 1, 2-DOF system with damper.....	36
21.	Response at DOF 2, 2-DOF system with damper.....	36
22.	Response at DOF 1, 3-DOF system with damper.....	37
23.	Response at DOF 2, 3-DOF system with damper.....	38
24.	Response at DOF 3, 3-DOF system with damper.....	38
25.	Response at DOF 1, 2-DOF system.....	42

26.	Response at DOF 2, 2-DOF system.....	42
27.	Response at DOF 1, 3-DOF system.....	43
28.	Response at DOF 2, 3-DOF system.....	43
29.	Response at DOF 3, 3-DOF system.....	44
30.	2DOF shear structure with diagonal [C]	45
31.	Response at DOF 1, 2-DOF system.....	47
32.	Response at DOF 2, 2-DOF system.....	47
33.	Response at DOF 1, 3-DOF system.....	48
34.	Response at DOF 2, 3-DOF system.....	48
35.	Response at DOF 3, 3-DOF system.....	49
36.	3DOF shear structure with added dashpots at all stories.....	50
37.	Response at DOF 1, 2-DOF system.....	52
38.	Response at DOF 2, 2-DOF system.....	52
39.	Response at DOF 1, 3-DOF system.....	53
40.	Response at DOF 2, 3-DOF system.....	53
41.	Response at DOF 3, 3-DOF system.....	54
42.	3DOF shear structure with dashpot added from top storey only.....	55
43.	Response at DOF 1, 2-DOF system.....	56
44.	Response at DOF 2, 2-DOF system.....	57
45.	Response at DOF 1, 3-DOF system.....	58
46.	Response at DOF 2, 3-DOF system.....	58
47.	Response at DOF 3, 3-DOF system.....	59
48.	Response at DOF 1, 2-DOF system with damper.....	61
49.	Response at DOF 2, 2-DOF system with damper.....	61
50.	Response at DOF 1, 3-DOF system with damper.....	62
51.	Response at DOF 2, 3-DOF system with damper.....	62
52.	Response at DOF 3, 3-DOF system with damper.....	63

Appendix

A1.	Experimental setup of force-controlled shake table.....	74
A2.	Experimental setup of displacement-controlled shake table.....	74
A3.	SDOF shear model structure.....	75
A4.	SDOF shear structure free vibration response.....	76
A5.	SDOF shear structure forced vibration response.....	77
A6.	2DOF shear model structure.....	79
A7.	Response at DOF 1, 2-DOF system.....	80
A8.	Response at DOF 2, 2-DOF system.....	80
A9.	3DOF shear model structure.....	81
A10.	Response at DOF 1, 3-DOF system.....	82
A11.	Response at DOF 2, 3-DOF system.....	82
A12.	Response at DOF 3, 3-DOF system.....	83
A13.	SDOF shear model structure with damper.....	85
A14.	Simple passive damping device.....	86
A15.	Load versus displacement comparison for stiffness evaluation.....	86
A16.	SDOF shear structure with damper, free vibration response.....	87
A17.	SDOF shear structure with damper, forced vibration test 1 response.....	88
A18.	SDOF shear structure with damper, forced vibration test 2 response.....	88
A19.	SDOF shear model structure with damper.....	89
A20.	SDOF shear structure with damper, forced vibration response.....	90
A21.	2DOF shear model structure with damper.....	91
A22.	Response at DOF 1, 2-DOF system with damper.....	92
A23.	Response at DOF 2, 2-DOF system with damper.....	92
A24.	3DOF shear model structure with damper.....	93
A25.	Response at DOF 1, 3-DOF system with damper.....	94
A26.	Response at DOF 2, 3-DOF system with damper.....	94
A27.	Response at DOF 3, 3-DOF system with damper.....	95
A28.	SDOF shear structure with damper on displacement-controlled shake table.....	96

A29.	SDOF shear structure with damper, forced vibration response.....	97
A30.	Response at DOF 1, 2-DOF system with damper.....	99
A31.	Response at DOF 2, 2-DOF system with damper.....	99
A32.	Response at DOF 1, 3-DOF system with damper.....	100
A33.	Response at DOF 2, 3-DOF system with damper.....	101
A34.	Response at DOF 3, 3-DOF system with damper.....	101
A35.	SDOF shear structure with damper, forced vibration response.....	102
A36.	Response at DOF 1, 2-DOF system with damper.....	104
A37.	Response at DOF 2, 2-DOF system with damper.....	104
A38.	Response at DOF 1, 3-DOF system with damper.....	105
A39.	Response at DOF 2, 3-DOF system with damper.....	106
A40.	Response at DOF 3, 3-DOF system with damper.....	106
A41.	Larger SDOF shear model structure.....	109
A42.	Larger SDOF shear structure, forced vibration response.....	109
A43.	Larger SDOF shear structure, free vibration response.....	110
A44.	Larger 2DOF shear model structure.....	111
A45.	Larger 2DOF shear model structure.....	112
A46.	Response at DOF 1, 2-DOF system.....	113
A47.	Response at DOF 2, 2-DOF system.....	113

List of Tables

Part II

1.	Comparison of modal damping ratios.....	64
----	---	----

Appendix

A1.	Summary of SDOF shear structure properties.....	77
A2.	Summary of SDOF properties used for modeling.....	78
A3.	Damping ratios from log decrement.....	87
A4.	SDOF shear structure with damper, properties used for modeling.....	90
A5.	SDOF shear structure with damper, properties used for modeling.....	97
A6.	SDOF shear structure with damper, properties used for modeling.....	102
A7.	Larger SDOF shear structure properties.....	110
A8.	Larger SDOF shear structure properties used for modeling.....	110

Part I

Introduction

1.1 Introduction

In recent years, significant research has been performed to study structures incorporating supplemental damping devices, base isolation, and tuned mass dampers [1,2,9]. To accurately model the response of a structure with these devices, a good understanding of their associated damping matrices is required. These damping matrices are created by assembling the damping matrix of the structure with that of the added device. Research efforts involving supplemental devices focus on the ability of these devices to improve a structure's earthquake response. Damping matrices for structures are typically created by assuming damping ratios for each mode, which may in turn be evaluated experimentally by impulse-hammer testing of the entire structure or a least squares solution of test data from transfer functions obtained from sine-sweep tests [3, 4, 7, 8].

Interestingly, very little research has been performed in correctly assembling the damping matrix of a structure alone. The main reason for this discrepancy is the importance of only a few low frequency modes for most common structures. When supplemental damping devices are added to a structure to reduce the response in the first mode, the damping in only the fundamental mode would need to be accurately modeled. Therefore errors in the damping matrix associated with higher frequency responses would not contribute appreciably to the response. Consequently, only limited research efforts have focused on evaluating and improving the damping matrices for structures.

In many structures, the addition of supplemental energy dissipation devices is prohibitively cost-intensive for widespread use. However, for structures incorporating secondary systems such as equipment and piping, these supplemental damping devices are relatively low-cost, high-performance options. This type of coupled primary-secondary

system is non-classically damped [5,10]. Unlike other structures, coupled primary-secondary systems are much more difficult to model due to the significant contributions from higher frequency modes [6]. For these types of structures, a thorough knowledge of the damping matrix of the structure itself is critical for predicting the vibration response of the structure including supplemental devices.

In this thesis, we begin by summarizing the various methods of evaluating damping matrices. Then, we illustrate the inconsistencies introduced by these methods. We also present the results from simple experimental studies conducted by us to illustrate that the currently used methods for creating damping matrices give incorrect responses.

Experimental results from 2-DOF and 3-DOF simple structures, both with and without passive damping devices, are presented. We propose several methods of creating damping matrices, one of which that gives relatively accurate responses. Each new formulation is derived and evaluated to determine its ability to accurately predict the response of these simple structures. The discussion in this thesis focuses only on linear elastic systems.

1.2 Objective

The objective of this research was to study various formulations of the damping matrix and evaluate their validity by conducting simple shake table experiments. A series of analytical studies was performed to evaluate the consistency of the various methods of creating the damping matrix. A series of case studies was used to demonstrate properties of the damping matrix and demonstrate the importance of its accuracy in determining the response of a system. The currently-used methods of assembling the damping matrix were evaluated based on results from simple shake table experiments. Because the results were

inconsistent, new formulations for assembling damping matrices were proposed to better predict the response of the structures. The following experimental investigations were undertaken:

- **Conduct experiments on shear structures.** Single, 2- and 3-storey shear building models were tested in the frequency domain to determine plots of transmissibility ratio.
- **Test potential supplemental damping devices.** Because of the size and scale of the simple shear model structures, a smaller damping device was needed. The device needed to provide less than 10% linear viscous damping and be able to be fitted to the structure. The properties of the device needed to be consistent from test to test.
- **Conduct experiments on structures with dampers.** Single, 2- and 3-DOF systems with damping devices were tested.
- **Verify results using displacement-controlled shake table.** Initial testing was performed on a small, less-powerful, force-controlled shake table. In order to verify the experimental results and relationships with analytical predictions, testing on a larger, displacement-controlled shake table was conducted.

1.3 Organization

This thesis consists of three parts and an appendix. Part I provides the introduction, objectives of the research, and organization of the thesis.

The second part contains a manuscript that will be submitted to a technical journal for review and publication. This manuscript contains the analytical background of various forms of the damping matrix, a discussion of the inconsistencies in these methods, results from simple laboratory experiments which reflect the inaccuracies in the currently-used formulations, and evaluations of several proposed alternative forms of the damping matrix.

The third part of the thesis contains a summary of results and conclusions from the research work. Suggestions for future work and extensions of this research are also provided.

The appendix contains a more detailed description of the experimental work conducted on the simple shear model structures. The appendix also contains several tables listing experimentally determined properties of the structures. A more thorough explanation of a method for solving the equation of motion directly for transmissibility ratio, with an example Matlab code, is provided at the end of the appendix.

References

1. ASCE. *Seismic Analysis of Safety-Related Nuclear Structures and Commentary*. ASCE Standard 4-98. 1998.
2. Chopra, Anil K. *Dynamics of Structures*. New Jersey: Prentice Hall, 1995.
3. Dyke S J, Spencer Jr B F, Quast P, Kaspari Jr D C and Sain M K 1996
Impelementation of an active mass driver using acceleration feedback control
Microcomputers in Civil Engineering (Special Issue on Active and Hybrid Structural Control) **11** 305-23
4. Dyke S J, Spencer Jr B F, Sain M K and Carlson J D 1996 Modeling and control of magnetorheological dampers for seismic response reduction *Smart Mater. Struct.* **5** 565-575
5. Gupta A, "Significance of Nonclassical Damping in Coupled System Analysis," *Proceedings of 15th International Conference on Structural Mechanics in Reactor Technology*, Vol. VIII, Seoul, South Korea, August 15-20, 1999.
6. Gupta A, Gupta AK. "Missing mass effect in coupled analysis I: complex modal properties." *Journal of Structural Engineering*, ASCE 1998; 124:490-495.

7. Qing S, Ling Z, Jinxiong Z and Qingxuan S 2003 Experimental study of the semi-active control of building structures using the shaking table *Earthquake Engineering and Structural Dynamics* **32** 2353-2376
8. Shiba K, Mase S, Yabe Y and Tamura K 1998 Active/passive vibration control systems for tall buildings *Smart Mater. Struct.* **7** 588-598
9. Soong TT, Dargush GF. *Passive Energy Dissipation Systems*. John Wiley and Sons, 1997.
10. Xu K, Igusa T. "Dynamic characteristics of non-classically damped structures." *Earthquake Engineering Structural Dynamics* 1991; 20:1127-1144.

Part II

Analytical and Experimental Investigation of the Damping Matrix in Shear Building Models

(planned for submission to a technical journal)

Analytical and Experimental Investigation of the Damping Matrix in Shear Building Models

*Michael E. Cropper, Master's Student
Dr. Abhinav Gupta, Associate Professor
North Carolina State University, Raleigh NC*

Abstract

In this thesis, we present a study conducted on investigating the nature of damping matrix associated with multi degree of freedom simple shear building models. The various conventional methods of creating damping matrices in structures are summarized and numerical examples are used to illustrate the inconsistencies among them. Numerical examples are also used to illustrate the significance of non-zero off diagonal terms in the transformed damping matrix obtained after pre and post multiplication with mode shape matrix, i.e. the significance of non-classical nature of damping matrix in certain cases. The analytical study is followed by the description of a laboratory experiment that is developed to evaluate the validity of analytical results. The results from experimental studies of simple 2-DOF and 3-DOF shear building models, both with and without supplemental damping devices, are presented to validate the inconsistencies associated with the conventional methods of creating damping matrices in structures. It is also shown that the incorrect formulation of damping matrix results in highly incorrect responses. Several formulations for damping matrices are then proposed and evaluated in an effort to better predict the response of these structures.

2.1 Introduction

In recent years, a significant research effort has been devoted to the study of structures with supplemental damping devices, base isolation, tuned mass dampers, etc [1,2,5]. All such structures represent systems with non-classical damping. Furthermore, the damping in

coupled primary-secondary systems such as building-piping is also non-classical [3,6]. The development of modern technology in some of these applications, such as supplemental damping devices, has been based on extensive experimental investigations. On the other hand, the research in some areas such as coupled primary-secondary systems is mostly analytical with very little experimental verification. Irrespective, the concept of non-classical damping in structures is well established. Experimental investigations in the area of supplemental damping devices clearly illustrate that the damping in such structures is governed by the high damping associated with the supplemental devices. In the analytical investigation for such structures, the damping associated with the supplemental damping devices is assembled with the damping matrix of the structure. Interestingly, very little research has been conducted on correctly assembling the damping matrix of a structure by itself, i.e. without the supplemental damping device. It appears that the main reason for this discrepancy in research efforts is related to the importance of only a few (mostly one) low frequency modes in a building. For example, let us consider a structure in which the fundamental mode is sufficient to evaluate the response quantities of interest such as, displacements, base shear and overturning moment. Consideration of supplementary damping devices to reduce the response in this structure would require that the damping of structure be modeled accurately only in the fundamental mode, and an error in the damping associated with the high frequency modes will not result in any appreciable error in the response quantities of interest. Consequently, only limited research efforts have focused on overcoming the limitations in the methods for developing damping matrices in structures.

While the development of supplementary damping devices was initiated by the perceived applications for improving life-safety in buildings and bridges, the technology is still in its incipient stages and often cost-intensive for wide spread consideration. On the contrary, a significant increase has been witnessed in the use of supplemental damping devices for improving the earthquake performance of secondary systems such as equipment and piping. This is due to several factors that relate to not only relatively inexpensive devices but also to more stringent performance requirements related to continued operability of various equipment in critical infrastructure facilities like hospitals during and after an earthquake. Unfortunately, the evaluation of response in secondary systems is much more complex than in the case of buildings because of significant contribution of modes other than the first few low frequency modes [4]. In such a case, it is critical to accurately evaluate the damping matrix of the structure prior to assembling the damping associated with the supplementary devices. In this thesis, we begin by summarizing the various methods of evaluating damping matrices. Then, we illustrate the inconsistencies introduced by these methods. Finally, we present the results from a simple experimental study conducted by us to illustrate that the currently used methods for creating damping matrices give incorrect responses. The discussion in this thesis focuses only on linear elastic systems.

2.2 Formation of Damping Matrix

2.2.1 Case-1: Damping Matrix in Simple Shear Buildings

In linear elastic systems, the damping is characterized as linear viscous and evaluated in terms of a modal damping ratio ξ from the free or forced vibration response of a structure.

For a single degree of freedom (SDOF) system, the relationship between the modal damping

ratio and the corresponding damping coefficient is well established, i.e. $c = 2m\xi\omega$ where m is the mass and ω is the circular natural frequency of the SDOF system. For simple multi-degree of freedom (MDOF) systems such as those considered in textbooks and research investigations, the damping matrix is created by assembling the damping coefficients associated with the individual story. The assembly of damping coefficients is performed in a manner identical to the assembly of stiffness matrix. For example, let us consider a 2-DOF system shown in Figure 1 that has damping coefficients c_1 and c_2 associated with the two individual stories. The damping matrix for the 2-DOF system is then created as follows:

$$[C] = \begin{bmatrix} c_1 + c_2 & -c_2 \\ -c_2 & c_2 \end{bmatrix} \quad (1)$$

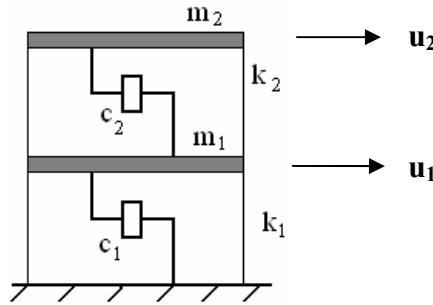


Figure 1 – Simple 2DOF Shear Building

Creation of damping matrix in this form introduces two key issues for further consideration. First, does this form of damping matrix result in classical (or proportional) damping? Second, does this form of damping matrix result in modal damping ratios that are similar or close to those evaluated from the free vibration tests of the individual SDOF systems? Let us consider an SDOF system with mass $m = 0.80 \text{ lb} \cdot \text{s}^2/\text{in}$, storey stiffness $k = 500 \text{ lb/in}$, and modal

damping ratio $\xi = 0.05$. For this system, the circular frequency $\omega = 25$ rad/s and the damping coefficient $c = 2.00 \text{ lb} \cdot \text{s} / \text{in}$. A 2-DOF system of the type shown earlier in Figure 1 is created by putting two such identical stories together, such that $m_1 = m_2 = 0.80 \text{ lb} \cdot \text{s}^2 / \text{in}$, $k_1 = k_2 = 500 \text{ lb} / \text{in}$, and $\xi = 0.05$. The damping matrix, the frequency vector and the mode shape matrix for the 2-DOF structure are given by

$$[C] = \begin{bmatrix} 4.00 & -2.00 \\ -2.00 & 2.00 \end{bmatrix} \quad (2)$$

$$\{\omega\} = \begin{Bmatrix} 15.45 \\ 40.45 \end{Bmatrix} \quad (3)$$

$$[\Phi] = \begin{bmatrix} -0.5878 & -0.9511 \\ 0.9511 & 0.5878 \end{bmatrix} \quad (4)$$

It can be seen that the damping matrix is proportional to the stiffness matrix. Consequently, it will be orthogonal to the modal matrix $[\Phi]$ even though the damping matrix was not considered explicitly in the solution of the eigenvalue problem. Therefore, the damping matrix given above is classical in nature. The transformed damping matrix $[\bar{C}]$ for this system is given by

$$[\bar{C}] = [\Phi^T] \cdot [C] \cdot [\Phi] = \begin{bmatrix} 0.9549 & 0 \\ 0 & 6.5451 \end{bmatrix} \quad (5)$$

The diagonal elements in the above equation give $\xi_1 = 0.0309$ and $\xi_2 = 0.0809$. These values of modal damping ratio are quite different from the corresponding value for the single story structure. To examine this issue further, let us consider a 3-DOF system that consists of three of the same SDOF systems. In this case it can be shown that $\xi_1 = 0.0223$, $\xi_2 = 0.0623$,

and $\xi_3 = 0.0901$. Consequently, the modal damping ratios in MDOF systems are very different from the damping ratio associated with the corresponding SDOF system. The damping ratios in MDOF systems are highly dependent upon the configuration of the system even though all the stories are identical. The question remains whether this is true for actual systems or not. We evaluate this effect later in this thesis using simple laboratory experiments.

Next, we consider a 2-DOF system in which the individual stories are made of the same materials but have somewhat different stiffness characteristics. For a system of the type shown in Figure 1, $m_1 = m_2 = 0.80 \text{ lb} \cdot \text{s}^2 / \text{in}$, $k_1 = 500 \text{ lb} / \text{in}$, $k_2 = 490 \text{ lb} / \text{in}$ and the damping in individual stories is taken as 5.0%. Then, $c_1 = 3.9799 \text{ lb} \cdot \text{s} / \text{in}$ and $c_2 = 1.9799 \text{ lb} \cdot \text{s} / \text{in}$. The damping matrix $[C]$ and the transformed damping matrix $[\bar{C}]$ of the 2-DOF system are given by

$$[C] = \begin{bmatrix} 3.9799 & -1.9799 \\ -1.9799 & 1.9799 \end{bmatrix} \quad (6)$$

$$[\bar{C}] = \begin{bmatrix} 0.9523 & -0.0113 \\ -0.0113 & 6.4975 \end{bmatrix} \quad (7)$$

The damping matrix for this structure is not proportional to the stiffness matrix. Therefore, the transformed damping matrix is not orthogonal to the mode shape matrix and contains non-zero off-diagonal terms. Let us first examine the significance of off-diagonal terms in the transformed damping matrix. To do so, we generated transmissibility curves for each degree of freedom by subjecting the 2-DOF to a harmonic excitation at the base, i.e.

$$[M]\{\ddot{u}\} + [C]\{\dot{u}\} + [K]\{u\} = -[M]\{u_b\}\ddot{u}_{g0} \sin(\Omega t) \quad (8)$$

in which $\{u_b\}$ is the influence vector for base excitation and \ddot{u}_{g0} is the amplitude of harmonic base excitation corresponding to a frequency of Ω rad/sec. The transmissibility ratios, TR_i , $i = 1, 2$ are then evaluated as the ratios of total steady-state acceleration amplitude at DOF i to that at the base (shake table).

$$TR_1(\Omega) = \frac{\ddot{u}_1^T}{\ddot{u}_{g0}} \quad (9)$$

$$TR_2(\Omega) = \frac{\ddot{u}_2^T}{\ddot{u}_{g0}} \quad (10)$$

in which $\ddot{u}_i^T = \ddot{u}_i(t) + \ddot{u}_g(t)$, $i=1, 2$. Figures 2 and 3 show a comparison of the two transmissibility curves obtained by neglecting and by considering the off-diagonal terms in the transformed damping matrix. As seen in these figures, the off-diagonal terms do not have any appreciable effect on the response of the structure. The two diagonal terms of the transformed damping matrix for this case give $\xi_1 = 0.0309$ and $\xi_2 = 0.0809$ which, as in the previous case, are different from the corresponding damping ratios associated with individual stories.

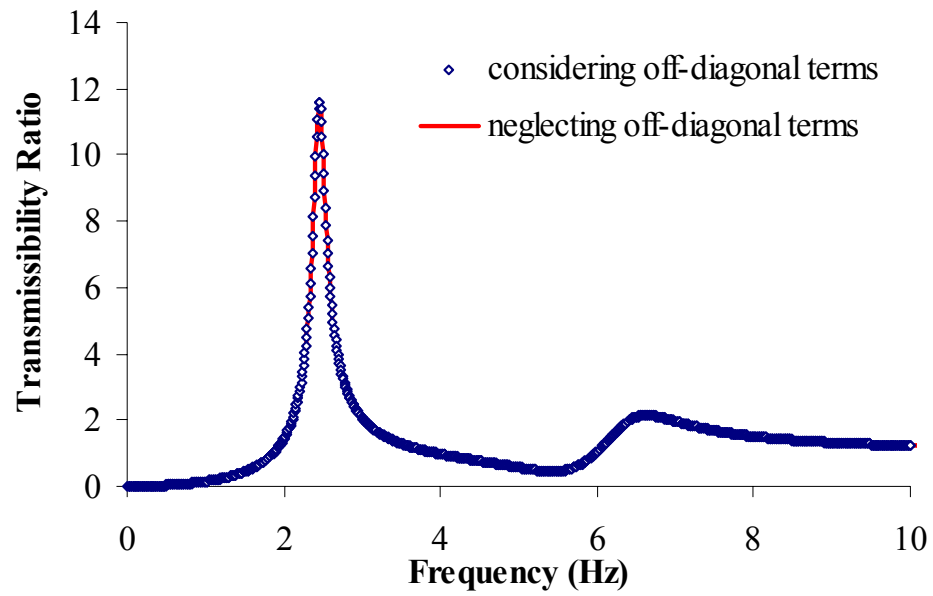


Figure 2 – Nearly tuned 2-DOF structure, response at DOF 1

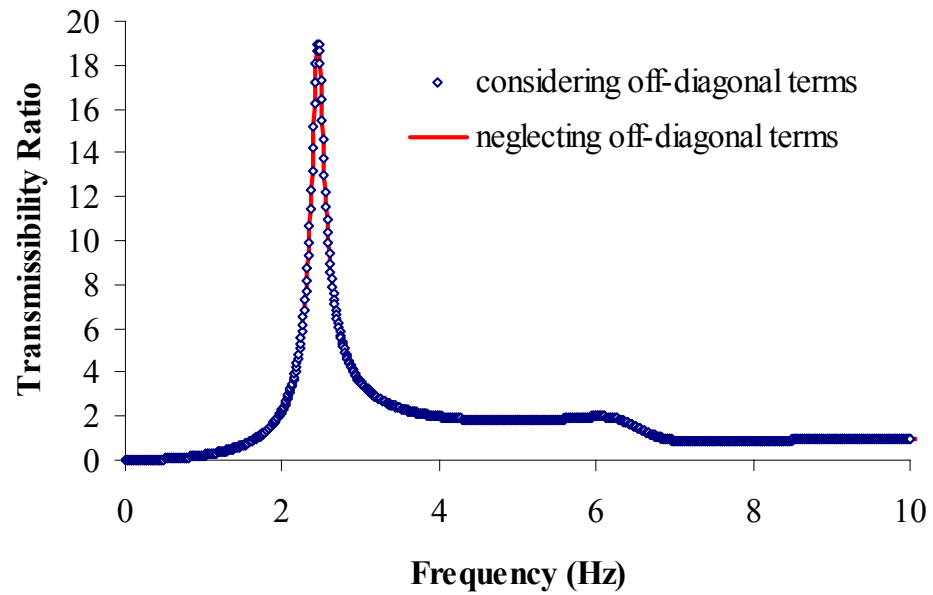


Figure 3 – Nearly tuned 2DOF structure, response at DOF 2

Let us consider another 2-DOF structure, with mass $m_1 = m_2 = 0.80 \text{ lb} \cdot \text{s}^2 / \text{in}$, and storey stiffness $k_1 = k_2 = 500 \text{ lb/in}$. The damping is taken as 5.0% in the first, and 2.0% in the second storey. The damping matrix and transformed damping matrix are given as

$$[C] = \begin{bmatrix} 2.8000 & -0.8000 \\ -0.8000 & 0.8000 \end{bmatrix} \quad (11)$$

$$[\bar{C}] = \begin{bmatrix} 0.7966 & 0.6708 \\ 0.6708 & 3.7034 \end{bmatrix} \quad (12)$$

The transformed damping matrix again has off-diagonal terms. These off-diagonal terms are now a larger percentage of the diagonal terms, although the transmissibility curves in Figures 4 and 5 demonstrate that their effect remains negligible.

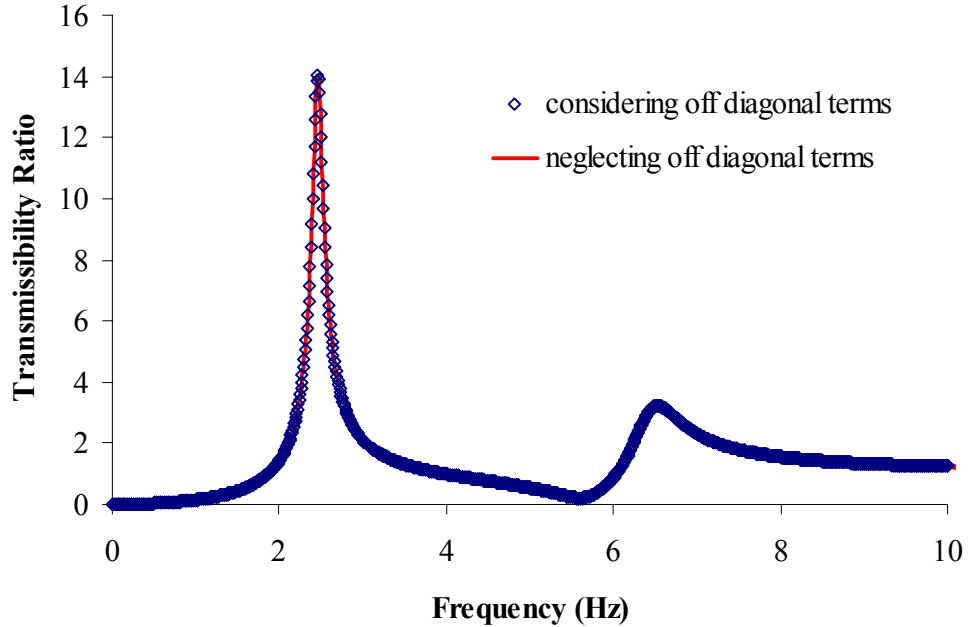


Figure 4 – 2DOF structure, response at DOF 1

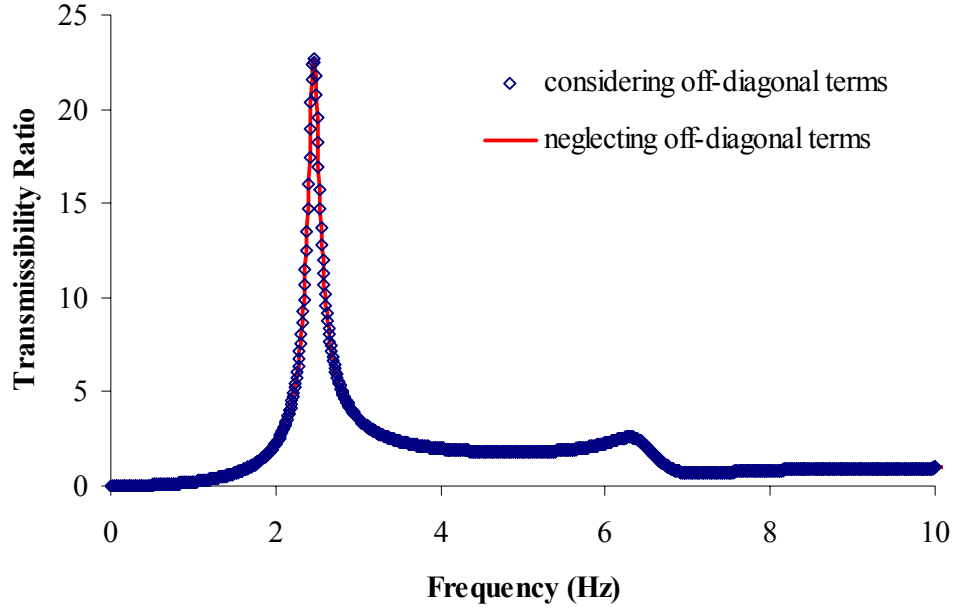


Figure 5 – 2DOF structure, response at DOF 2

We will now consider a structure that is nearly tuned, with a larger primary system mass and different storey damping. Let us consider that $m_1 = 0.80 \text{ lb} \cdot \text{s}^2 / \text{in}$, $m_2 = 0.080 \text{ lb} \cdot \text{s}^2 / \text{in}$, $k_1 = 500 \text{ lb/in}$ and $k_2 = 49 \text{ lb/in}$. The damping in the primary system is 5.0%, and it is 2.0% in the secondary system. The damping matrix and transformed damping matrix are

$$[C] = \begin{bmatrix} 2.8000 & -0.8000 \\ -0.8000 & 0.8000 \end{bmatrix} \quad (13)$$

$$[\bar{C}] = \begin{bmatrix} 0.7966 & 0.6708 \\ 0.6708 & 3.7034 \end{bmatrix} \quad (14)$$

Again, the transformed damping matrix is not diagonal, and the off-diagonal terms are significant compared to the diagonal terms. Figures 6 and 7 demonstrate that the predicted response of the structure is not affected by neglecting these off-diagonal terms.

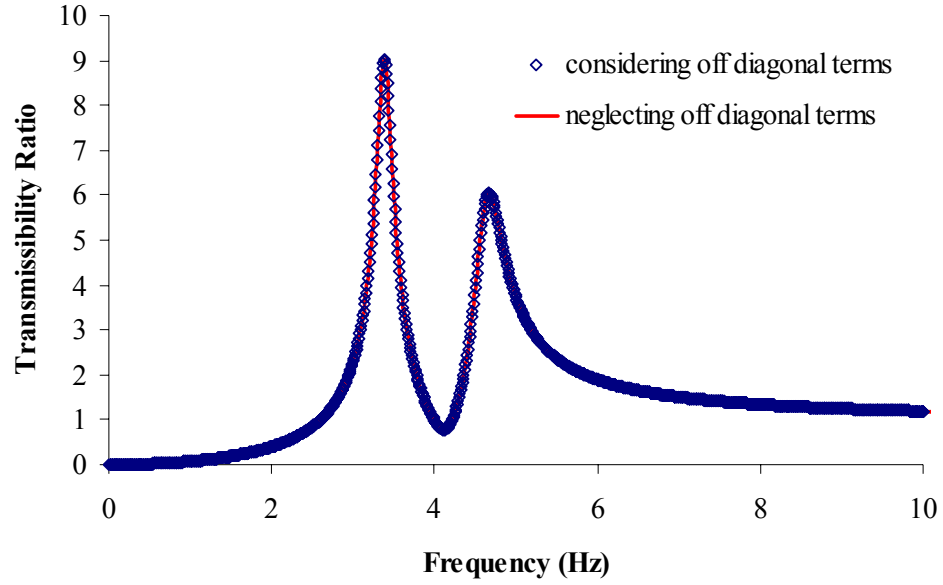


Figure 6 – Response at primary system DOF

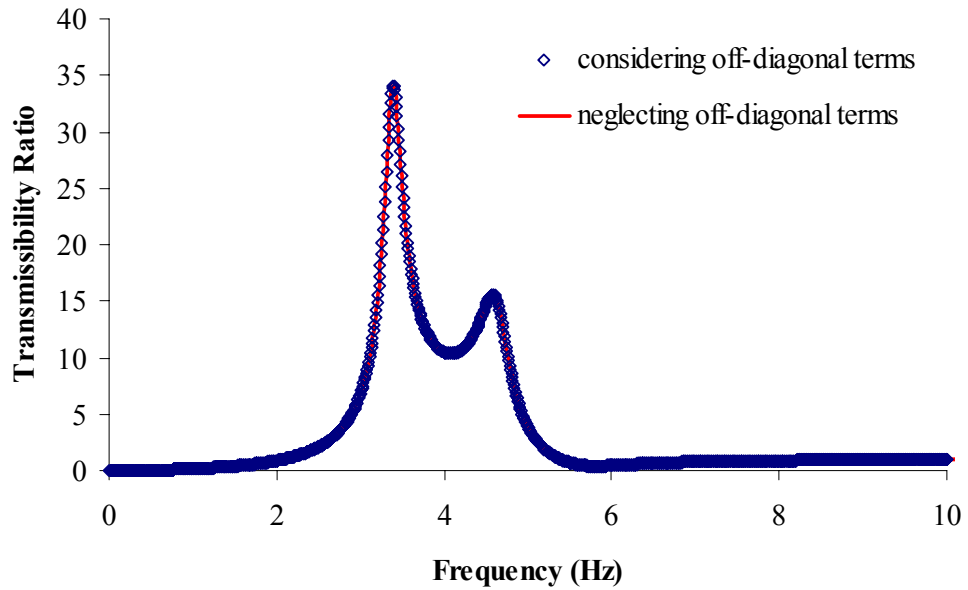


Figure 7 – Response at secondary system DOF

The examples given above validate the conventional practice in the building research wherein the off-diagonal terms in the transformed damping matrix are neglected. However, it is not appropriate to do so under all circumstances. For example, numerous studies have been

conducted on coupled primary-secondary systems that illustrate the significance of the off-diagonal terms [3,6]. To illustrate this effect, let us consider a nearly tuned SDOF primary-SDOF secondary (2-DOF coupled) system shown in Figure 8. Let us consider that $m_1 = 0.80 \text{ lb} \cdot \text{s}^2 / \text{in}$, $m_2 = 0.000080 \text{ lb} \cdot \text{s}^2 / \text{in}$, $k_1 = 500 \text{ lb/in}$, $k_2 = 0.049 \text{ lb/in}$ and the damping in the primary system is 5.0% and that in the secondary system is 2.0%. Consequently, the damping matrix $[C]$ and the transformed damping matrix $[\bar{C}]$ for this coupled system are:

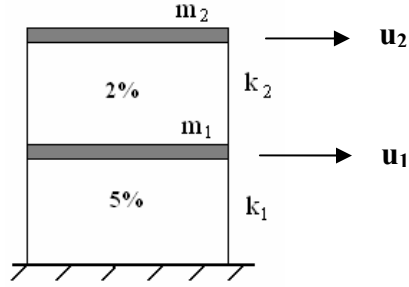


Figure 8 – Primary-secondary system

$$[C] = \begin{bmatrix} 2.0000 & -7.92 \times 10^{-5} \\ -7.92 \times 10^{-5} & 7.92 \times 10^{-5} \end{bmatrix} \quad (15)$$

$$[\bar{C}] = \begin{bmatrix} 1.1975 & 0.5201 \\ 0.5201 & 2.2925 \end{bmatrix} \quad (16)$$

The transformed damping matrix contains off-diagonal terms. The effect of off-diagonal terms on the structure's response for this case is illustrated in Figures 9 and 10 that compare the transmissibility curves obtained by ignoring and by considering the off-diagonal terms. As seen in these figures, the off-diagonal terms do not have any appreciable influence on the response of primary system. However, the secondary system response is excessively higher

when the off-diagonal terms are neglected. Therefore, it is not appropriate to ignore the off-diagonal terms (non-classical nature of damping matrix) for such a case.

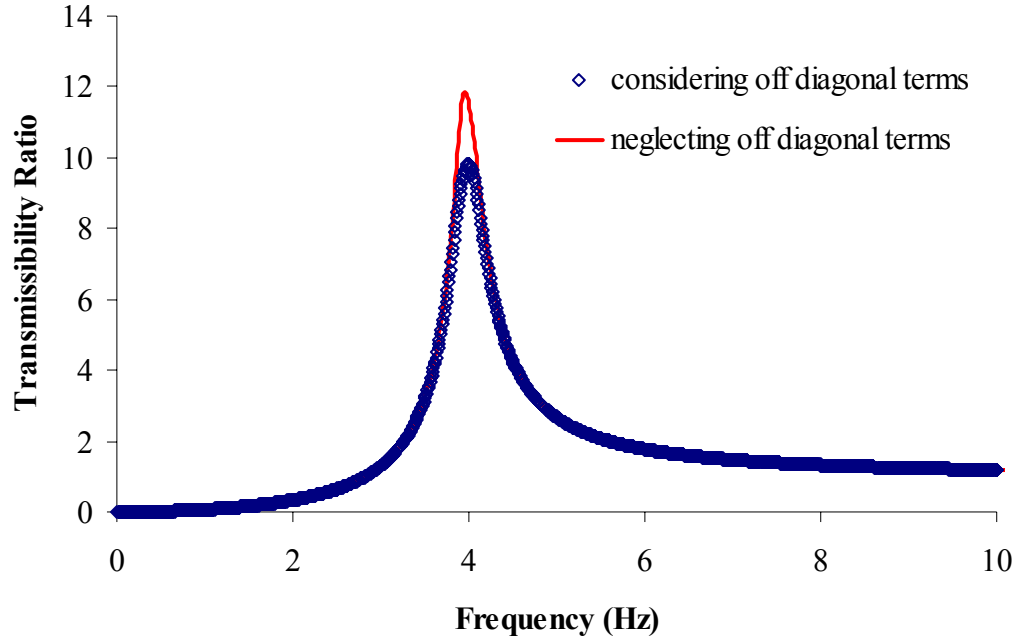


Figure 9 – Response at primary system DOF

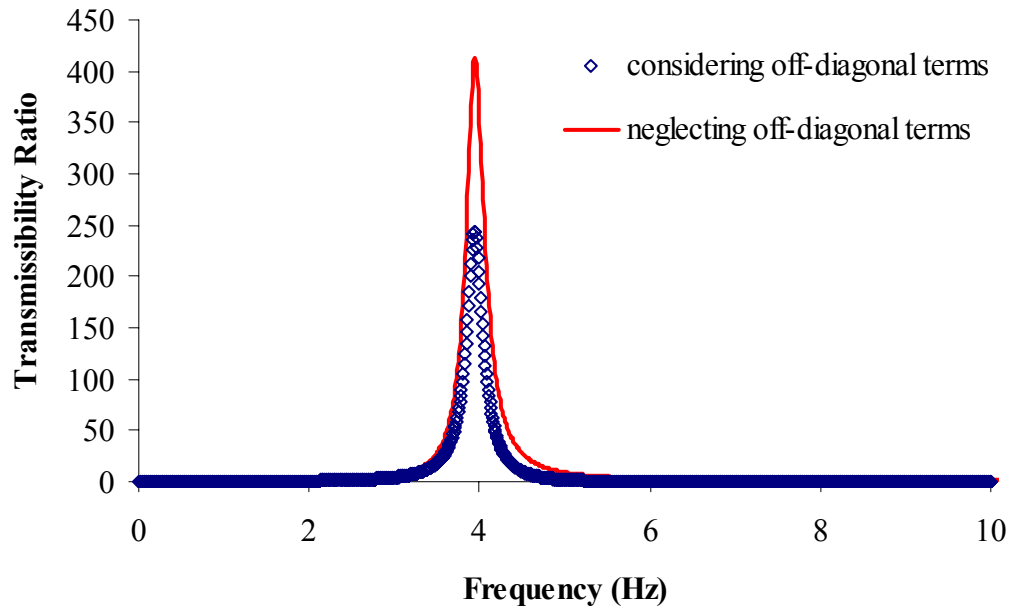


Figure 10 – Response at secondary system DOF

2.2.2 Case-2: Damping Matrix using Rayleigh's Method:

In structural systems that are more realistic or complex, the damping matrix cannot be assembled in a manner described above. The damping matrix in such cases can be evaluated by using Rayleigh's method in which the damping matrix is considered proportional to both the mass and the stiffness matrix of the structure, i.e. $[C] = \alpha \cdot [M] + \beta \cdot [K]$. The primary reason for considering this form of damping matrix is that it makes the damping matrix orthogonal to the mode shape matrix and in turn simplifies the solution of equations of motion by decoupling the equations for each mode. The coefficients α and β are evaluated by rewriting the above relationship after transforming it using the mode shape vectors for each mode, i.e. $2\xi_i\omega_i = \alpha + \beta\omega_i^2$. Damping ratios and frequencies in two modes are then used to calculate the coefficients α and β which in turn give the damping matrix $[C]$. The damping ratios in the two modes considered for this purpose are specified arbitrarily. In many cases, these damping ratios are taken as those evaluated from the free vibration response of the SDOF system for the particular type of material. The discussion presented in the previous section illustrates that it may not be appropriate to consider damping ratios based on SDOF responses. Another inconsistency introduced in this method relates to the damping in modes other than the two modes in which ξ_i is specified because the damping ratios in such modes do not correspond to a true behavior. These damping ratios are clearly governed by the mathematical expression, i.e. they are a function of structural frequencies.

2.2.3 Case-3: Damping Matrix by Superposition

This method of forming damping matrix avoids the frequency dependence of damping ratio encountered in the Rayleigh's method but maintains the orthogonal nature of the damping matrix. In this method, the damping ratios are specified in all the non-rigid modes to start with a transformed damping matrix that is diagonal. The damping matrix is then evaluated as follows

$$[\bar{C}] = [\Phi^T] \cdot [C] \cdot [\Phi] \quad (17)$$

$$[\bar{C}] = \begin{bmatrix} 2\xi_i \omega_i & 0 \\ 0 & 2\xi_j \omega_j \end{bmatrix} \quad (18)$$

We can then write

$$[C] = [\Phi^T]^{-1} \cdot [\bar{C}] \cdot [\Phi]^{-1} \quad (19)$$

Furthermore, $[\Phi^T] \cdot [M] \cdot [\Phi] = [I]$ gives

$$[\Phi^T]^{-1} = [M] \cdot [\Phi] \quad (20)$$

and

$$[\Phi]^{-1} = [\Phi^T] \cdot [M] \quad (21)$$

Therefore,

$$[C] = [M] \cdot [\Phi] \cdot [\bar{C}] \cdot [\Phi^T] \cdot [M] \quad (22)$$

A key limitation of this method lies in the requirement that the damping ratio of each mode needs to be known for formation of damping matrix. As illustrated in Section 2.2.1 above, the damping ratio in each mode cannot be same as that associated with the corresponding SDOF system.

2.2.4 Direct Solution of the Equation of Motion

The equation of motion for harmonic excitation can be written alternatively as shown below.

By substituting in for the quantities $\{u\} = \{u_0\} \cdot e^{i\Omega t}$, $\{\dot{u}\} = i\Omega \cdot \{u_0\} \cdot e^{i\Omega t}$ and

$\{\ddot{u}\} = -\Omega^2 \cdot \{u_0\} \cdot e^{i\Omega t}$, the equation of motion can be transformed as follows:

$$[M]\{\ddot{u}\} + [C]\{\dot{u}\} + [K]\{u\} = -[M]\{u_b\}\ddot{u}_{g0} e^{i\Omega t} \quad (23)$$

For a 2-DOF structure, in which $\{u_0\}^T = [u_{10} \quad u_{20}]$, the equation becomes:

$$[-m_1\Omega^2 + i\Omega c_{11} + k_{11}] \cdot u_{10} + [i\Omega c_{12} + k_{12}] \cdot u_{20} = -m_1 \ddot{u}_{g0} \quad (24)$$

$$[i\Omega c_{21} + k_{21}] \cdot u_{10} + [-m_2\Omega^2 + i\Omega c_{22} + k_{22}] \cdot u_{20} = -m_2 \ddot{u}_{g0} \quad (25)$$

Since acceleration records measured during experiments directly give \ddot{u}_{10} and \ddot{u}_{20} , we can write:

$$\frac{1}{\Omega^2 m_1} [-m_1\Omega^2 + i\Omega c_{11} + k_{11}] \cdot \ddot{u}_{10} + \frac{1}{\Omega^2 m_1} [i\Omega c_{12} + k_{12}] \cdot \ddot{u}_{20} = \ddot{u}_{g0} \quad (26)$$

$$\frac{1}{\Omega^2 m_2} [i\Omega c_{21} + k_{21}] \cdot \ddot{u}_{10} + \frac{1}{\Omega^2 m_2} [-m_2\Omega^2 + i\Omega c_{22} + k_{22}] \cdot \ddot{u}_{20} = \ddot{u}_{g0} \quad (27)$$

The expressions can be simplified using the following notation

$$A_{11} \cdot \ddot{u}_{10} + A_{12} \cdot \ddot{u}_{20} = \ddot{u}_{g0} \quad (28)$$

$$A_{21} \cdot \ddot{u}_{10} + A_{22} \cdot \ddot{u}_{20} = \ddot{u}_{g0} \quad (29)$$

$$[A]\{\ddot{u}_0\} = \{\ddot{u}_{g0}\} \quad (30)$$

Solving the system of equations for \ddot{u}_{10} we have:

$$\ddot{u}_{10} \cdot (A_{22}A_{11} - A_{12}A_{21}) = (A_{22} - A_{12}) \cdot \ddot{u}_{g0} \quad (31)$$

Which can be simplified in the form of:

$$\ddot{u}_{10} \cdot (A_1 + iB_1) = (C_1 + iD_1) \cdot \ddot{u}_{g0} \quad (32)$$

In which the coefficients $A_1 - D_1$ are provided in the appendix in Equations (A15)-(A18).

Therefore the transmissibility ratio at the first storey can be expressed as:

$$TR_1 = \frac{\ddot{u}_{10}}{\ddot{u}_{g0}} = \frac{\sqrt{C_1^2 + D_1^2}}{\sqrt{A_1^2 + B_1^2}} \quad (33)$$

Similarly, solving the system of equations for \ddot{u}_{20} we have:

$$\ddot{u}_{20} \cdot (A_{21}A_{12} - A_{11}A_{22}) = (A_{21} - A_{11}) \cdot \ddot{u}_{g0} \quad (34)$$

Which can be simplified in the form of:

$$\ddot{u}_{20} \cdot (A_2 + iB_2) = (C_2 + iD_2) \cdot \ddot{u}_{g0} \quad (35)$$

In which the coefficients $A_2 - D_2$ are provided in the appendix in Equations (A22)-(A25).

Therefore the transmissibility ratio at the second storey can be expressed as:

$$TR_2 = \frac{\ddot{u}_{20}}{\ddot{u}_{g0}} = \frac{\sqrt{C_2^2 + D_2^2}}{\sqrt{A_2^2 + B_2^2}} \quad (36)$$

The above equations represent the solution to a 2-DOF structure. A 3-DOF structure can be solved in a similar manner. Solving the equation of motion directly in this manner eliminates assumptions that would otherwise be needed regarding the orthogonality of the damping matrix with regard to mode shapes. The expressions developed for transmissibility ratios using these methods are closed-form. The expressions also consider the complete damping matrix. Throughout the rest of the thesis, this direct solution method is used to determine the curves of transmissibility ratio.

2.3 Laboratory Experiments

2.3.1 Shear Structure Experiments – Force Controlled Shake Table

To better understand the formation of damping matrix, we developed and conducted shake table experiments. Each structure consisted of thin aluminum columns and heavy steel girders. For shear-building behavior, rotation of the floor girders was eliminated by making them much stiffer than the columns. As shown in Figure 11, end caps were used to create rigid connections so that the columns could not rotate at the joints. Multiple storied models consisted of identical stories stacked on top of one another. Accelerometers were mounted at each storey to measure the acceleration response. Simple harmonic motion was used as input excitation into the shake table. Steady-state responses were measured to determine transmissibility ratio plots.

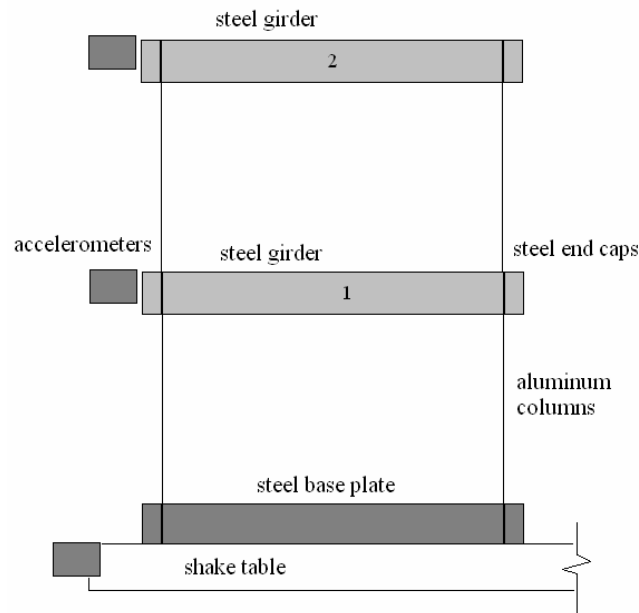


Figure 11 –2DOF shear model structure

As a first step, several single storey shear building models were tested in order to determine the natural frequency and damping ratio associated with each storey individually. The natural frequencies were calculated by making physical measurements on the column dimensions for calculating stiffness and on girder for weight. Columns were 1" wide and 1/16" thick. The effective length for the columns was 5.25". Each column had a mass of $0.0001085 \text{ lb} \cdot \text{s}^2/\text{in}$ and the mass of the girder was $0.005887 \text{ lb} \cdot \text{s}^2/\text{in}$. Both free vibration and forced harmonic vibration tests were performed. The free vibration tests were then used to evaluate the frequencies and damping ratios. The free vibration acceleration time histories were used in MS-Excel solver to evaluate these parameters. Damping ratios were also calculated using logarithmic decrement. The various methods reproduced the values for frequencies and damping ratios consistently in each single degree of freedom structure (individual storey). For forced harmonic excitation, a series of tests were run near the resonant frequency of the single-storey structure to develop a transmissibility ratio curve directly using the measured amplitudes of total acceleration at the girder level and at the base (shake table). The natural frequency and damping ratios were then calculated by using the following closed-form equation for transmissibility ratio in MS-Excel solver.

$$\frac{\ddot{u}_0}{\ddot{u}_{g0}} = \frac{\sqrt{1 + (2\xi\beta)^2}}{\sqrt{(1 - \beta^2)^2 + (2\xi\beta)^2}} \quad (37)$$

$$\beta = \frac{\Omega}{\omega} \quad (38)$$

The natural frequencies evaluated from forced vibration tests of individual stories were also very close and almost identical to those evaluated earlier from free vibration tests. We also determined if the individual stories were different from each other with respect to their

dynamic characteristics. The test results showed that the differences were insignificant for the purposes of this study. Therefore, an MDOF structure made of these stories could be considered to be made up of a series of identical SDOF stories with a frequency of 13.17 Hz and a modal damping ratio of 0.126 %. The comparison of directly measured curve and that obtained using Eq. (37) is given in Figure 12.

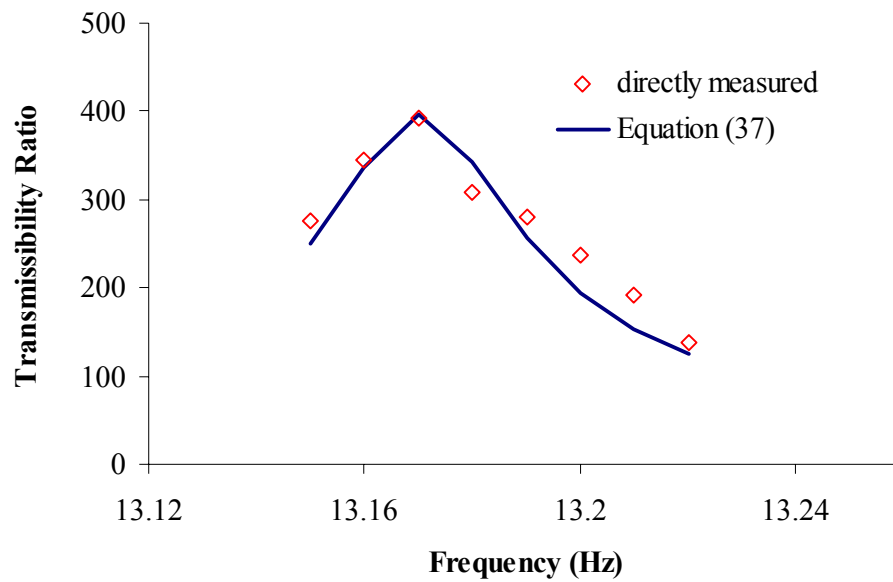


Figure 12 – System identification of SDOF structure

Once the properties of the system were determined, forced harmonic excitation tests were conducted for a 2-DOF structure. Testing was performed in an adequate frequency range to capture all structural modes. Excitation frequencies were spaced closely in the resonance regions. The transmissibility ratios plots were developed from directly measured amplitudes of total acceleration at each degree of freedom and at base (shake table). These curves were then compared with the corresponding curves evaluated by direct solution of the equation of motion using the damping matrix given in Eq. (1). These comparisons are shown in Figures

13 and 14 for the 2-DOF system. Clearly, the damping matrix created in accordance with Eq. (1) gives highly incorrect results. In terms of damping ratios, one can use the experimentally obtained transmissibility ratios at each storey to determine the experimentally obtained damping ratio. These values at the first storey level were found to be 0.35% and 0.28% in two modes. For the second storey, these values were 0.35% and 0.26%. As evaluated earlier, the damping ratio for the corresponding SDOF structure was found to be 0.126%. Therefore, the damping ratios in the modes of an MDOF system are not equal to the damping ratio associated with the corresponding SDOF systems. Furthermore, the damping matrix evaluated by assembling the damping coefficients for each SDOF storey is not correct.

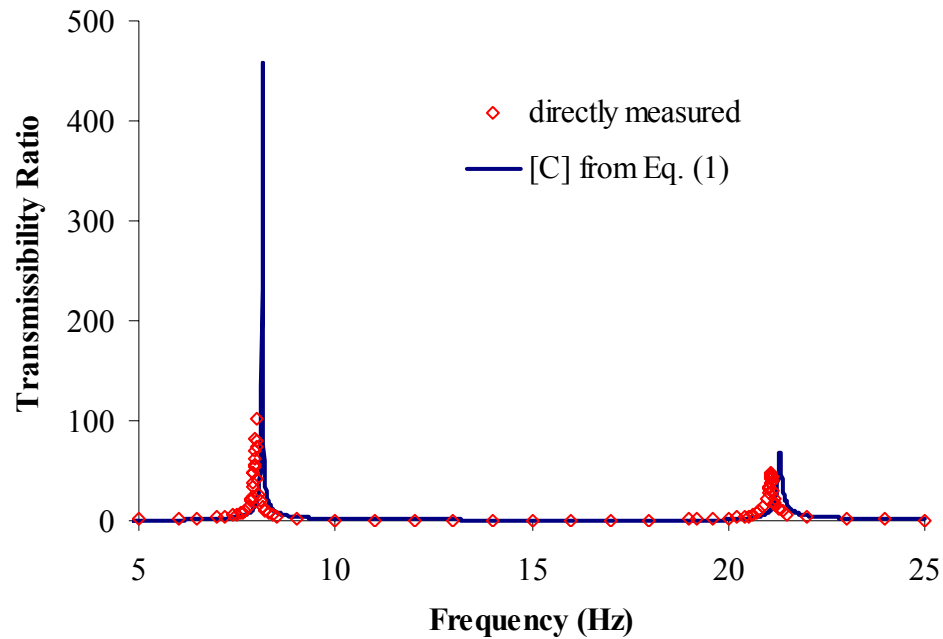


Figure 13 – Response at DOF 1, 2-DOF system

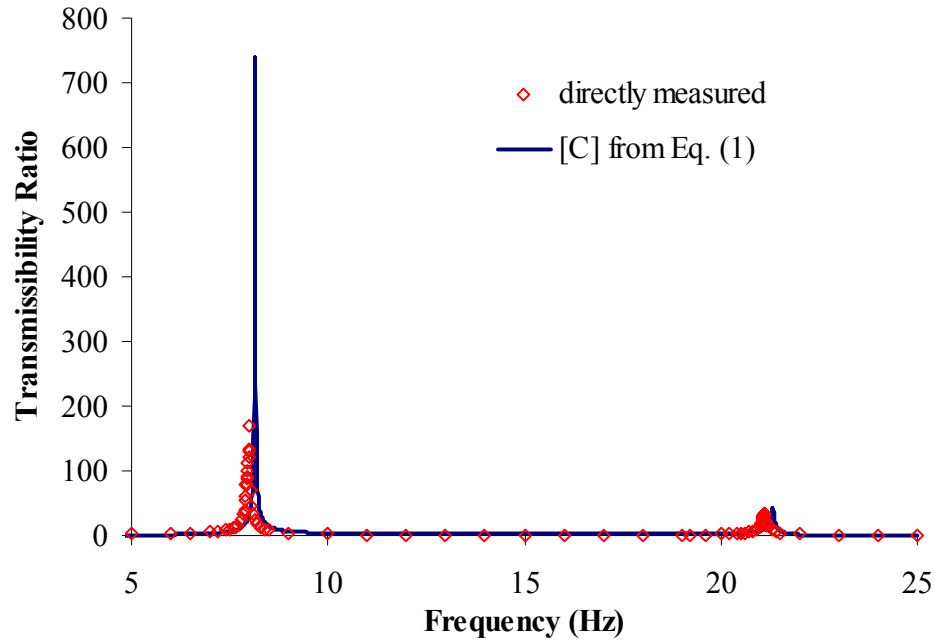


Figure 14 – Response at DOF 2, 2-DOF system

A 3-DOF structure consisting of the identical stories was constructed and tested in forced harmonic vibration. Transmissibility ratios were measured at each DOF and are compared with the results from a direct solution of the equation of motion in Figures 15 - 17. Similarly to the 2-DOF testing, excitation frequencies were more closely spaced in the regions of the structural modes. As in the 2-DOF case, the damping matrix created in accordance with Eq. (1) gives highly incorrect results. At the first storey level, damping ratios were found to be 0.21%, 0.50% and 0.34% in three modes. For the second storey, these values were 0.22%, 0.52% and 0.37%. For the third storey, the damping ratios were 0.24%, 0.45% and 0.31% for three modes. These values contradict the damping ratio for the corresponding SDOF structure of 0.126%.

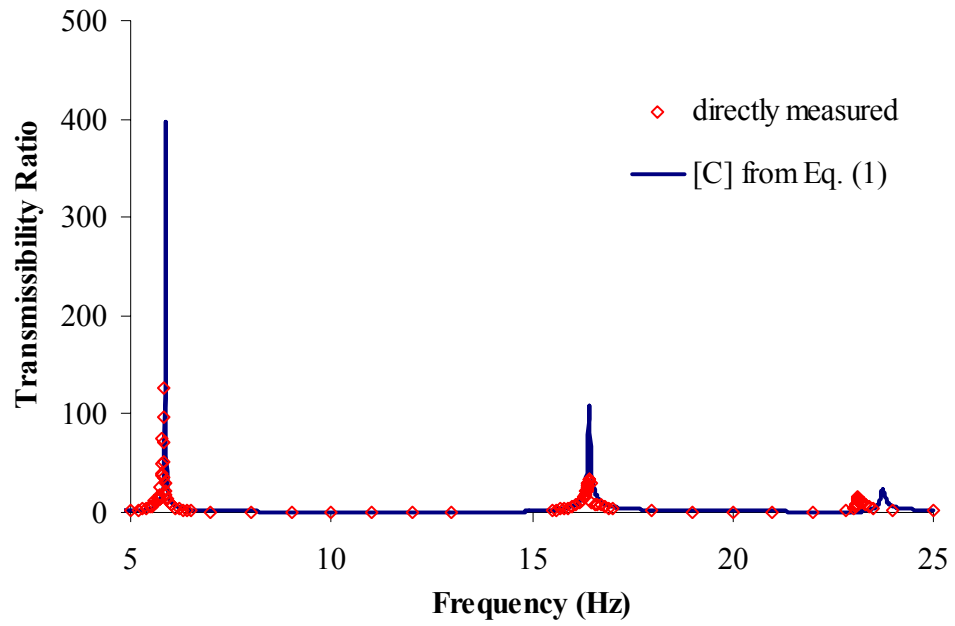


Figure 15 – Response at DOF 1, 3-DOF system

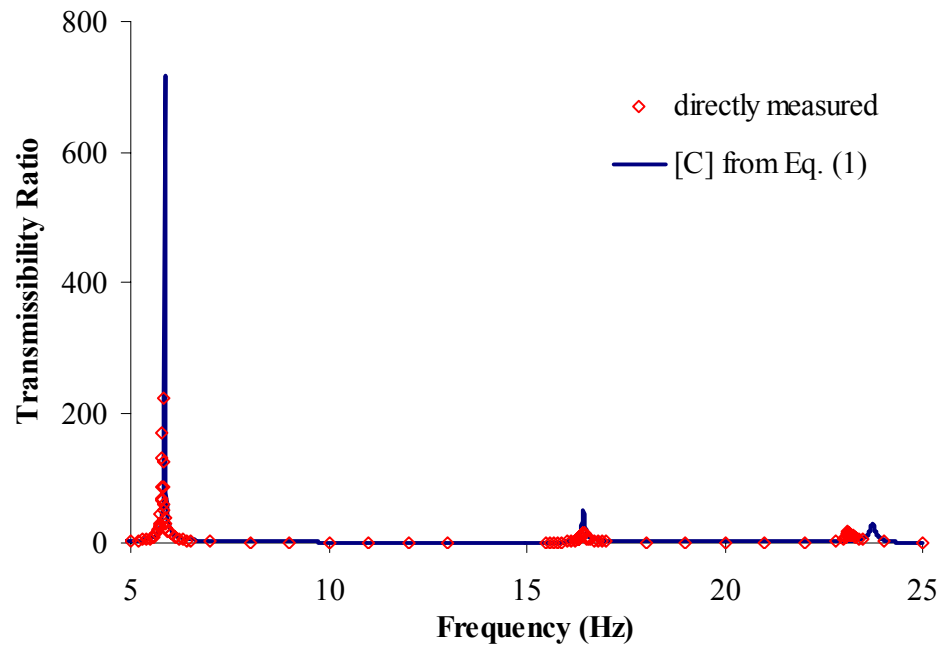


Figure 16 – Response at DOF 2, 3-DOF system

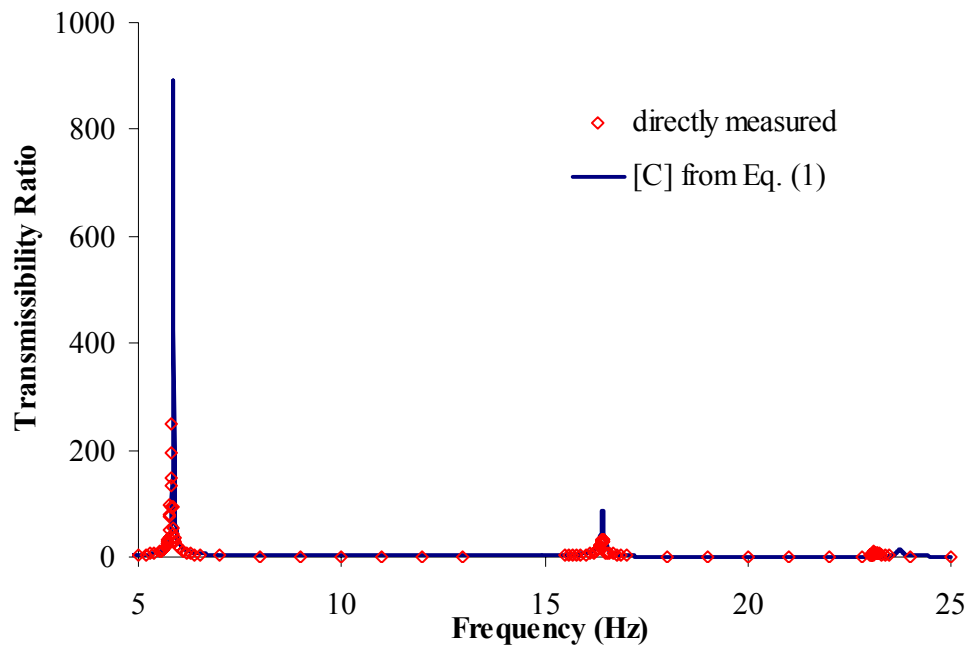


Figure 17 – Response at DOF 3, 3-DOF system

2.3.2 Structure with Damper Experiments – Displacement Controlled Shake Table

The current rise in the use of supplemental damping devices makes the understanding of the damping matrix even more important. For complex analysis of critical structures that employ these emerging technologies, an accurate knowledge of the structure's damping matrix is essential before including any supplemental devices. To examine the effects of adding supplemental damping to a structure, we elected to use a simple shock absorber to act as a damping device in the shear models. The shock absorber, originally intended for use in remote-controlled automobiles, is shown in Figure 18. The overall extended length of the device is 4" inches, and the stroke length is 1.25". The device is oil-filled and incorporates interchangeable flow caps to vary the resistance of the plunger. Free vibration test data confirmed approximate linear-viscous behavior of the damper, and consecutive sets of forced vibration experiments were run to ensure consistent damping properties for the damper. Tests to measure the stiffness of a SDOF system with and without a damper confirmed that the device provided negligible additional stiffness to the system.



Figure 18 – Simple shock absorber

The same simple shear model structures used in earlier tests were outfitted with a damping device and tested in forced harmonic vibration. The structures were tested on a more powerful displacement-controlled shake table. In addition to being displacement-controlled, the shake table setup also incorporated analog signal filters to ensure clearer acceleration data. For the SDOF system identification, it was found that the natural frequency of the structure remained unchanged at 13.17 Hz. The damping ratio of the structure without the damper was found to be 0.1866%, and with the damper it was 0.4763%.

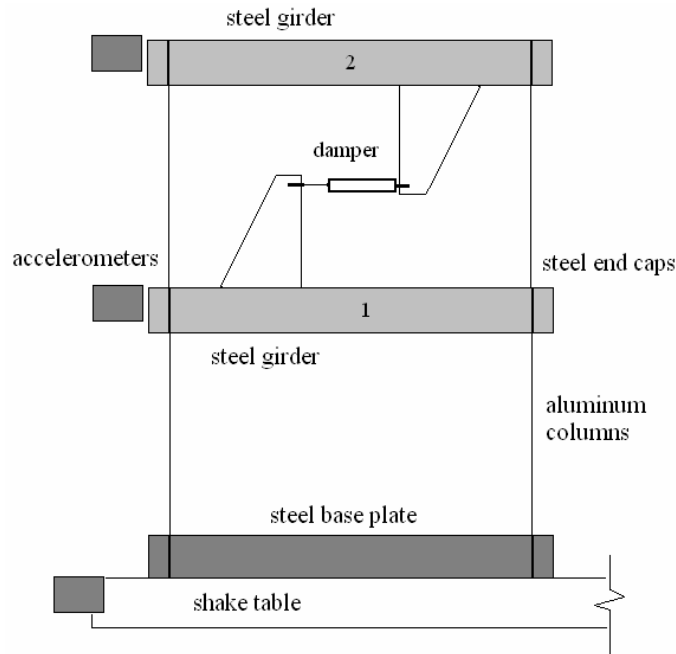


Figure 19 – 2DOF shear structure with damper

For analytical modeling of the structure, the structure's damping matrix was established based upon the damping ratio of the forced vibration testing. As shown in Eq. (39), the damping coefficient from the damper alone was used to create a supplemental damping matrix, which was then added to the original damping matrix.

$$[C] = \begin{bmatrix} c_1 + c_2 & -c_2 \\ -c_2 & c_2 \end{bmatrix} + \begin{bmatrix} c_D & -c_D \\ -c_D & c_D \end{bmatrix} \quad (39)$$

A 2-DOF structure incorporating a damping device in the top storey, as shown in Figure 19, was tested in forced vibration. The experimental results of transmissibility ratio are plotted versus the direct solution in Figures 20 and 21. Due to the presence of the damping device, higher structural modes were very difficult to excite. Therefore, only results from the first mode are shown. Similarly to the experiments without damping devices, the analytical methods yield much higher peak responses than what were measured experimentally. For the first mode, the modal damping ratio in the first storey was 0.32% and 0.42% in the second storey.

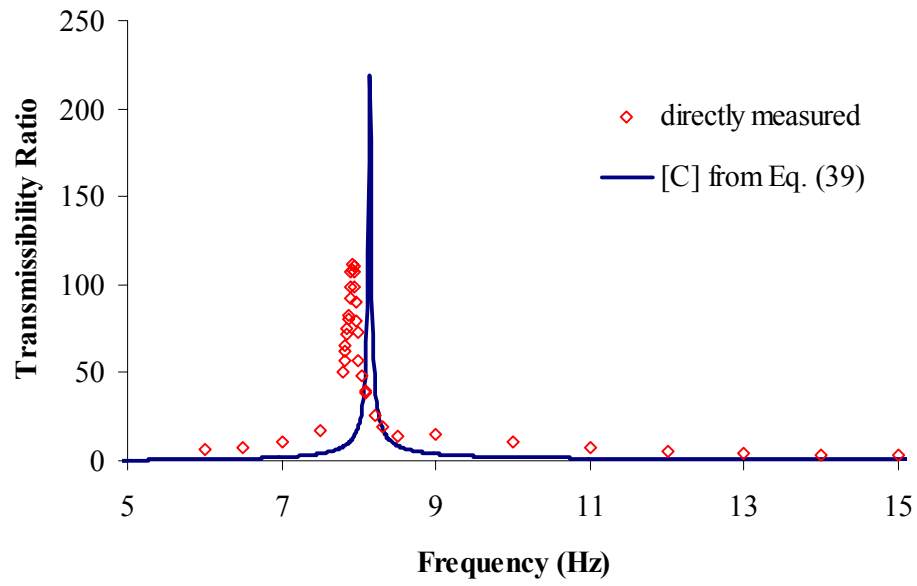


Figure 20 – Response at DOF 1, 2-DOF system with damper

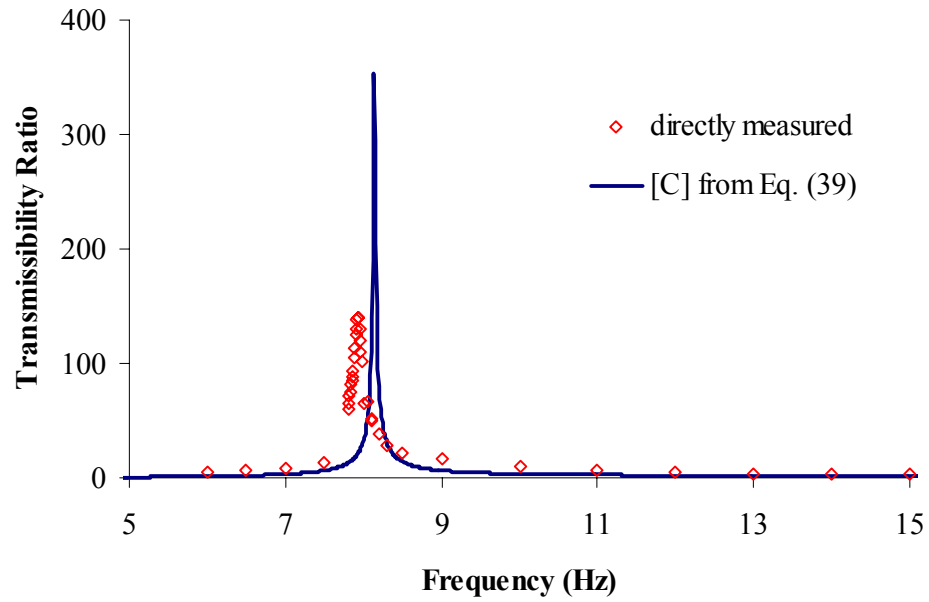


Figure 21 – Response at DOF 2, 2-DOF system with damper

A 3-DOF structure was also outfitted with a damper in the top storey and was tested in forced vibration. The damping matrix is created as shown in Eq. (40) below. The experimental results for transmissibility ratio are plotted versus the direct solution for each DOF in Figures 22 - 24. As in the 2-DOF experiments, only results from the first structural mode are shown. For the first mode of vibration, the modal damping ratios were 0.27%, 0.49%, and 0.40% for the three stories.

$$[C] = \begin{bmatrix} c_1 + c_2 & -c_2 & 0 \\ -c_2 & c_2 + c_3 & -c_3 \\ 0 & -c_3 & c_3 \end{bmatrix} + \begin{bmatrix} 0 & 0 & 0 \\ 0 & c_D & -c_D \\ 0 & -c_D & c_D \end{bmatrix} \quad (40)$$

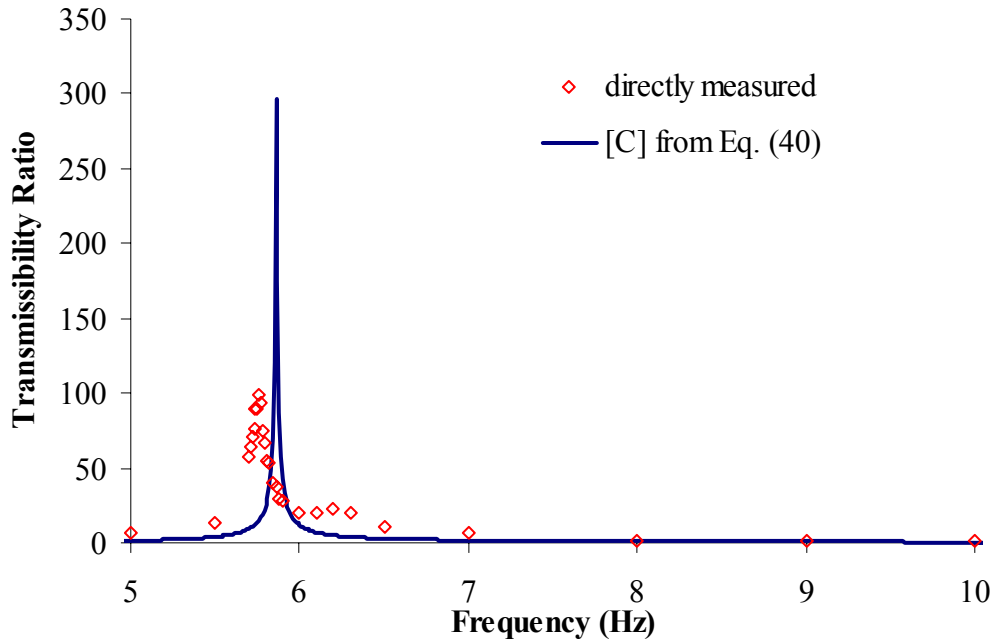


Figure 22 – Response at DOF 1, 3-DOF system with damper

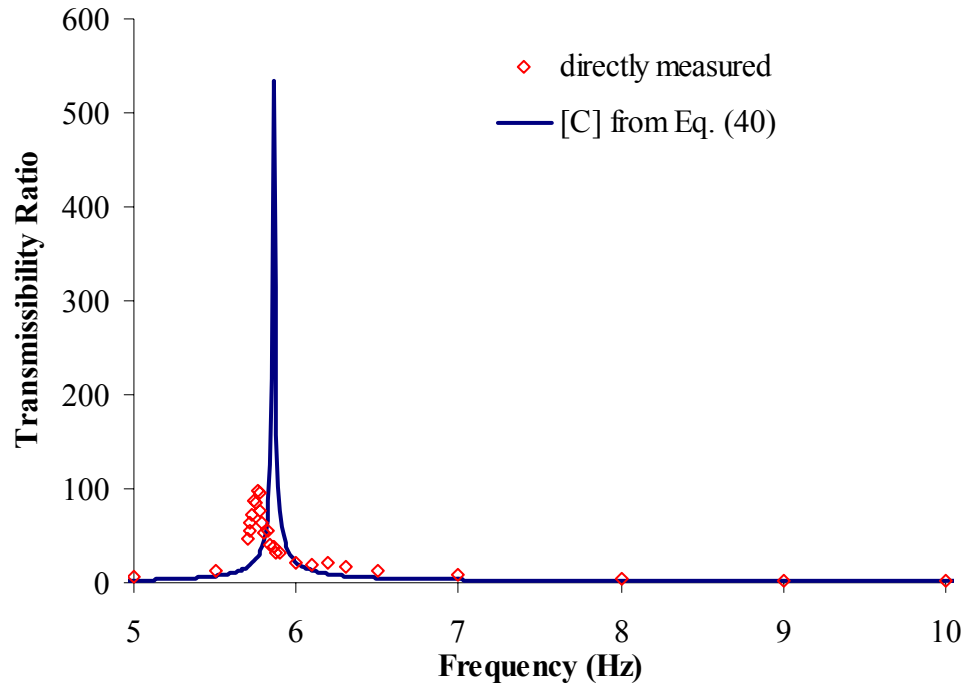


Figure 23 – Response at DOF 2, 3-DOF system with damper

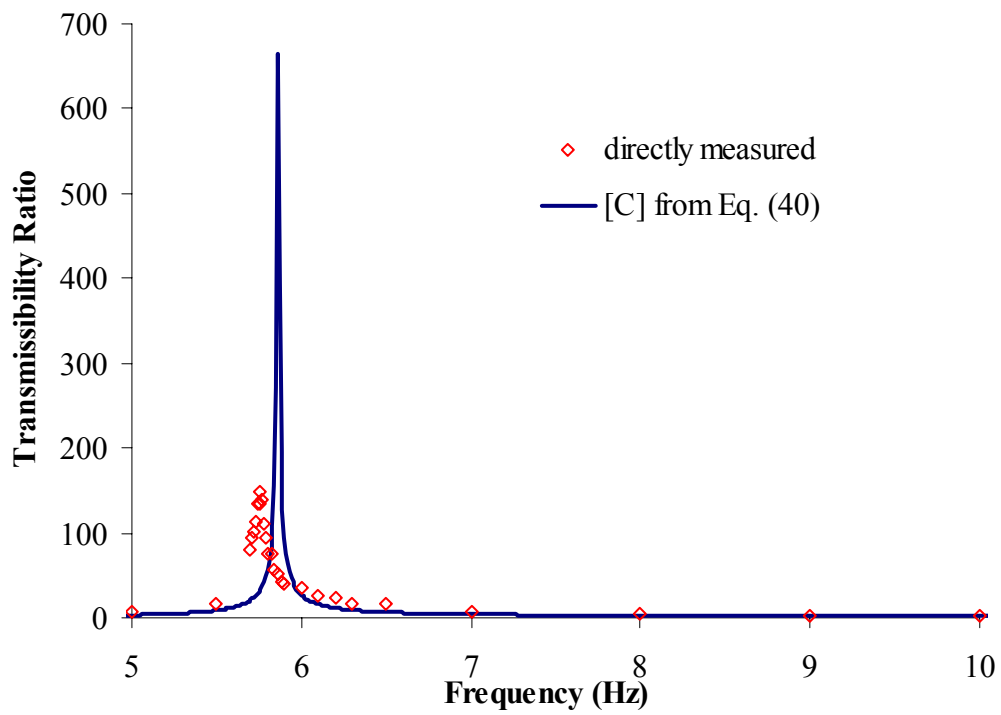


Figure 24 – Response at DOF 3, 3-DOF system with damper

2.4 Proposed Damping Matrix

The results presented for both the original structure as well as a structure with a supplemental damping device clearly show a remarkable difference in the predicted and measured frequency domain response. Because the analytical models are based on a direct solution to the equations of motion, which accounts for the entire damping matrix, we will now consider alternative methods of formulating the damping matrix itself.

2.4.1 Damping Matrix Using Mode Shapes

Exact shape functions for a beam can be used to determine a model for damping in a MDOF structure. For a simple beam, let us consider only the two translational degrees-of-freedom in order to represent a column placed in a shear model structure. The exact shape functions for the deformation of the beam are:

$$\Psi_1(x) = 1 - 3\left(\frac{x}{L}\right)^2 + 2\left(\frac{x}{L}\right)^3 \quad (41)$$

$$\Psi_2(x) = 3\left(\frac{x}{L}\right)^2 - 2\left(\frac{x}{L}\right)^3 \quad (42)$$

For a one storey structure sitting on a shake table, the damping coefficient can be found using Equation (44), where \bar{c} is the effective damping per unit length of the beam. From experimental testing, we can determine c using the modal damping ratio and natural frequency. From these two expressions, we can find that:

$$c = \int_0^L \bar{c} \cdot [\Psi_2(x)]^2 dx \quad (43)$$

$$c = 2\xi\omega m \quad (44)$$

$$\bar{c} = \frac{35c}{13L} \quad (45)$$

$$c_{ij} = \int_0^L \bar{c} \cdot \Psi_i(x) \cdot \Psi_j(x) dx \quad (46)$$

For a 2-DOF structure, the damping in the first storey is found using Eq. (43) since the second mode shape determines the storey motion. For the second storey, however, there is a combination of modes included in the response. Therefore, we must determine the damping coefficients using Eq.(46). Once the damping coefficients from the first and second stories have been determined, the damping matrix of the structure is assembled to yield the following result:

$$[c] = \begin{bmatrix} 2c & \frac{63}{182}c \\ \frac{63}{182}c & c \end{bmatrix} \quad (47)$$

For a 3-DOF structure, the damping matrix as determined using mode shapes therefore becomes:

$$[c] = \begin{bmatrix} 2c & \frac{63}{182}c & 0 \\ \frac{63}{182}c & 2c & \frac{63}{182}c \\ 0 & \frac{63}{182}c & c \end{bmatrix} \quad (48)$$

Using the example structure from Section 2.2.1, we can examine the properties of the damping matrix for this type of formulation. For the 2-DOF structure, the damping matrix is

$$[C] = \begin{bmatrix} 4.0000 & 0.6923 \\ 0.6923 & 2.0000 \end{bmatrix} \quad (49)$$

The transformed damping matrix can be computed to be

$$[\bar{C}] = \begin{bmatrix} 3.9650 & 1.5050 \\ 1.5050 & 3.5350 \end{bmatrix} \quad (50)$$

Unlike the damping matrix given in Eq. (1), damping matrix from exact shape functions is non-proportional. The diagonal elements in the transformed damping matrix give

$\xi_1 = 0.1283$ and $\xi_2 = 0.0437$. As in the earlier discussion, let us consider a 3-DOF system that consists of three of the same SDOF systems. In this case it can be shown that $\xi_1 = 0.212$, $\xi_2 = 0.0675$, and $\xi_3 = 0.0395$.

To experimentally evaluate the damping matrix created using exact shape functions for a beam, measured responses were compared with transmissibility curves generated using the new damping matrix. Experimental data for a 2-DOF structure is compared to the results predicted by using the damping matrix in Eq. (47) in Figures 25 and 26. The analytical model better predicts the actual response of the structure in the first mode compared with the original damping matrix from Eq. (1). Figures 27 – 29 compare the prediction using Eq. (48) to the experimentally measured response for a 3-DOF structure. It is clear from the plots that the new damping matrix significantly under-predicts the response in the first mode at each storey.

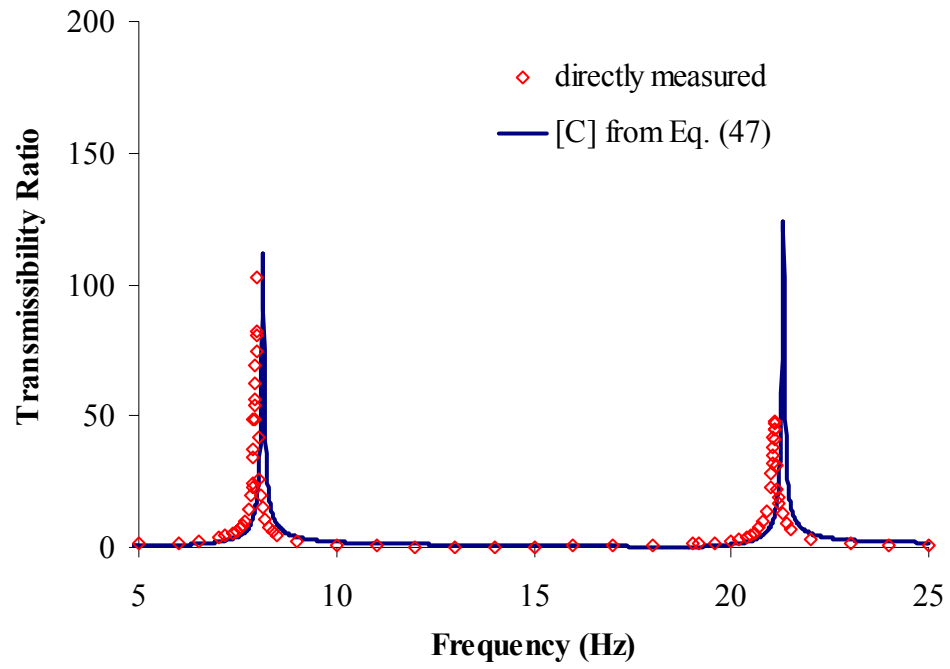


Figure 25 – Response at DOF 1, 2-DOF system

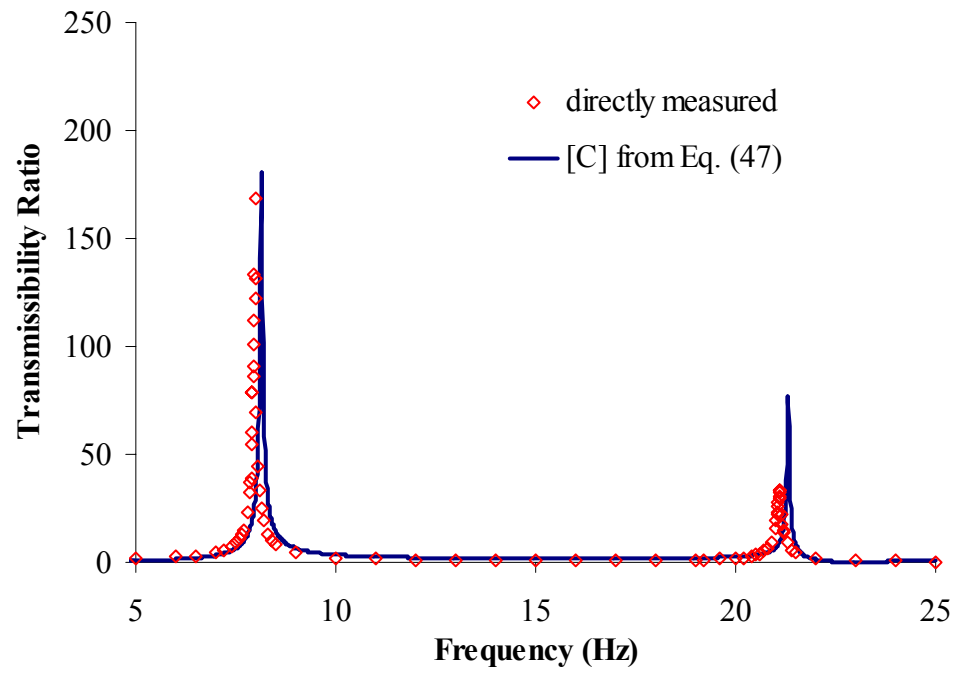


Figure 26 – Response at DOF 2, 2-DOF system

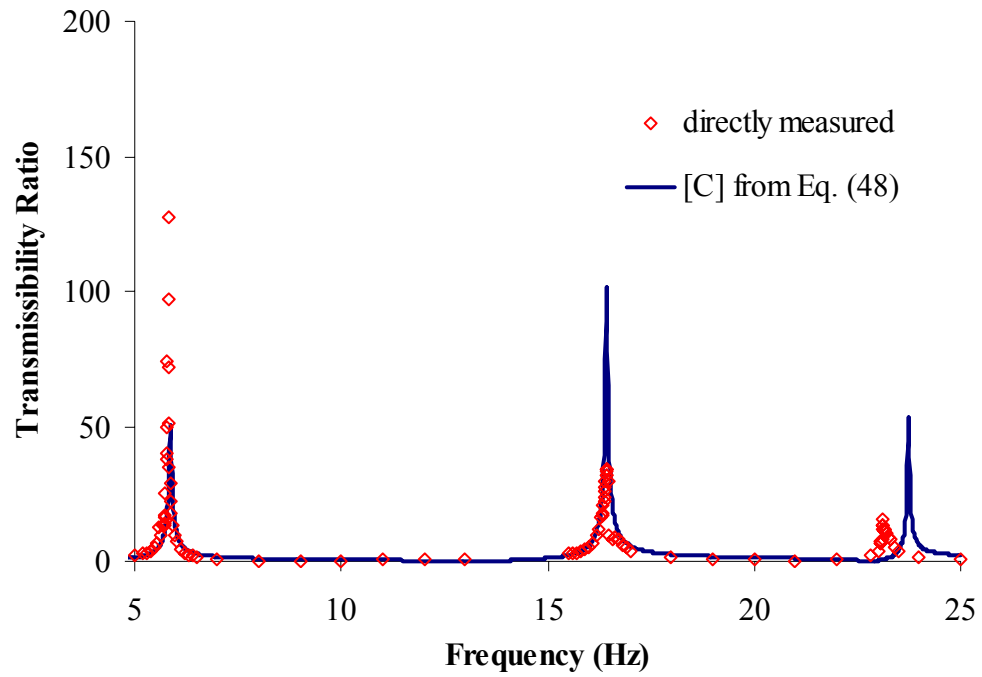


Figure 27 – Response at DOF 1, 3-DOF system

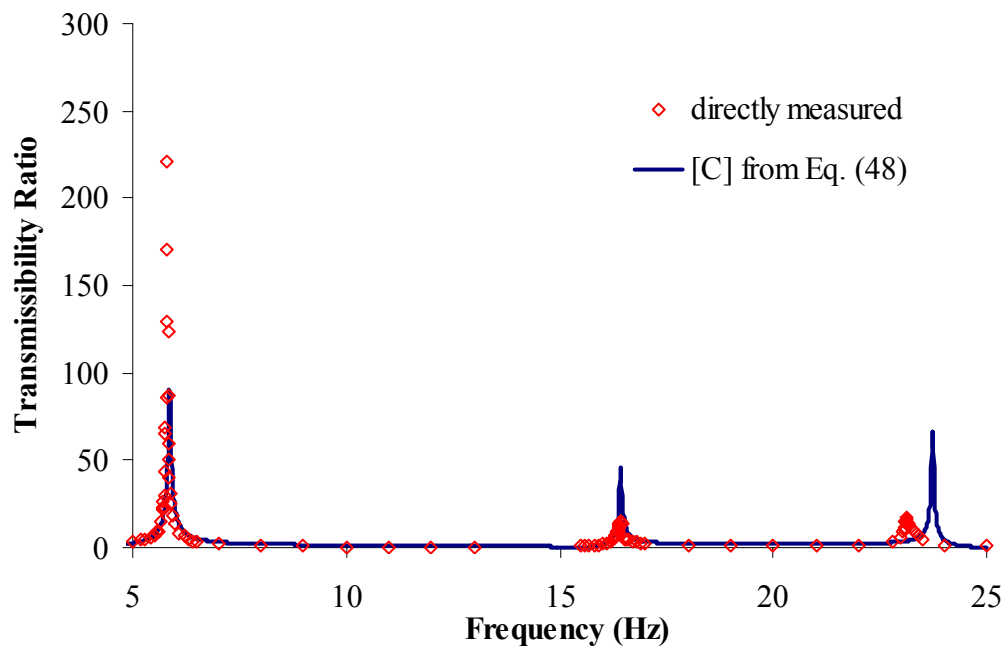


Figure 28 – Response at DOF 2, 3-DOF system

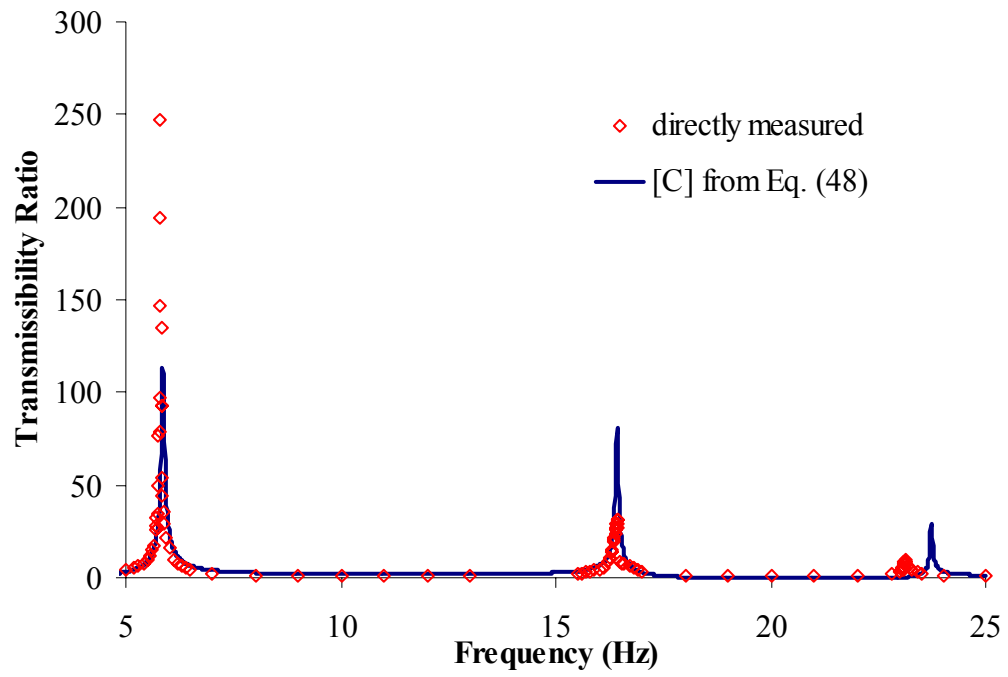


Figure 29 – Response at DOF 3, 3-DOF system

2.4.2 Diagonal Damping Matrix

Let us assemble a damping matrix using an alternate form to that considered in Eq. (1). This damping matrix only incorporates dashpots from each storey to the ground, as shown in Figure 30. The damping matrix is then created as follows for a 2-DOF and 3-DOF structure:

$$[C] = \begin{bmatrix} c_1 & 0 \\ 0 & c_2 \end{bmatrix} \quad (51)$$

$$[C] = \begin{bmatrix} c_1 & 0 & 0 \\ 0 & c_2 & 0 \\ 0 & 0 & c_3 \end{bmatrix} \quad (52)$$

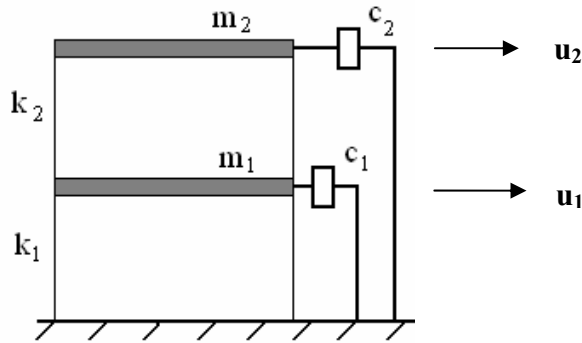


Figure 30 – 2DOF shear structure with diagonal $[C]$

Using the example structure from Section 2.2.1, we can examine the properties of the damping matrix for this type of formulation. For the 2-DOF structure, the damping matrix is

$$[C] = \begin{bmatrix} 2.0000 & 0 \\ 0 & 2.0000 \end{bmatrix} \quad (53)$$

The transformed damping matrix can be computed to be

$$[\bar{C}] = \begin{bmatrix} 2.5000 & 0 \\ 0 & 2.5000 \end{bmatrix} \quad (54)$$

Similar to the damping matrix given in Eq. (1), the damping matrix described by Eq. (51) is proportional. The diagonal elements in the transformed damping matrix give $\xi_1 = 0.0809$ and $\xi_2 = 0.0309$. As in the earlier discussion, let us consider a 3-DOF system that consists of three of the same SDOF systems. The damping matrix is again proportional, and it can be shown that $\xi_1 = 0.112$, $\xi_2 = 0.0401$, and $\xi_3 = 0.0277$.

To experimentally evaluate the damping matrix assembled in a diagonal manner, measured responses were compared with transmissibility curves generated using the new damping matrix. For the 2-DOF structure presented in Section 2.3.1, the experimentally measured transmissibility curves at each DOF are compared with the predicted response using the form of the damping matrix shown in Equation (51) in Figures 31 and 32. Response for the 3-DOF structure is then compared in Figures 33 – 35.

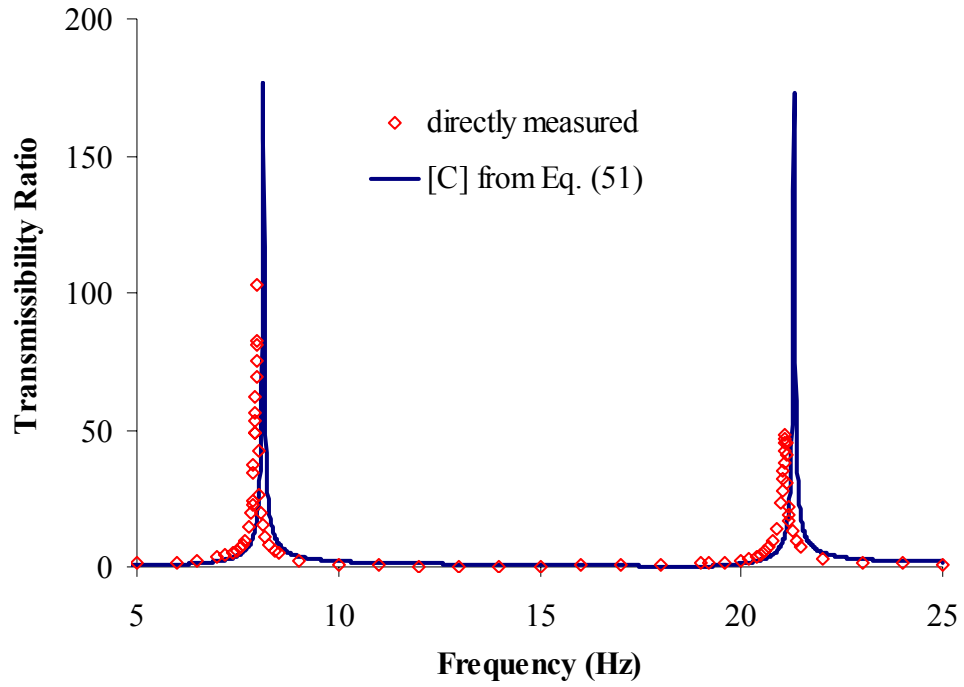


Figure 31 – Response at DOF 1, 2-DOF system

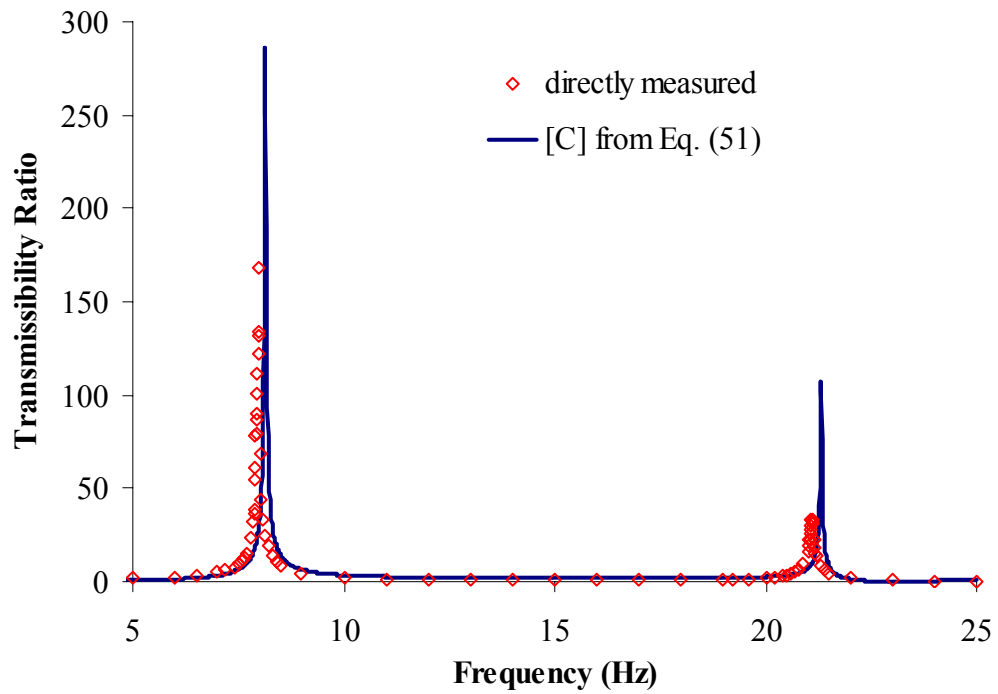


Figure 32 – Response at DOF 2, 2-DOF system

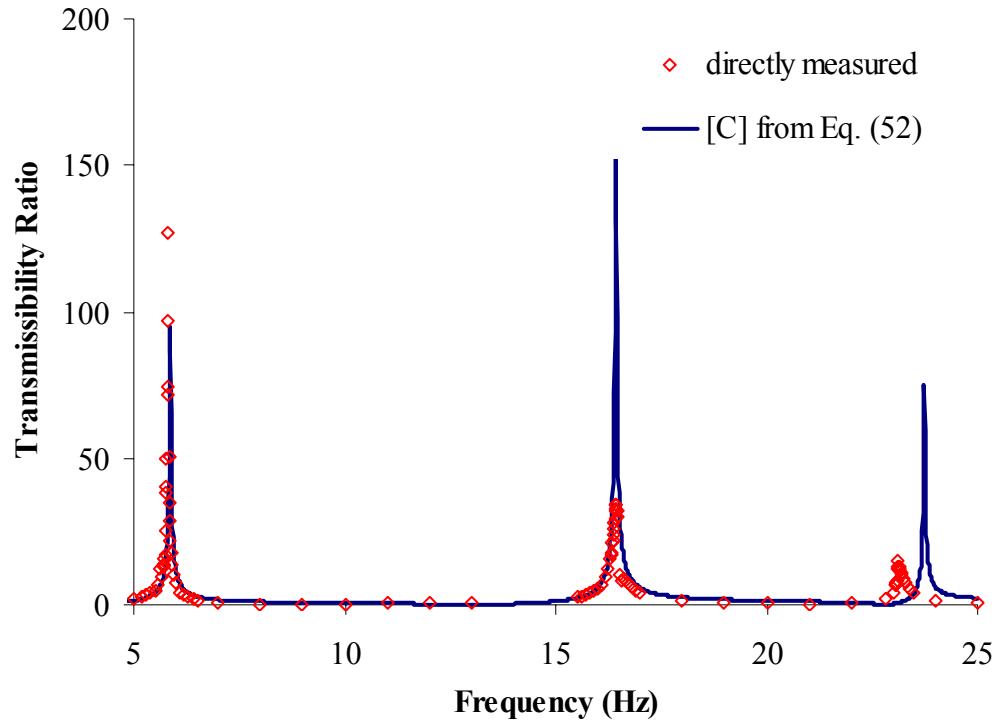


Figure 33 – Response at DOF 1, 3-DOF system

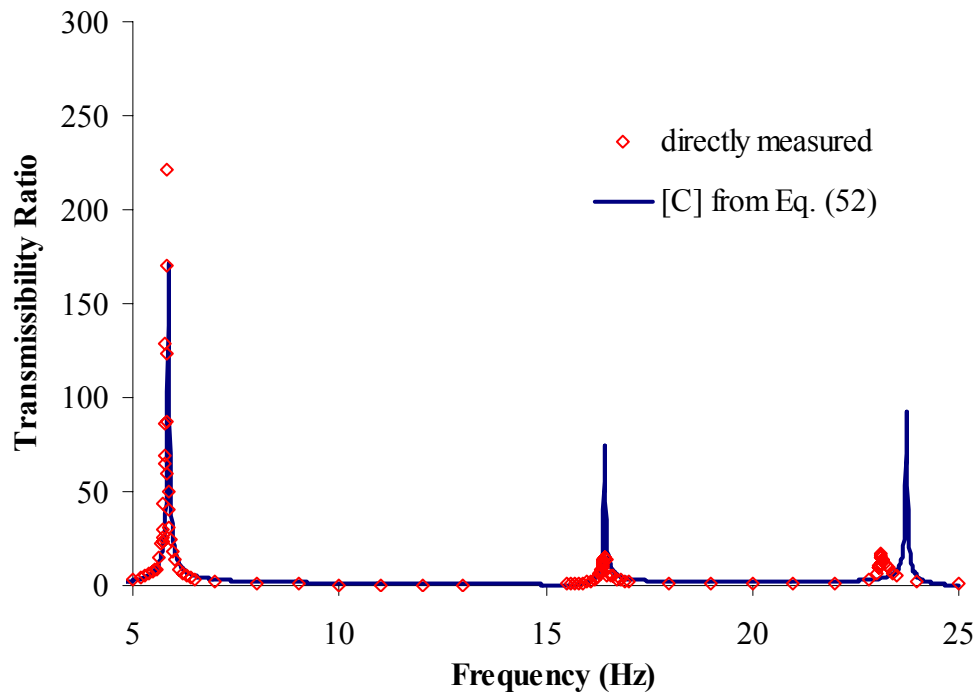


Figure 34 – Response at DOF 2, 3-DOF system

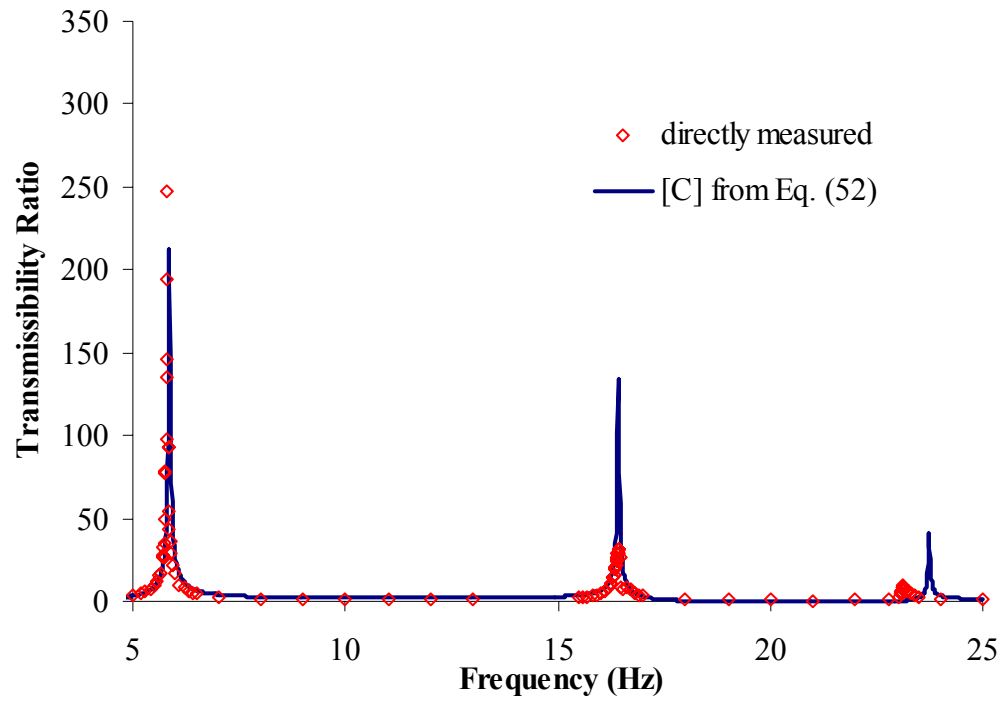


Figure 35 – Response at DOF 3, 3-DOF system

2.4.3 Damping Matrix using Additional Dashpots

Let us consider a form of the damping matrix where additional dashpots are attached from each storey to the ground. This damping matrix considers additional damping terms, as shown in Figure 36. The damping matrix is then created as follows for a 2-DOF and 3-DOF structure:

$$[C] = \begin{bmatrix} c_1 + c_2 & -c_2 \\ -c_2 & 2c_2 \end{bmatrix} \quad (55)$$

$$[C] = \begin{bmatrix} c_1 + c_2 & -c_2 & 0 \\ -c_2 & 2c_2 + c_3 & -c_3 \\ 0 & -c_3 & 2c_3 \end{bmatrix} \quad (56)$$

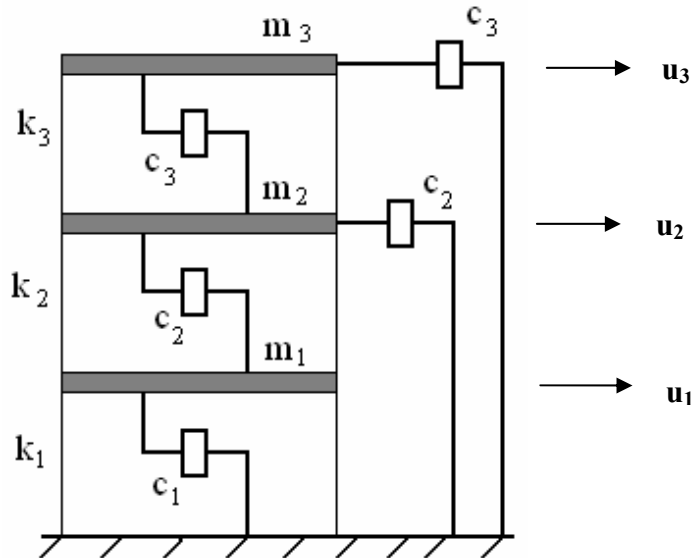


Figure 36 – 3DOF shear structure with added dashpots at all stories

Using the example structure from Section 2.2.1, we can examine the properties of the damping matrix for this type of formulation. For the 2-DOF structure, the damping matrix is

$$[C] = \begin{bmatrix} 4.0000 & -2.000 \\ -2.000 & 4.0000 \end{bmatrix} \quad (57)$$

The transformed damping matrix can be computed to be

$$[\bar{C}] = \begin{bmatrix} 2.7639 & -1.1180 \\ -1.1180 & 7.2361 \end{bmatrix} \quad (58)$$

Unlike the damping matrix given in Eq. (1), the damping matrix described by Eq. (55) is non-proportional. The diagonal elements in the transformed damping matrix give

$\xi_1 = 0.0894$ and $\xi_2 = 0.0894$. As in the earlier discussion, let us consider a 3-DOF system that consists of three of the same SDOF systems. In this case it can be shown that $\xi_1 = 0.122$, $\xi_2 = 0.0807$, and $\xi_3 = 0.108$.

To experimentally evaluate the damping matrix including the additional dashpots, measured responses were compared with transmissibility curves generated using the new damping matrix. For the 2-DOF structure presented in Section 2.3.1, the experimentally measured transmissibility curves at each DOF are compared with the predicted response using the form of the damping matrix shown in Equation (55) in Figures 37 and 38. Response for the 3-DOF structure is then compared in Figures 39 – 41.

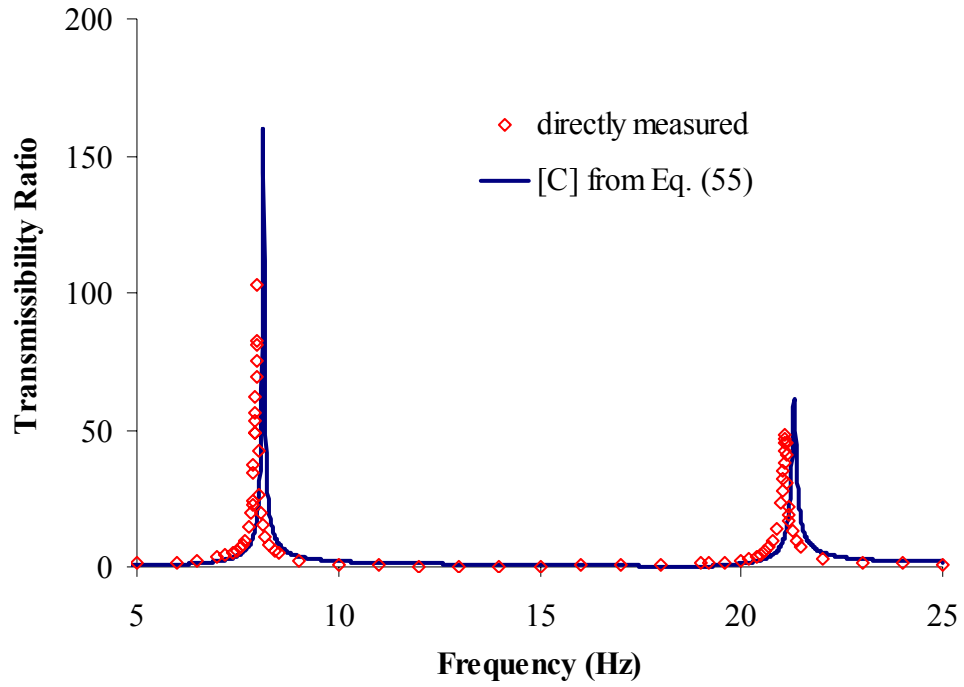


Figure 37 – Response at DOF 1, 2-DOF system

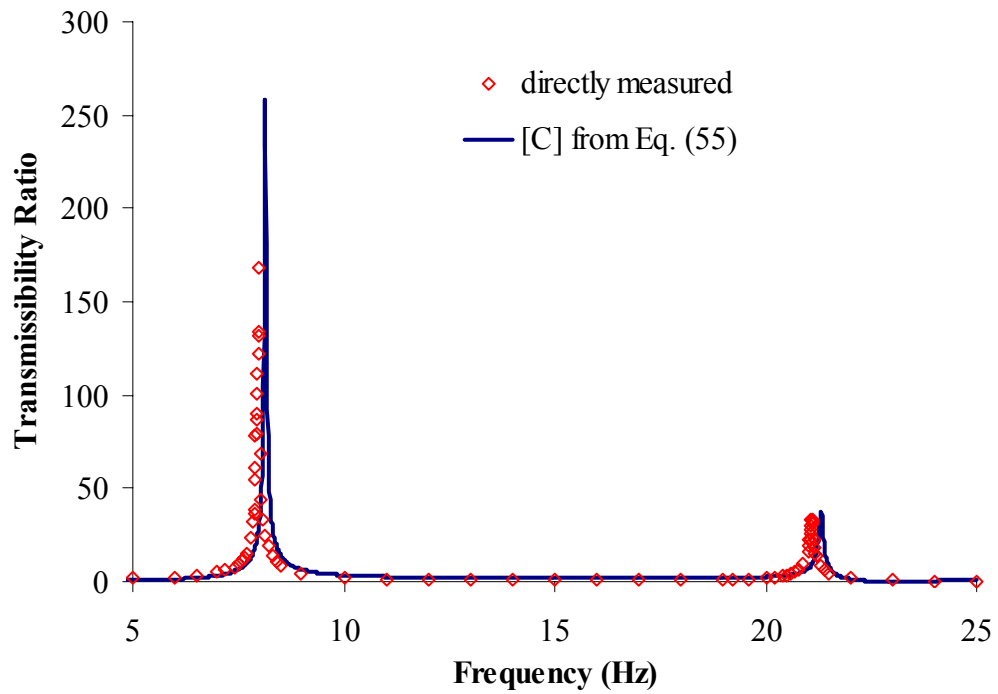


Figure 38 – Response at DOF 2, 2-DOF system

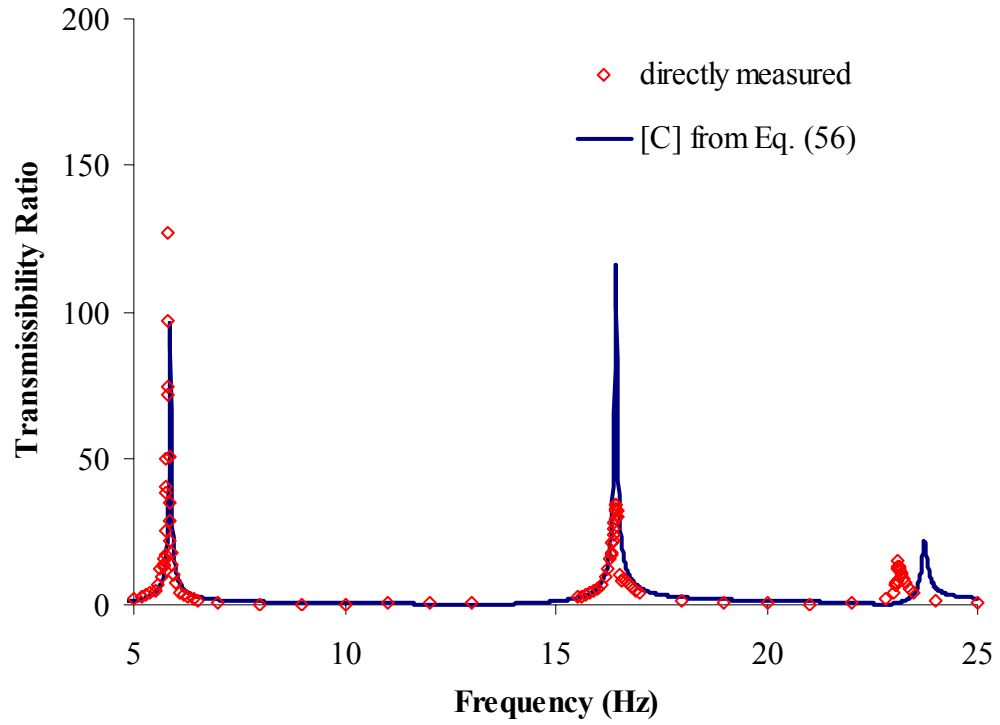


Figure 39 – Response at DOF 1, 3-DOF system

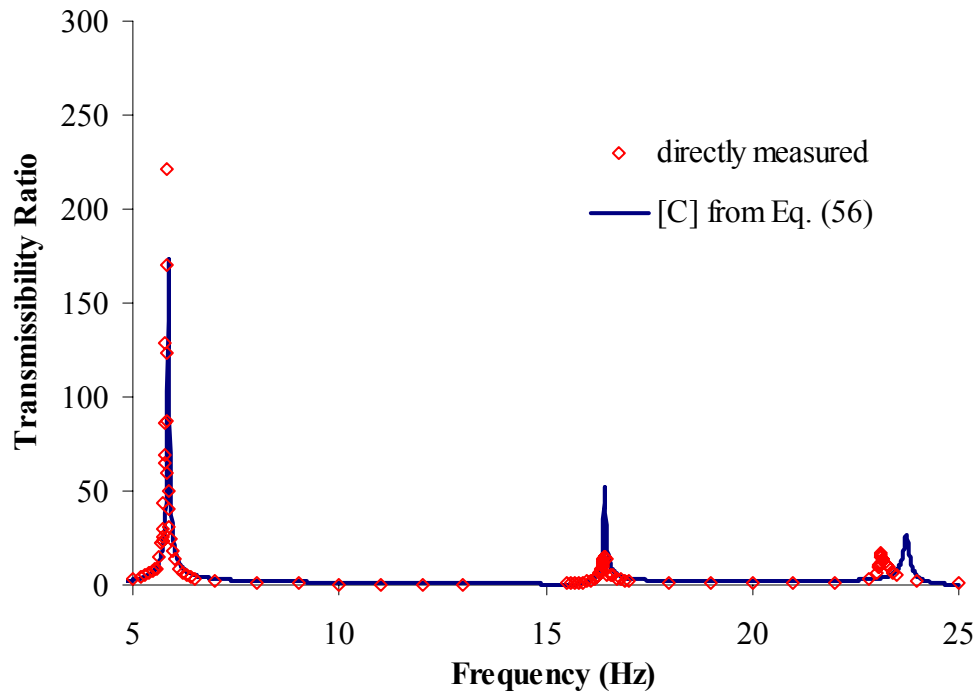


Figure 40 – Response at DOF 2, 3-DOF system

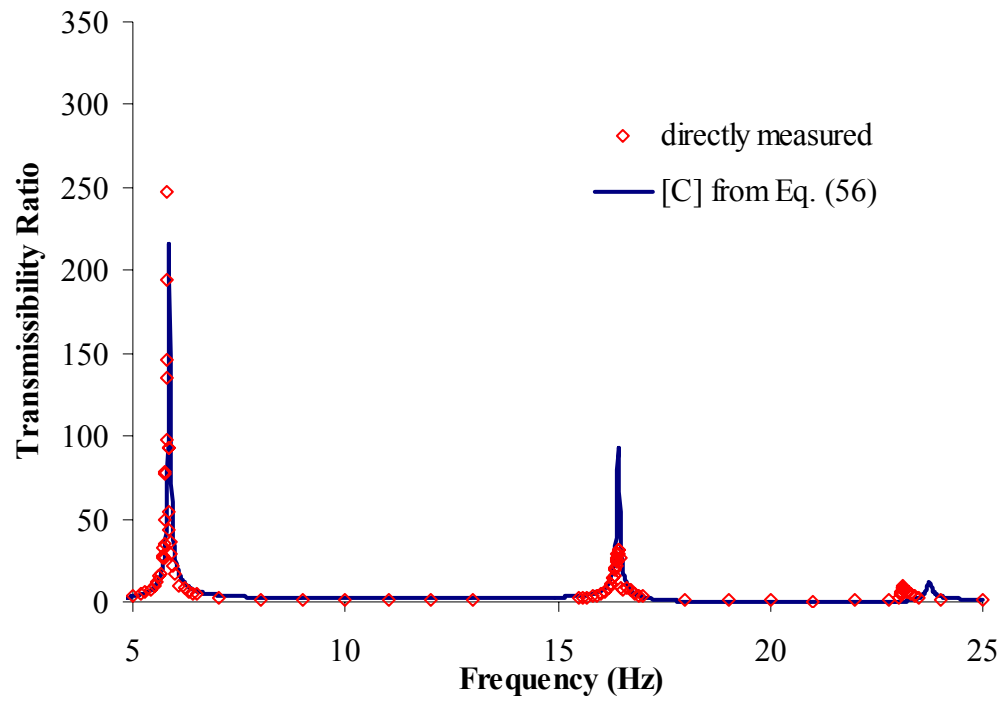


Figure 41 – Response at DOF 3, 3-DOF system

2.4.4 Damping Matrix by Additional Dashpot from Top Storey Only

Let us consider a damping matrix of an alternate form to that considered in Eq. (1). This damping matrix includes an additional damping term which represents a discrete damper, having a damping coefficient equal to that of a single storey, attached from the top storey of the structure to the ground, as illustrated in Figure 42. For a 2-DOF structure, the damping matrix is created as in Eq. (55), and for a 3-DOF structure it is created as follows:

$$[C] = \begin{bmatrix} c_1 + c_2 & -c_2 & 0 \\ -c_2 & c_2 + c_3 & -c_3 \\ 0 & -c_3 & 2c_3 \end{bmatrix} \quad (59)$$

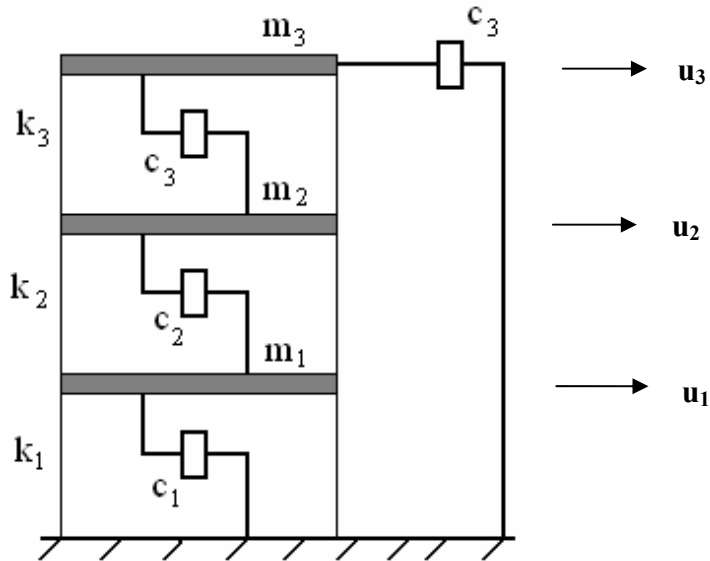


Figure 42 – 3DOF shear structure with dashpot added from top storey only

Using the example structure from Section 2.2.1, we can examine the properties of the damping matrix for this type of formulation. For the 2-DOF structure, the damping matrix and transformed damping matrix are the same as in Equations (57) and (58). As in the earlier

discussion, let us consider a 3-DOF system that consists of three of the same SDOF systems. For the case of the damping matrix created by with an additional dashpot at the top storey, it can be shown that $\xi_1 = 0.0833$, $\xi_2 = 0.0764$, and $\xi_3 = 0.0931$.

To experimentally evaluate the damping matrix created by an additional term at the top storey only, measured responses were compared with transmissibility curves generated using the new damping matrix. For the 2-DOF structure presented in Section 2.3.1, the experimentally measured transmissibility curves at each DOF are compared with the predicted response using the form of the damping matrix shown in Equation (55) in Figures 43 and 44. Response for the 3-DOF structure is then compared in Figures 45– 47. This form of the damping matrix gives much more representative results for the response of the structure when compared to the earlier forms.

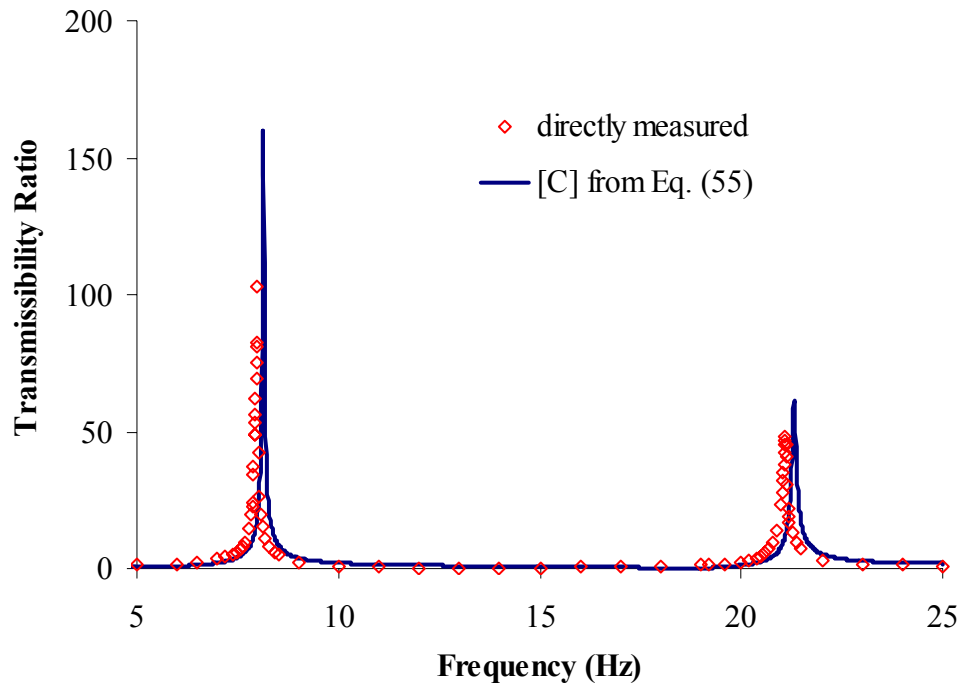


Figure 43 – Response at DOF 1, 2-DOF system

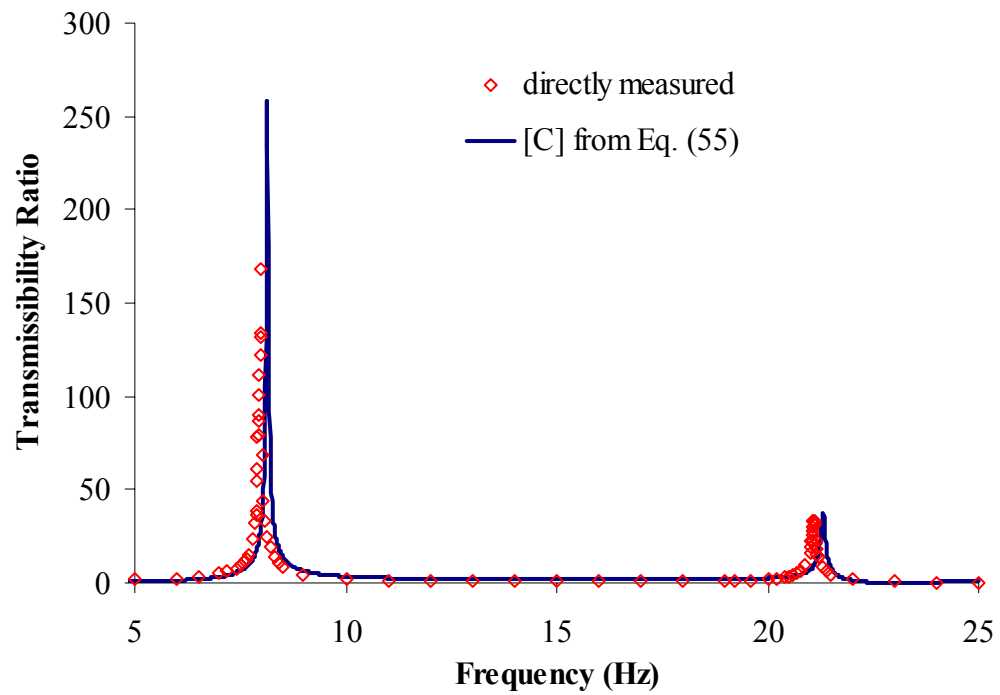


Figure 44 – Response at DOF 2, 2-DOF system

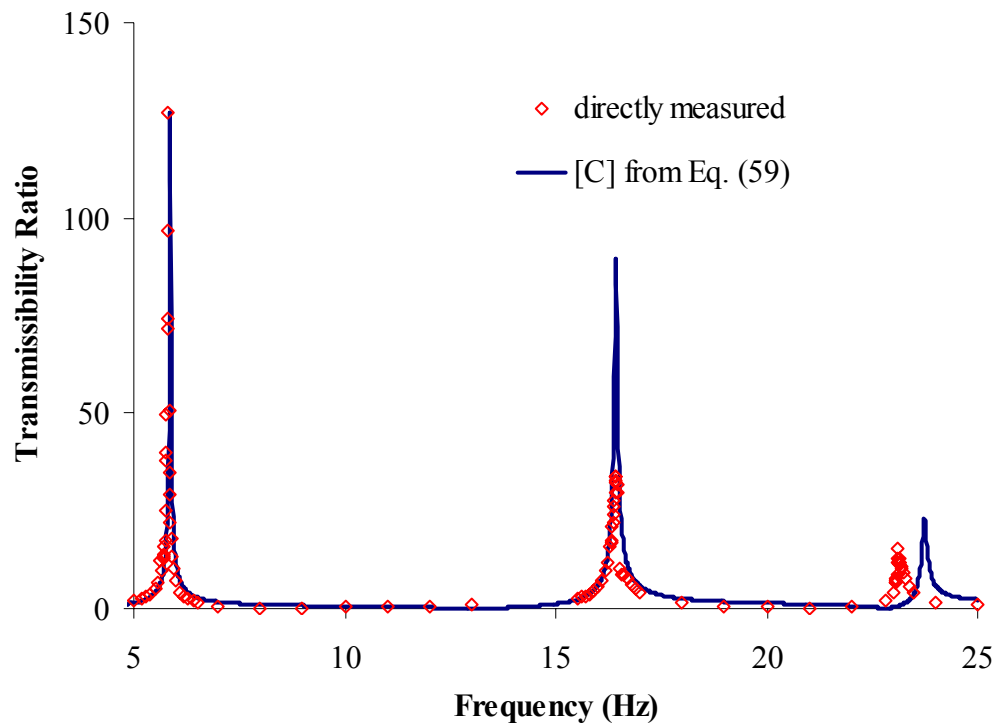


Figure 45 – Response at DOF 1, 3-DOF system

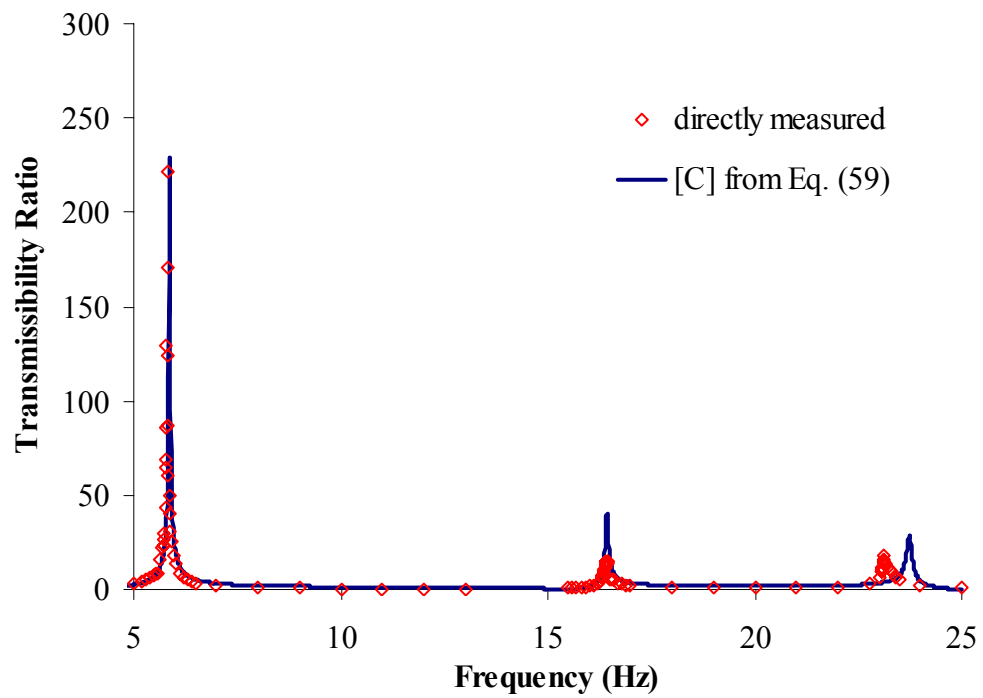


Figure 46 – Response at DOF 2, 3-DOF system

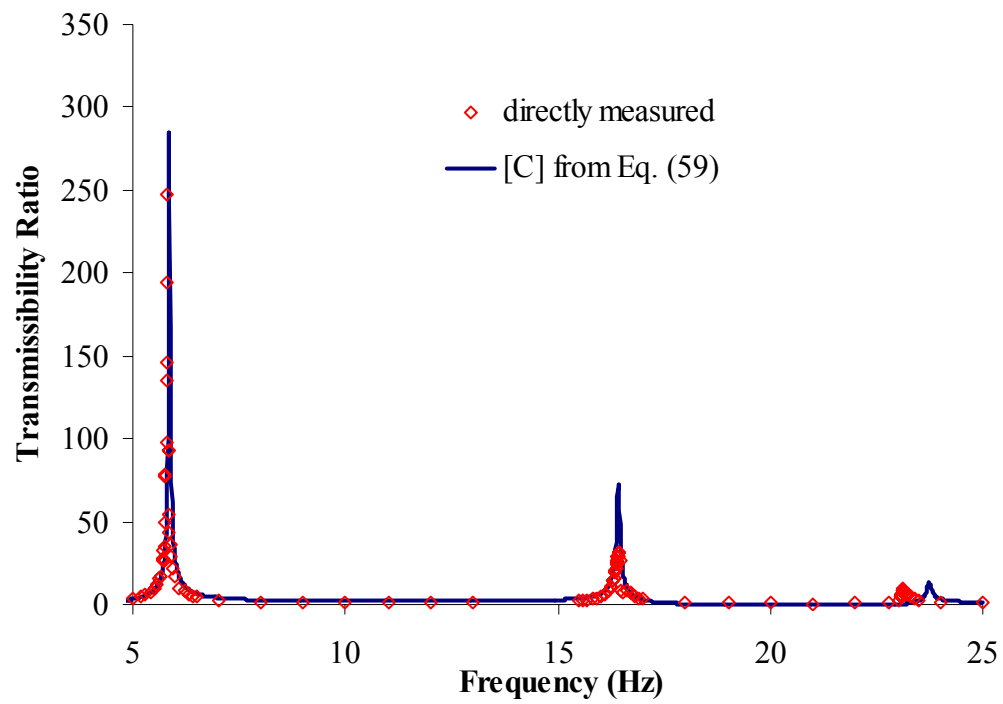


Figure 47 – Response at DOF 3, 3-DOF system

As with the earlier forms of the damping matrix, we can also compare the results for structures incorporating a discrete damper. The total damping matrix, shown in Equations (60) and (61), is a summation of the damping matrix of a structure and the damping matrix from the effect of the discrete damper. Figures 48 and 49 demonstrate the improved prediction for a 2-DOF structure incorporating a damper in the top floor. Results for a 3-DOF structure are shown in Figures 50 – 52.

$$[C] = \begin{bmatrix} c_1 + c_2 & -c_2 \\ -c_2 & 2c_2 \end{bmatrix} + \begin{bmatrix} c_D & -c_D \\ -c_D & c_D \end{bmatrix} \quad (60)$$

$$[C] = \begin{bmatrix} c_1 + c_2 & -c_2 & 0 \\ -c_2 & c_2 + c_3 & -c_3 \\ 0 & -c_3 & 2c_3 \end{bmatrix} + \begin{bmatrix} 0 & 0 & 0 \\ 0 & c_D & -c_D \\ 0 & -c_D & c_D \end{bmatrix} \quad (61)$$

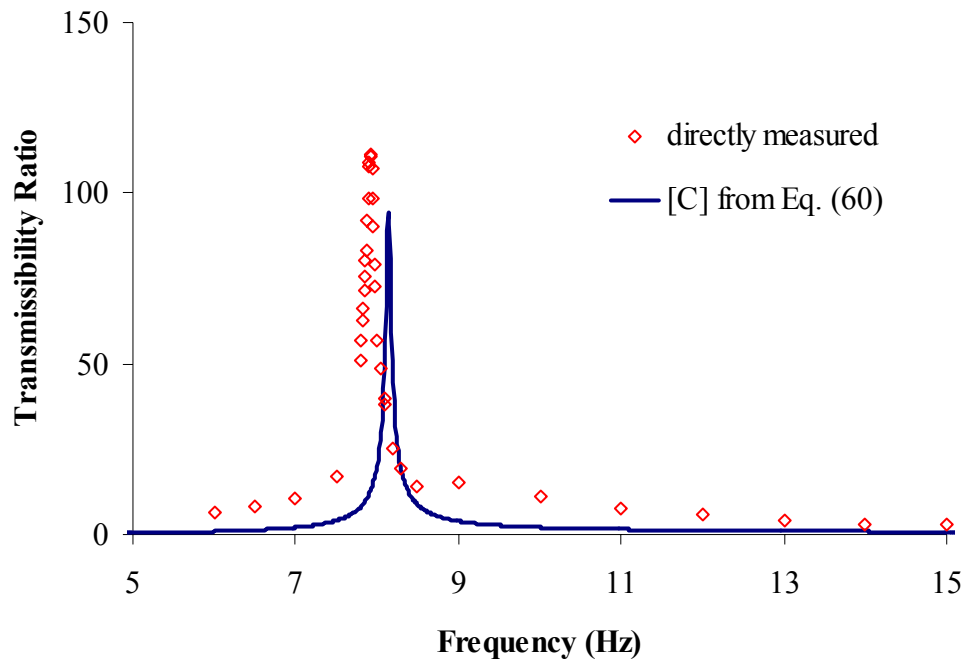


Figure 48 – Response at DOF 1, 2-DOF system with damper

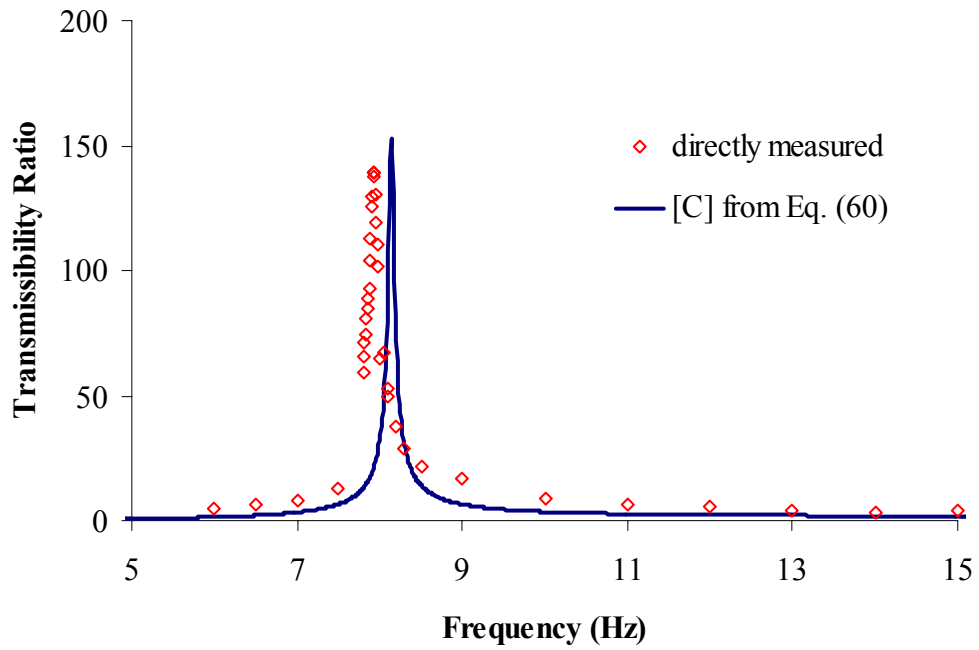


Figure 49 – Response at DOF 2, 2-DOF system with damper

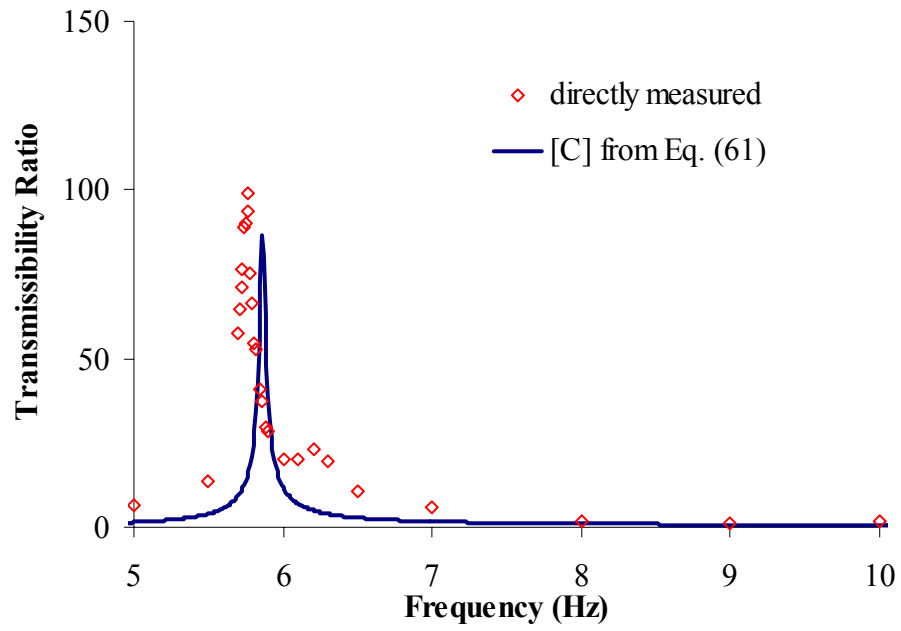


Figure 50 – Response at DOF 1, 3-DOF system with damper

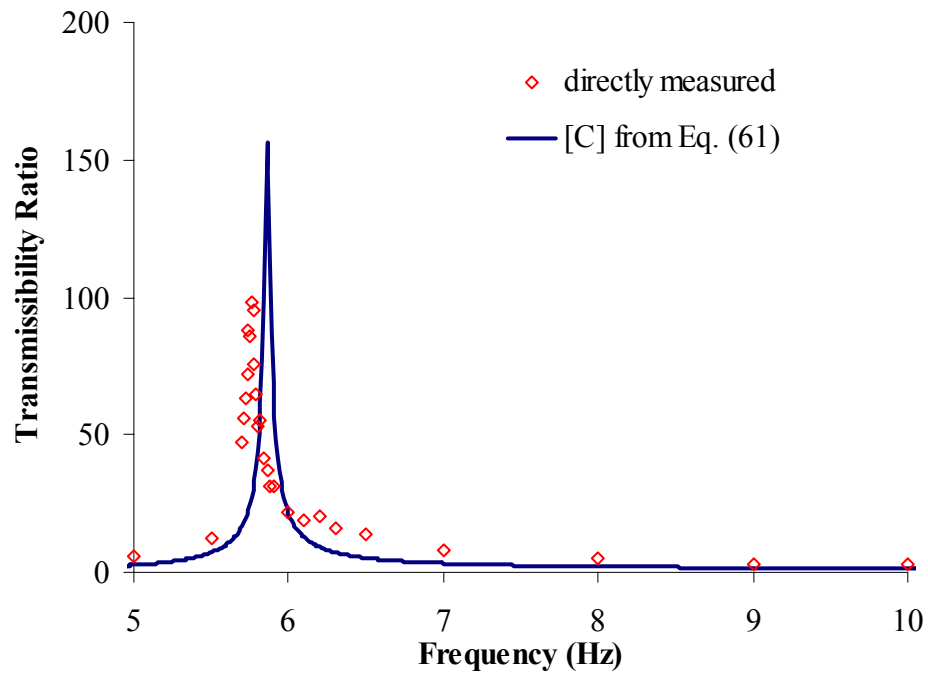


Figure 51 – Response at DOF 2, 3-DOF system with damper

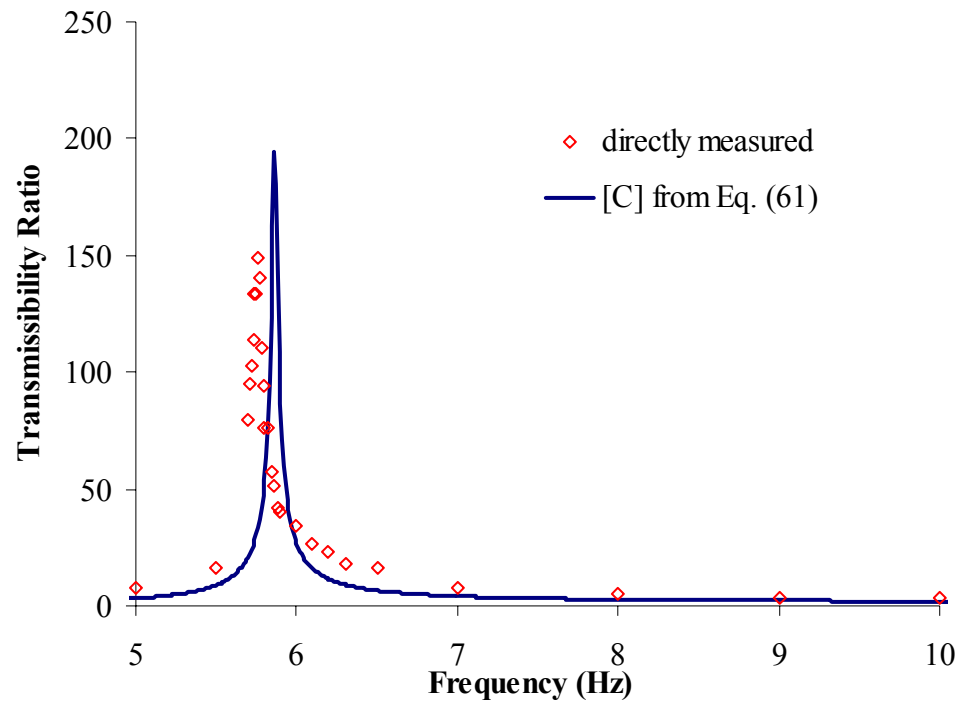


Figure 52 – Response at DOF 3, 3-DOF system with damper

2.4.5 Comparison of Results

Earlier figures have graphically demonstrated the differing performance of several forms of the damping matrix in modeling the transmissibility response of simple shear structures, with and without damping devices. As shown in the earlier figures, the damping matrix constructed with an additional dashpot from the top floor, presented in Section 2.4.4, most accurately models the experimental data from shear structures with and without dampers. We can quantify the performance of this damping matrix by comparing the experimental and analytical damping ratios for the first structural mode, which is presented in Table 1.

Table 1 – Comparison of modal damping ratios

Structure	DOF 1	DOF 2	DOF 3	[C] from Fig. 42
2-DOF	0.0035	0.0035	-----	0.0023
2-DOF w/ damper	0.0032	0.0042	-----	0.0038
3-DOF	0.0021	0.0022	0.0024	0.0021
3-DOF w/ damper	0.0027	0.0049	0.0040	0.0032

2.5 Conclusions and Future Work

The proposed study investigates inconsistencies in the formation of damping matrix for MDOF systems and proposes two new methods of formulating the damping matrix. The inconsistencies among various methods are illustrated analytically using numerical examples of simple representative two- and three- DOF systems. A simple laboratory test is developed to evaluate these inconsistencies experimentally. Results of experimental studies for single, two- DOF, and three- DOF systems illustrate that the current analytical methods give damping characteristics in MDOF systems that are very different from that evaluated experimentally. The large differences observed between experimental results and analytical

methods of creating damping matrices in MDOF system led to several new methods of formulating the damping matrix. The most accurate model of the damping matrix was constructed using an additional damping term from the top storey to the ground. The analytical results using this proposed damping matrix more accurately model the experimental data, both with and without a supplemental damper, than the other forms that were evaluated. Because the form of the damping matrix used in analytical modeling can have far-reaching implications in the earthquake response of structures, additional testing and verification is needed. Structures with a higher damping ratio will be tested to verify the accuracy of the proposed damping matrix.

2.6 Acknowledgements

We would like to thank the National Science Foundation Graduate Research Fellowship Program as well as the Civil Engineering Department at NC State University for their support and commitment to this research.

2.7 References

1. ASCE. *Seismic Analysis of Safety-Related Nuclear Structures and Commentary*. ASCE Standard 4-98. 1998.
2. Chopra, Anil K. *Dynamics of Structures*. New Jersey: Prentice Hall, 1995.
3. Gupta A, "Significance of Nonclassical Damping in Coupled System Analysis," *Proceedings of 15th International Conference on Structural Mechanics in Reactor Technology*, Vol. VIII, Seoul, South Korea, August 15-20, 1999.
4. Gupta A, Gupta AK. "Missing mass effect in coupled analysis I: complex modal properties." *Journal of Structural Engineering*, ASCE 1998; 124:490-495.
5. Soong TT, Dargush GF. *Passive Energy Dissipation Systems*. John Wiley and Sons, 1997.
6. Xu K, Igusa T. "Dynamic characteristics of non-classically damped structures." *Earthquake Engineering Structural Dynamics* 1991; 20:1127-1144.

Part III

Summary and Conclusions

3.1 Summary

While there are several methods of constructing the damping matrix for a structure, it is shown that these methods have inconsistencies in their formulations. For a system made of identical SDOF structures, assembly of the damping matrix yields a proportional, or classically damped system. However, it was shown that the modal damping ratios for both a 2-DOF and 3-DOF structure are much different from the damping ratio of an individual storey. If the 2-DOF structure is instead composed of a slightly different stiffness in one storey, the damping becomes non-proportional, meaning there are off-diagonal terms in $[\bar{c}]$. However, it can be seen that the response of the structure is the same whether the off-diagonal terms are included or neglected. This is not the case for a non-classically damped primary-secondary system where the masses and damping ratios between the stories are much different. For such a system, we have shown that neglecting the off-diagonal terms leads to significant errors in the response of the secondary system. If we consider Rayleigh damping, in which the damping matrix is proportional, reliable information about two modal damping ratios is required to construct the matrix. And as previously shown, using a damping ratio from SDOF testing may not be appropriate. Using modal superposition, we can use modal damping ratios to create a damping matrix that is proportional. However, specific knowledge of damping ratios in all important structural modes is required for this method.

To evaluate some of these inconsistencies and the validity of currently-used damping matrix formulations, simple shake table experiments were performed. Several shear model structures with and without supplemental dampers were tested in forced vibration to develop

transmissibility curves. The directly measured results were compared with results using several different forms of the damping matrix.

- **Currently-used assembly of the damping matrix.** The damping matrix is constructed in a similar manner to the stiffness matrix.
- **Damping matrix from exact shape functions for a beam.** The damping matrix is constructed by using the exact shape functions for a beam.
- **Damping matrix that is diagonal.** The damping matrix is assembled as a series of dashpots from each storey to the ground, with no dashpots interacting between the floors.
- **Damping matrix using additional dashpots.** The damping matrix is constructed similarly to the stiffness matrix, but additional dashpots are attached from each floor to the ground.
- **Damping matrix using an additional dashpot from the top storey only.** The damping matrix is constructed as it was originally, but with an additional dashpot from the top storey to the ground.

3.2 Conclusions

From the analytical discussion of the damping matrix, it is clear that inconsistencies and limitations exist. Experimental testing of simple shear model structures has shown that the currently-used assembly of the damping matrix does not accurately predict the response of the structure. The first mode damping ratio is significantly lower than experimentally observed, both with and without supplemental dampers. Other forms of the damping matrix also did not provide an accurate representation of the experimental data. However, the form of the damping matrix which incorporates an additional dashpot from the top storey gives an accurate model of the experimental data. Both with and without a damper, this damping matrix predicted the structure's response at each DOF.

3.3 Future Work

There are several extensions to this research and areas for future research that would be useful in gaining a better understanding of the damping matrix.

- **Construct structures with higher damping.** The simple shear models used in these experiments have very light damping, which makes measuring modal peak responses difficult. Higher damping in the structure would lower the peak responses and make experimental measurements easier and more accurate.
- **Add damping devices to a larger structure.** A larger structure incorporating a damping device would help to eliminate any effects of scale on the results. Using a larger structure would allow for a damping device with higher capacity and more consistent properties.
- **Incorporate free vibration testing.** Free vibration testing would provide an additional method to validate the various forms of the damping matrix. Multiple-DOF systems could be tested, but the initial conditions of the free vibration would need to be known or estimated.
- **Evaluate proposed damping matrix in earthquake response.** The earthquake response of a simple structure could be compared to the predicted response from the forms of the damping matrix considered earlier.

APPENDIX

A.1 Laboratory Experiments

Simple laboratory experiments were conducted to experimentally investigate the frequency-domain behavior of simple shear building models. To better understand the formation of damping matrix, we developed and conducted shake table experiments. The experiments were designed to be simple and repeatable analyses of the motion of shear building models. Each structure consisted of thin aluminum columns and heavy steel girders. For shear-building behavior, rotation of the floor girders was eliminated by making them much stiffer than the columns. As shown in the figures, end caps were used to create rigid connections so that the columns could not rotate. Multiple storied models consisted of identical stories stacked on top of one another. Accelerometers were mounted at each storey to measure the acceleration response. Simple harmonic motion was used as input excitation into the shake table. Steady-state responses were measured to determine transmissibility ratio plots.

The model structures were tested on both a force-controlled and a displacement-controlled shake table. The force-controlled shake table, shown in Figure A1, is driven by an electromagnetic shaker with no feedback system. The storey accelerations are recorded by a data acquisition system on a locally mounted computer station. The displacement-controlled shake table, shown in Figure A2, is driven by a hydraulic actuator that responds to displacement input. The storey accelerations are filtered through a series of analog signal filters before getting to the computer data acquisition system.

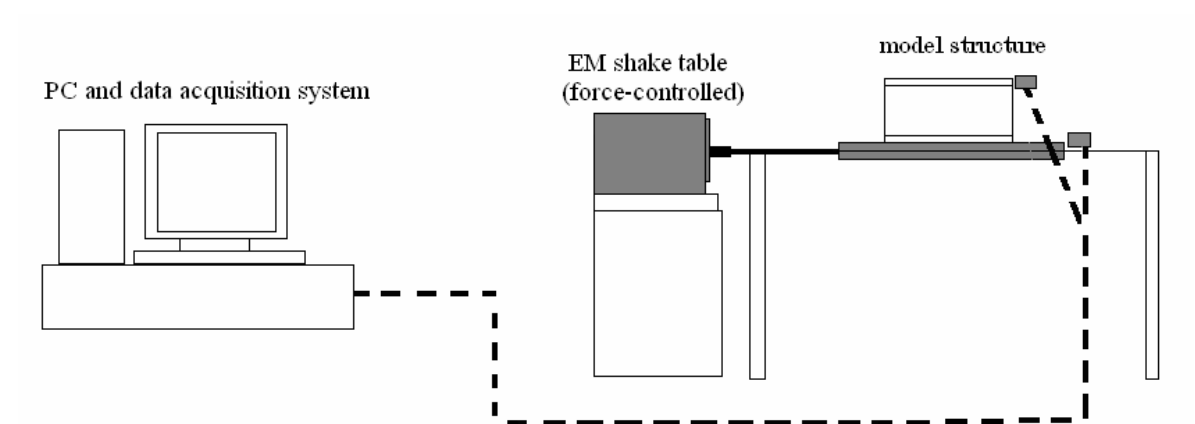


Figure A1 - Experimental setup of force-controlled shake table

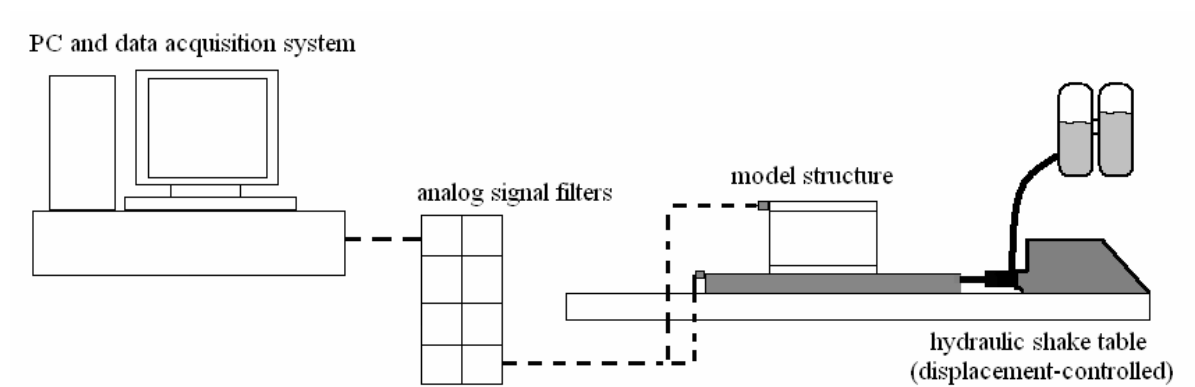


Figure A2 - Experimental setup of displacement-controlled shake table

A.2 Shear Structure Experiments – Force Controlled Shake Table

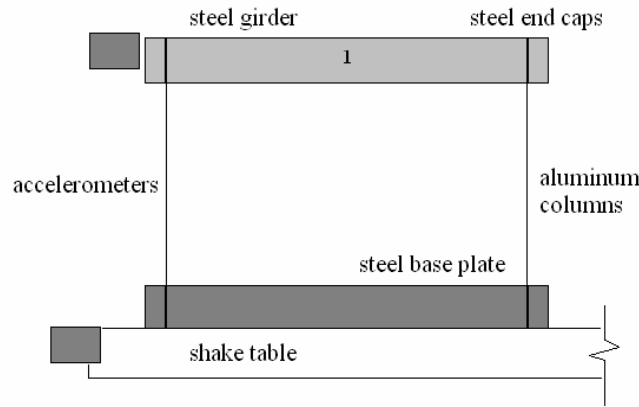


Figure A3 - SDOF shear model structure

As a first step, several single storey shear building models were tested in order to determine the natural frequency and damping ratio associated with each storey individually. The natural frequencies were calculated by making physical measurements on the column dimensions for calculating stiffness and on girder for weight. Columns were 1" wide and 1/16" thick. The length of the columns considering the centerline to centerline distance between the girders was 5.25". The clear distance of the columns between the girders was 4.5". The storey stiffness could be calculated using both lengths, using Equation (A1), and then averaged, yielding an estimated stiffness of 46.3 lb/in . Each column had a mass of 0.0001085 $lb \cdot s^2/in$ and the mass of the girder was 0.005887 $lb \cdot s^2/in$. Using Equation (A2), the single degree-of-freedom natural frequency was found to be 14.0 Hz.

$$k = \frac{24EI}{L^3} \quad (A1)$$

$$\omega = \frac{1}{2\pi} \sqrt{\frac{k}{m}} \quad (A2)$$

Both free vibration and forced harmonic vibration tests were performed using the force-controlled shake table to experimentally determine the natural frequency and damping ratio of the structure. The free vibration acceleration time histories, like that shown in Figure A4, were used in MS-Excel solver to evaluate these parameters. Damping ratios were also calculated using logarithmic decrement. The various methods reproduced the values for frequencies and damping ratios consistently in each single degree of freedom structure (individual storey).

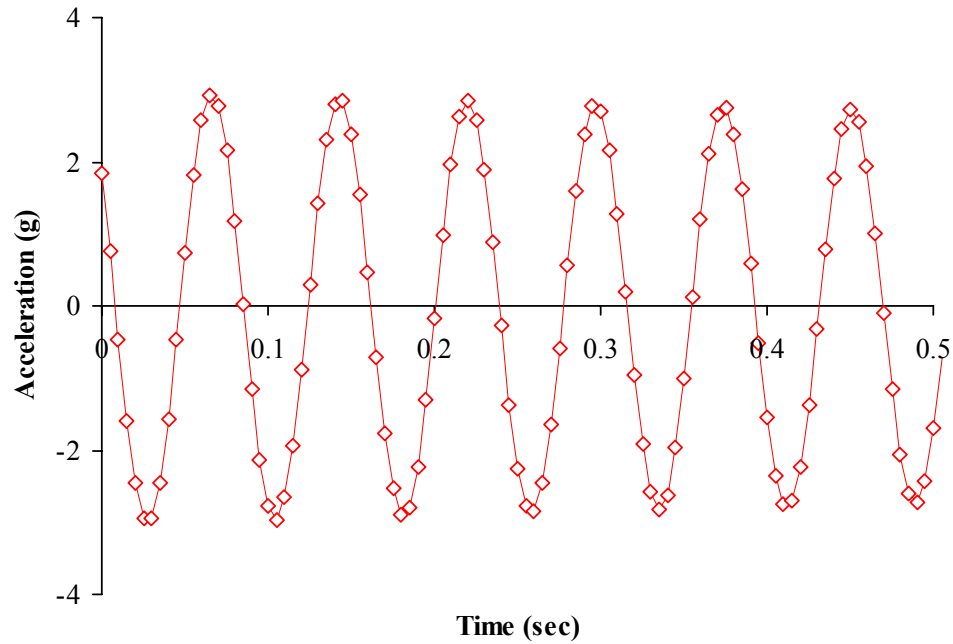


Figure A4 –SDOF shear structure free vibration response

For forced harmonic excitation, a series of tests was run near the resonant frequency of the single-storey structure to develop a transmissibility ratio curve directly using the measured amplitudes of total acceleration at the girder level and at the base (shake table). A plot of transmissibility ratio versus forcing frequency is shown in Figure A5. The natural frequency and damping ratios were then calculated by using the following closed-form equation for

transmissibility ratio in MS-Excel solver. Table A1 compares the experimental results for determining the structure's natural frequency and damping ratio.

$$\frac{\ddot{u}}{\ddot{u}_{g0}} = \frac{\sqrt{1 + (2\xi\beta)^2}}{\sqrt{(1 - \beta^2)^2 + (2\xi\beta)^2}} \quad (\text{A3})$$

$$\beta = \frac{\Omega}{\omega} \quad (\text{A4})$$

Table A1 - Summary of SDOF shear structure properties

	Free vibration	Forced vibration	Logarithmic decrement
Natural Frequency (Hz)	13.00	13.17	12.90
Damping Ratio	0.002668	0.001263	0.002025

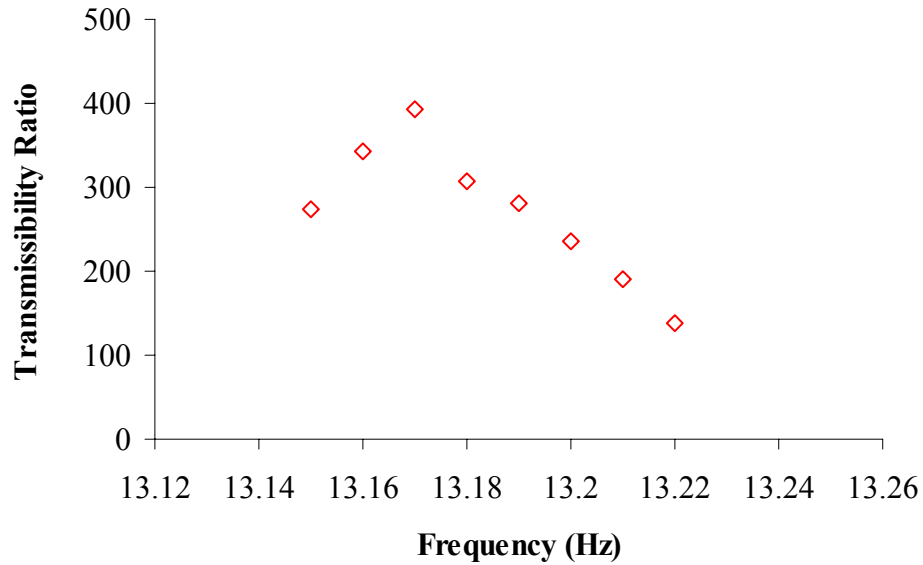


Figure A5 –SDOF shear structure forced vibration response

As stated earlier, single storey testing was utilized to establish properties of the system for multiple degree-of-freedom structures. Although testing revealed differences in natural

frequency and damping ratio between each storey, the differences were considered negligible for the purposes of this study. Because the physical system properties were necessary for analytical modeling and prediction, the storey stiffness was determined using the storey mass and experimental natural frequency. For the structure, Table A2 lists the properties that were used for subsequent analytical modeling of the identical-storied structures.

Table A2 - Summary of SDOF properties used for modeling

Storey mass ($lb \cdot s^2/in$)	0.00600
Natural frequency (Hz)	13.17
Storey stiffness (lb/in)	41.1
Damping ratio	0.001263

A two storey structure composed of identical SDOF systems was constructed and tested in the frequency domain. The setup for the 2-DOF model structure is shown in Figure A6.

Transmissibility ratios were directly measured at various frequencies of shake table excitation, with more concentrated measurements taking place near the structural modes.

Plots of transmissibility ratio versus forcing frequency are shown for each degree of freedom in Figures A7 and A8.

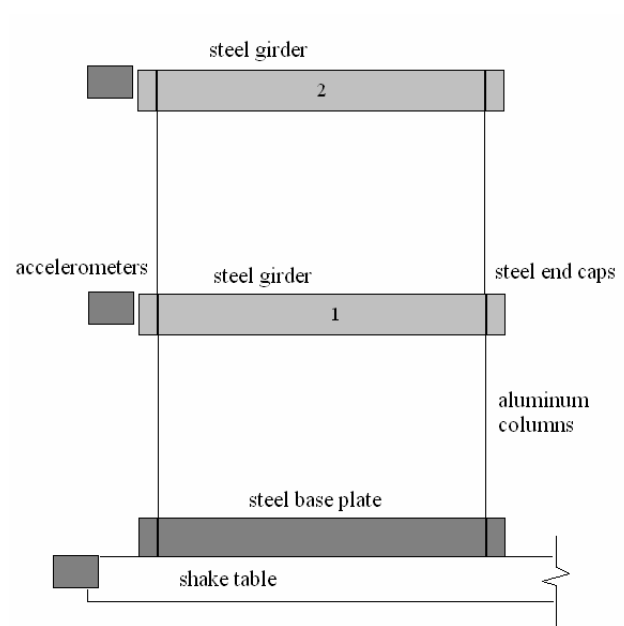


Figure A6 – 2DOF shear model structure

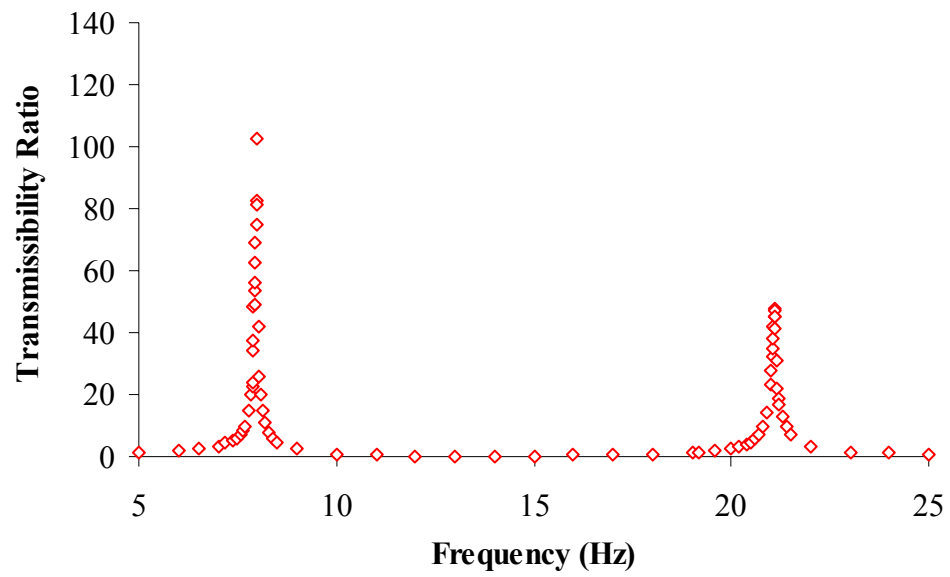


Figure A7 – Response at DOF 1 2-DOF system

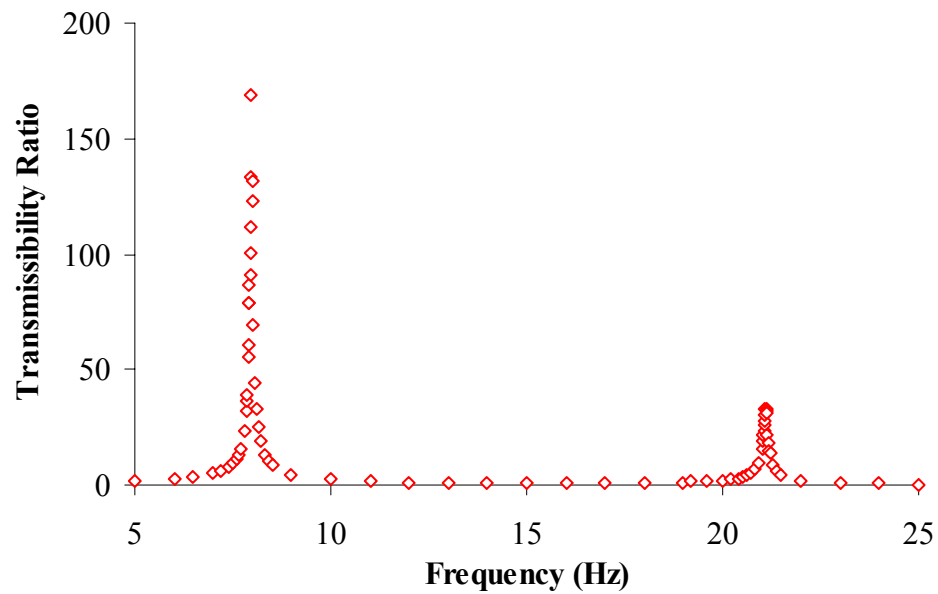


Figure A8 – Response at DOF 2, 2-DOF system

The three storey structure shown in Figure A9 was also tested in the frequency domain. Similar to the 2-DOF structure, measurements were taken more closely near the structural modes to accurately capture the resonant behavior of the system. The transmissibility response of the structure at each DOF is shown in Figures A10 - A12.

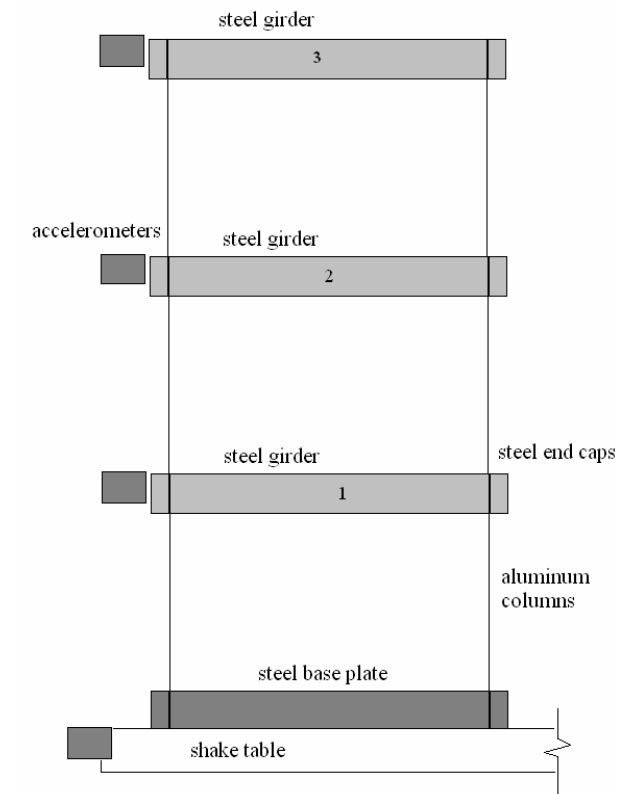


Figure A9 –3DOF shear model structure

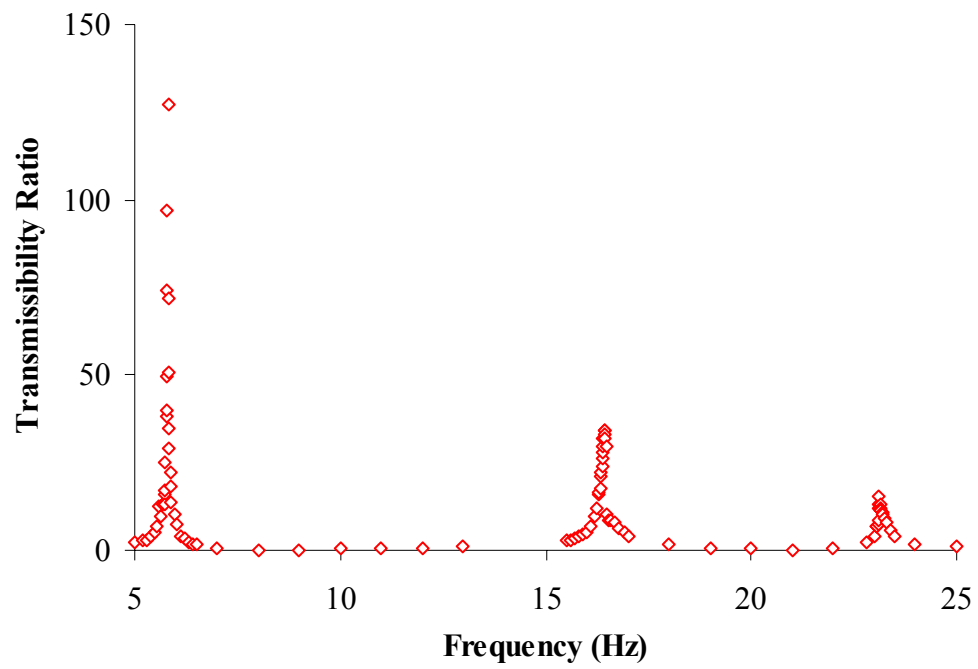


Figure A10 – Response at DOF 1 3DOF system

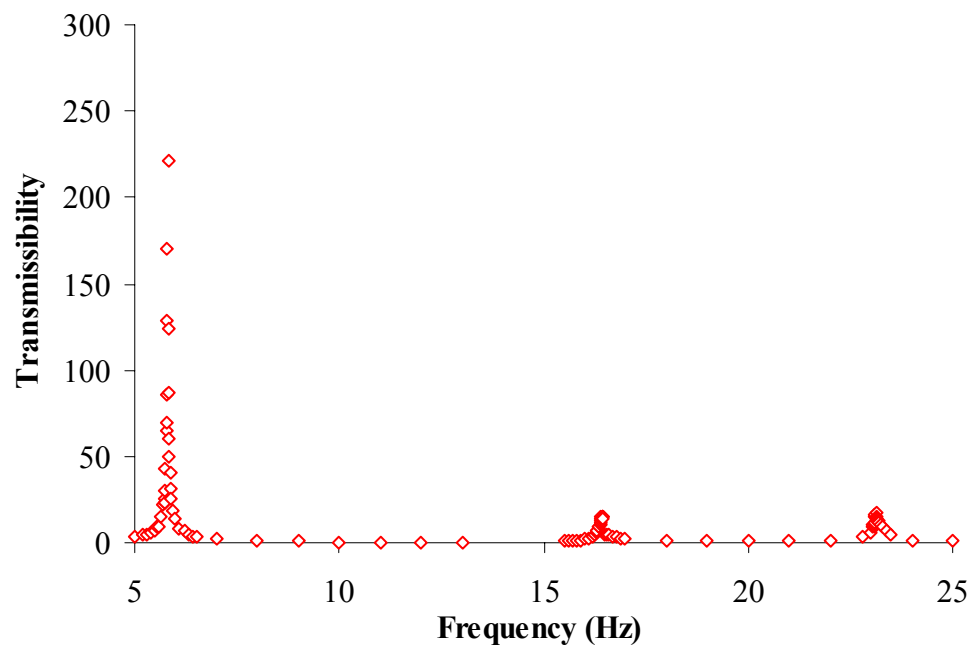


Figure A11 – Response at DOF 2, 3-DOF system

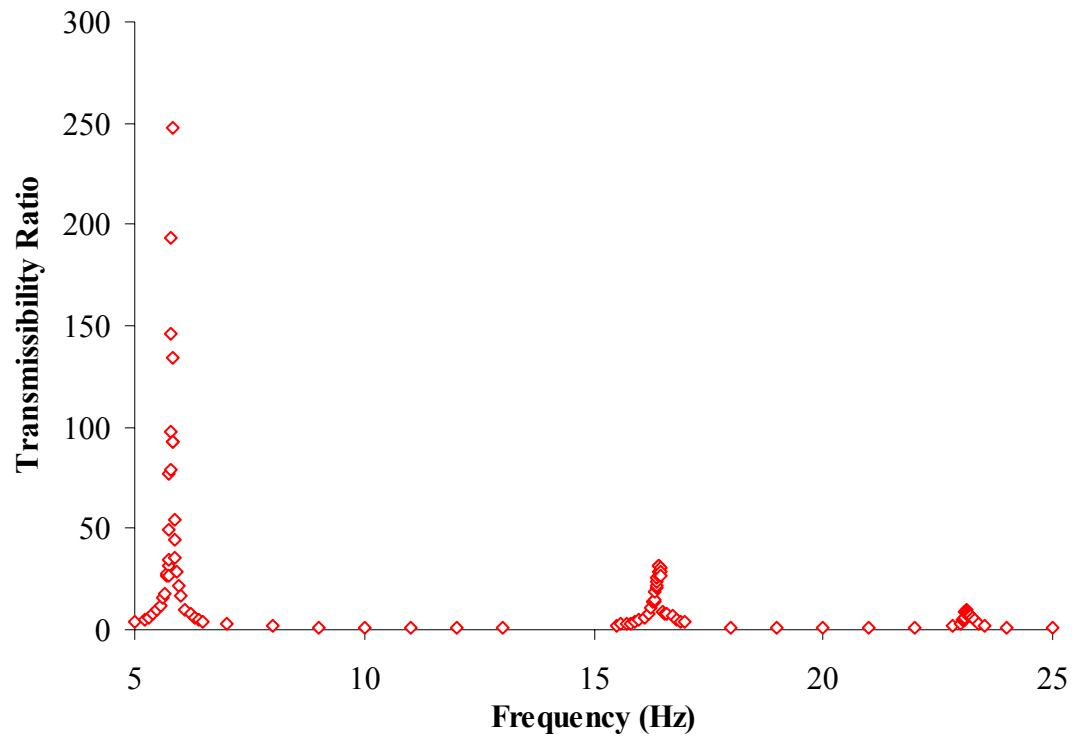


Figure A12 – Response at DOF 3, 3-DOF system

A.3 Structure with Damper Experiments – Force Controlled Shake Table

A.3.1 Damper properties

The current rise in the use of supplemental damping devices makes the understanding of the damping matrix even more important. For complex analysis of critical structures that employ these emerging technologies, an accurate knowledge of the structure's damping matrix is essential before including any supplemental devices. To examine the effects of adding supplemental damping to a structure, we elected to use a simple shock absorber to act as a damping device in the shear models. The shock absorber, originally intended for use in remote-controlled automobiles, is shown in Figure A14. The overall extended length of the device is 4" inches, and the stroke length is 1.25". The device is oil-filled and incorporates interchangeable flow caps to vary the resistance of the plunger.

Including supplemental dampers was essential to the study for two reasons. Firstly, experimental results with dampers would verify the necessity of having an accurate damping matrix for the structure before including the devices. Secondly, the additional damping provided by the device would lower the peak resonant responses of the system, making experimental verification more accurate.

To equip the structure with a damping device, adjustable supports were created so that the damper could be attached in a horizontal position in line with the structure. The supports were positioned to give adequate stroke for the damper in the positive and negative direction. Static tests of the structure were conducted to ensure that the damper did not add any

appreciable stiffness. Hung vertically, weights were imposed and the displacement of the structure was measured. The plots of displacement versus load, both with and without damper, are plotted in Figure A15. It is clear that the damper does not provide any additional stiffness to the system.

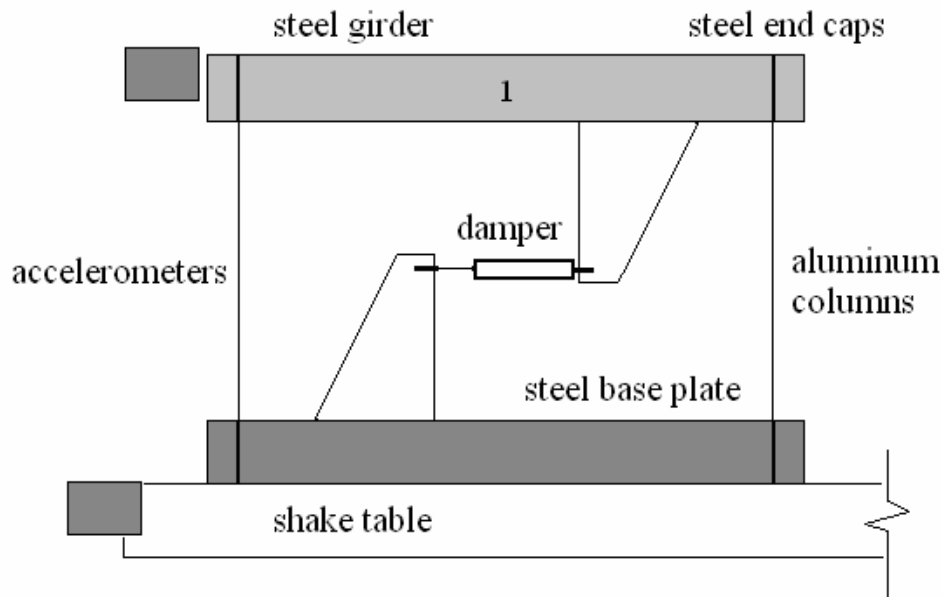


Figure A13 - SDOF shear model structure with damper

To determine the properties of the damping device, single degree-of-freedom free and forced vibration tests were performed. Free vibration test data confirmed that the damping provided by the device is approximately linear in nature. Data from logarithmic decrement is presented in Table A3, demonstrating that the measured damping ratios between successive peaks in the response are nearly identical. Forced vibration testing was also performed to determine the natural frequency and damping ratio of the structure incorporating the damper. Successive forced vibration tests were conducted to demonstrate the consistency of the

results. Although the damping ratio varied slightly from test to test, Figures A17 and A18 show the consistency in peak responses exhibited by one test to the next.



Figure A14 - Simple passive damping device

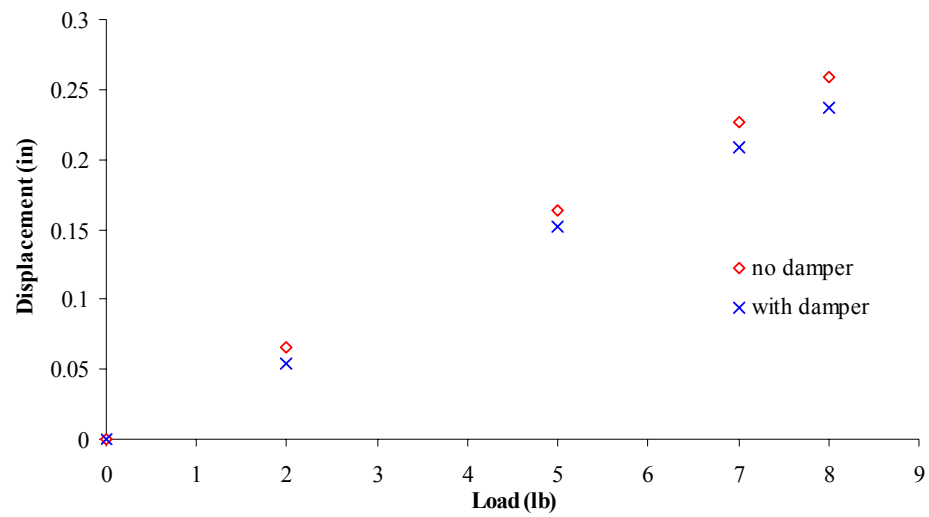


Figure A15 - Load versus displacement comparison for stiffness evaluation

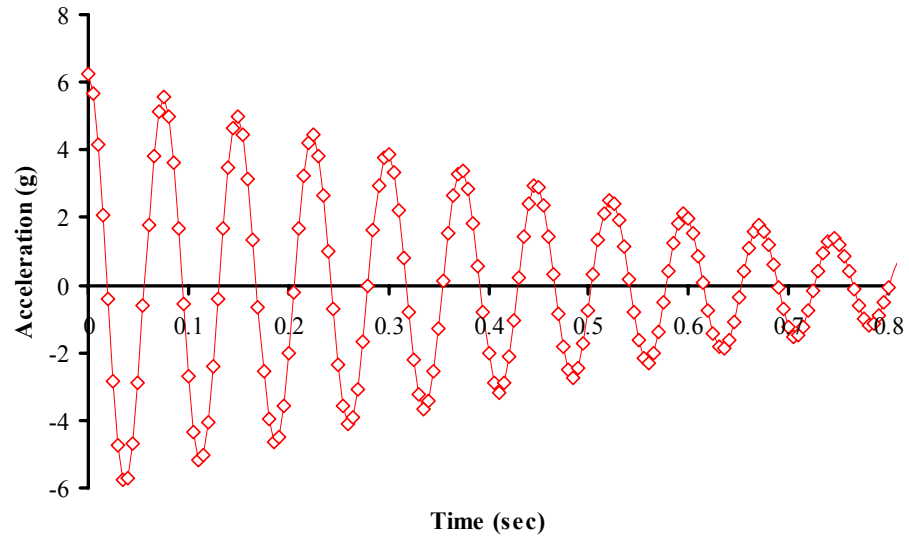


Figure A16 – SDOF shear structure with damper, free vibration response

Table A3 - Damping ratios from log decrement

Peak Response	Measured Damping Ratio
1 – 2	0.01751
2 – 3	0.01733
3 – 4	0.01963
4 – 5	0.02119

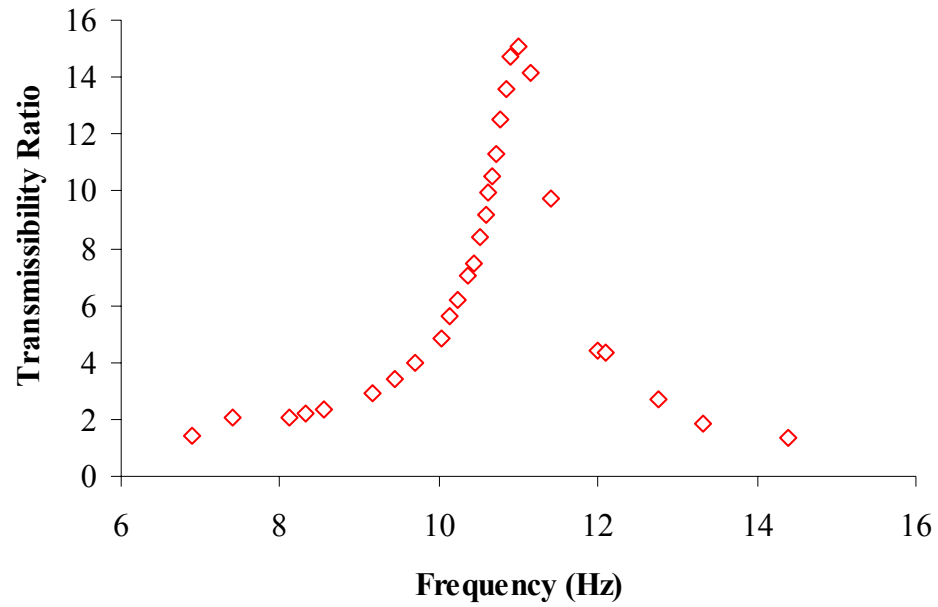


Figure A17 – SDOF shear structure with damper, forced vibration test 1 response

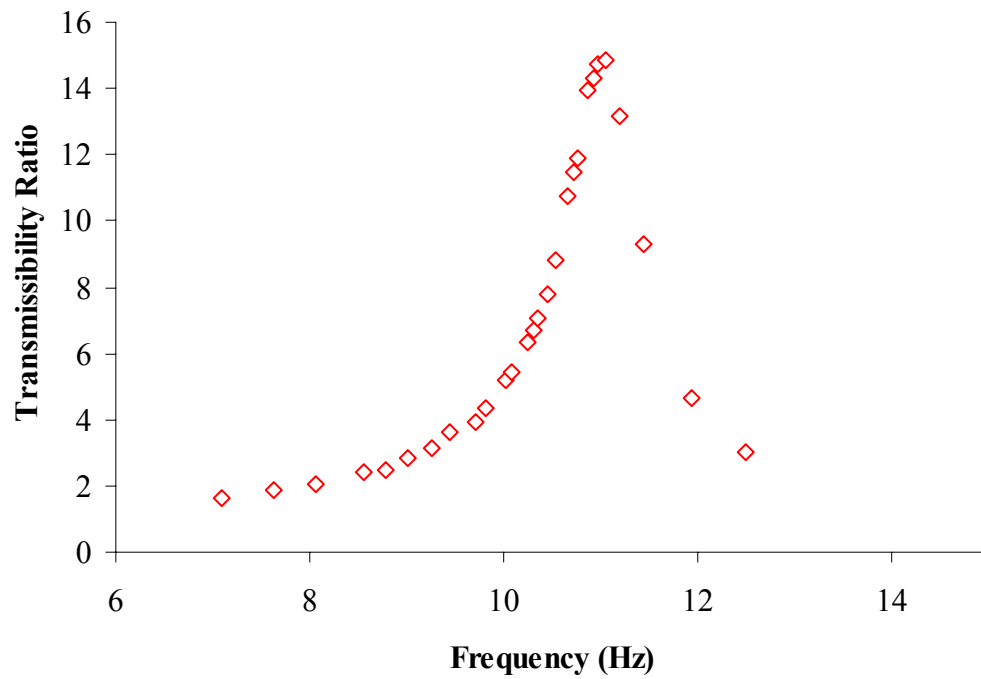


Figure A18 - SDOF shear structure with damper, forced vibration test 2 response

Before testing multiple degree-of-freedom structures incorporating a damper, the single storey structure was tested using the methods described for the structure without the damper. Transmissibility data from forced vibration testing of the SDOF structure is provided in Figure A20. To accurately determine the damping ratio for the structure with the supplemental device, a series of 5 consecutive forced vibration tests were performed. For the SDOF system, forced vibration testing showed that the average damping ratio of the system was 0.02912. This damping ratio still includes the effect of damping from the structure itself. Therefore, to include the effect of the damping device in analytical models of the structure, this difference was accounted for. For analytical modeling of the system, the properties listed in Table A4 were used.

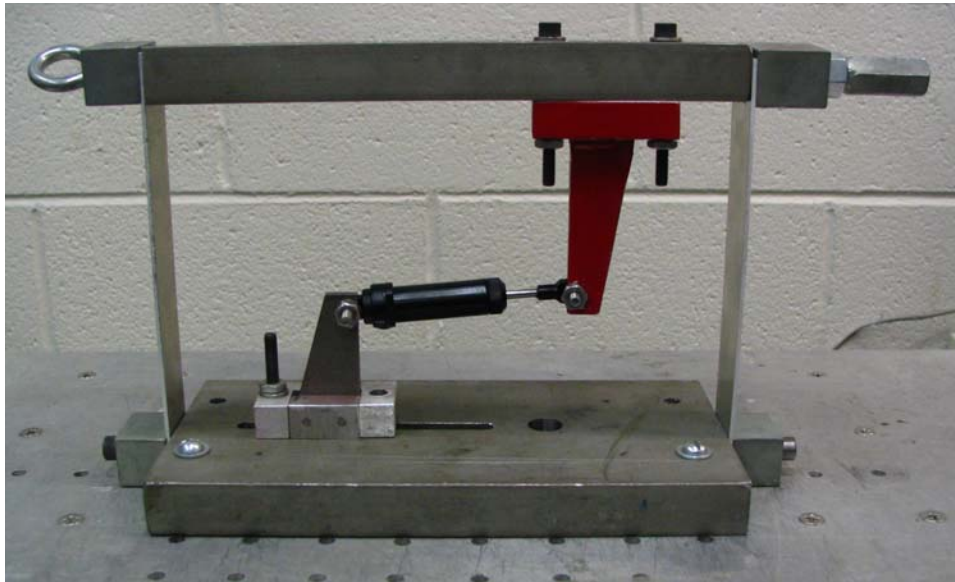


Figure A19 - SDOF shear model structure with damper

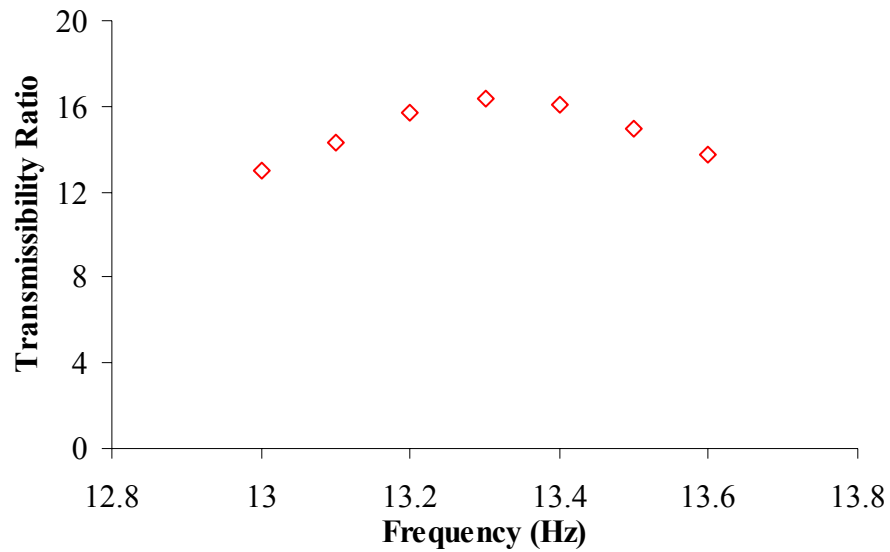


Figure A20 – SDOF shear structure with damper, forced vibration response

Table A4 – SDOF shear structure with damper, properties used for modeling

Storey mass ($lb \cdot s^2/in$)	0.00600
Storey stiffness (lb/in)	41.1
Damping ratio	0.02912

A 2-DOF structure incorporating a damper in the top floor, shown in Figure A21, was tested in forced vibration to evaluate its response. The testing was conducted similarly to the original structure in order to accurately measure the resonant behavior of the system. The presence of the damper significantly lowered the modal peaks, which became especially noticeable for the second structural mode. The data shown in Figures A22 and A23 show the structure's frequency domain response.

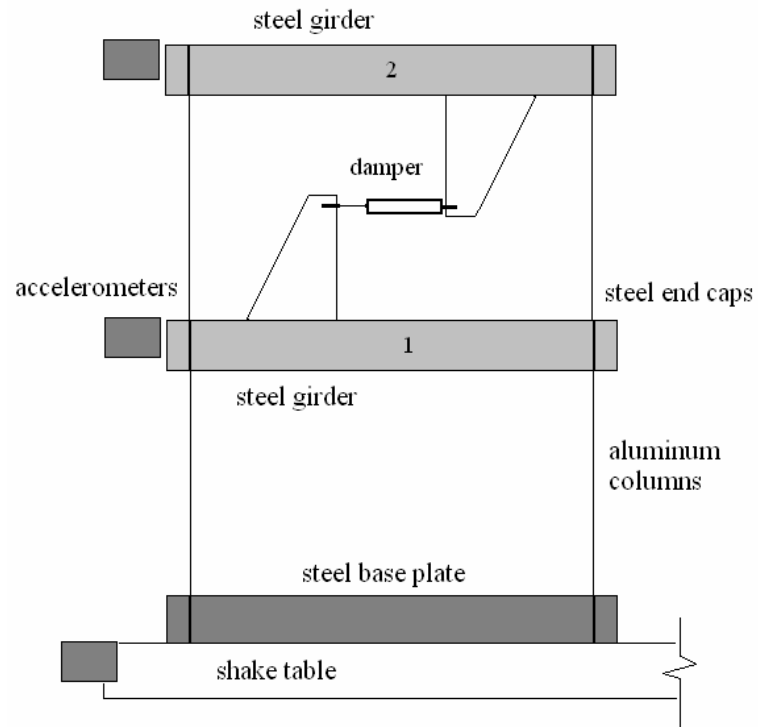


Figure A21 - 2DOF shear model structure with damper

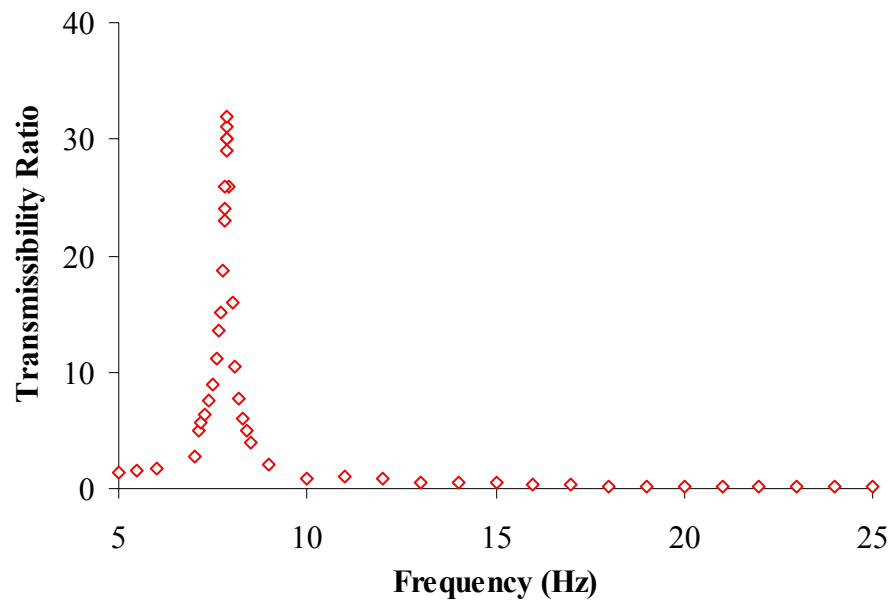


Figure A22 - Response at DOF 1, 2-DOF system with damper

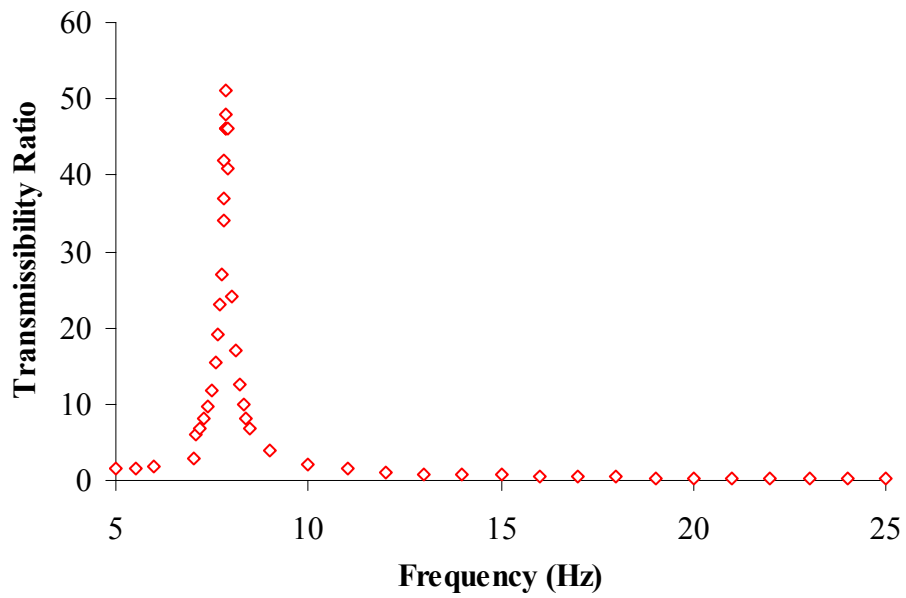


Figure A23 - Response at DOF 2, 2-DOF system with damper

A 3-DOF structure incorporating the damping device, shown in Figure A24, was constructed and tested in forced vibration. The transmissibility response of the structure at each DOF is shown in Figures A25 – A27. As with the 2-DOF system, higher structural modes were difficult to excite experimentally due to the presence of the damper. Therefore the plots of the frequency domain response of the system focus on the first mode response.

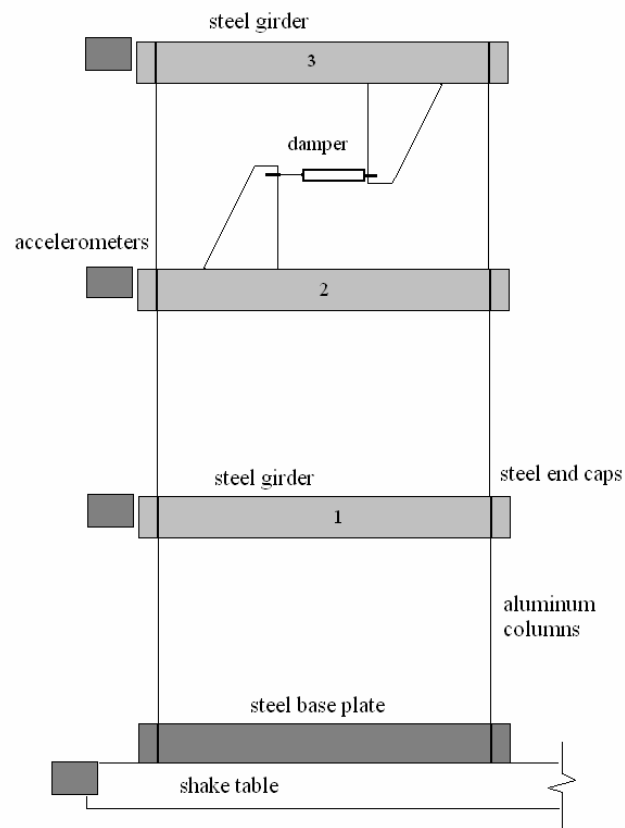


Figure A24 - 3DOF shear model structure with damper

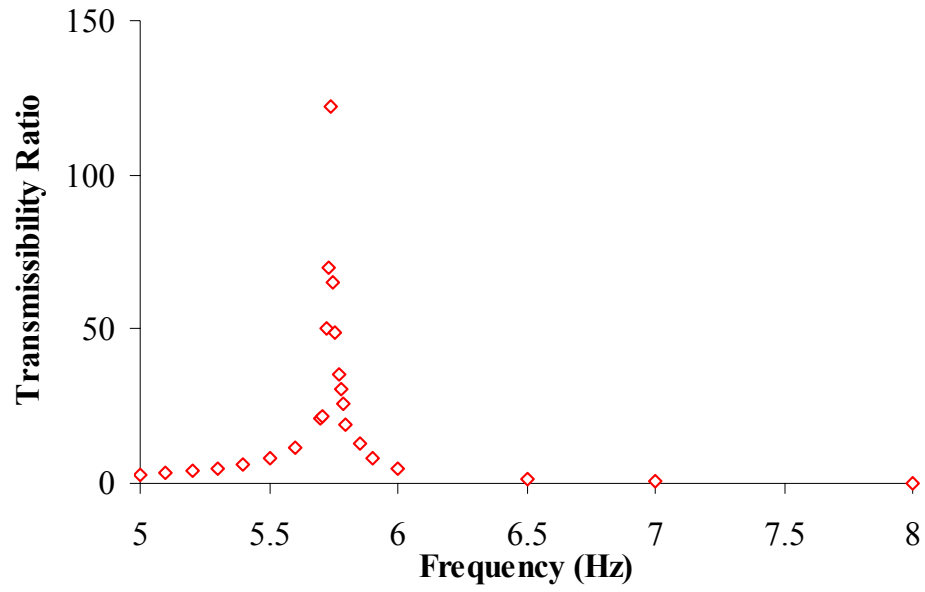


Figure A25 - Response at DOF 1, 3-DOF system with damper

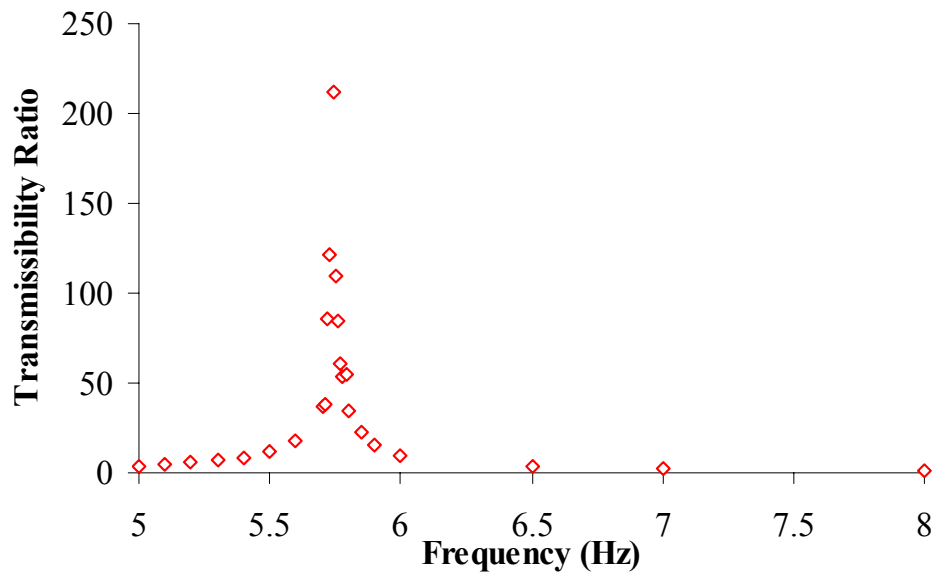


Figure A26 - Response at DOF 2, 3-DOF system with damper

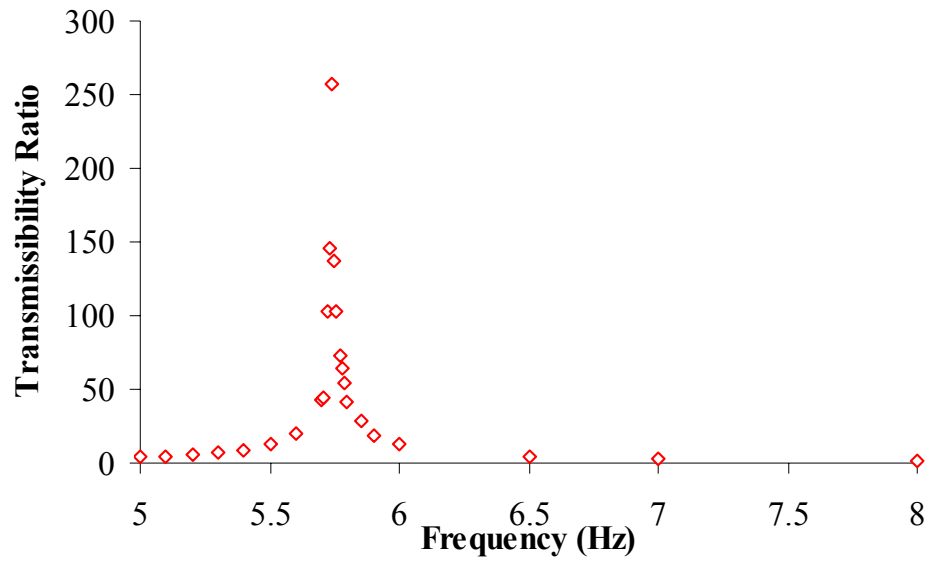


Figure A27 - Response at DOF 3, 3-DOF system with damper

A.4 Structure with Damper Experiments – Displacement Controlled Shake Table

To confirm the behavior of the multiple degree-of-freedom systems, additional testing was performed on a larger displacement-controlled device. The displacement-controlled shake table has a displacement feedback control system. The data collection system also incorporates analog signal filters to provide clearer signal from the accelerometers.

The simple shear models tested previously were tested in the same manner on the new shake table. First, SDOF testing was performed both with and without the damper to determine the structural properties of the system. The SDOF system tested with the damper is shown in Figure A28. Forced vibration test data for the structure is provided in Figure A29, and Table A5 gives the system properties with the damper in place. Once again, two forced vibration tests were performed with the damper to ensure consistent results.

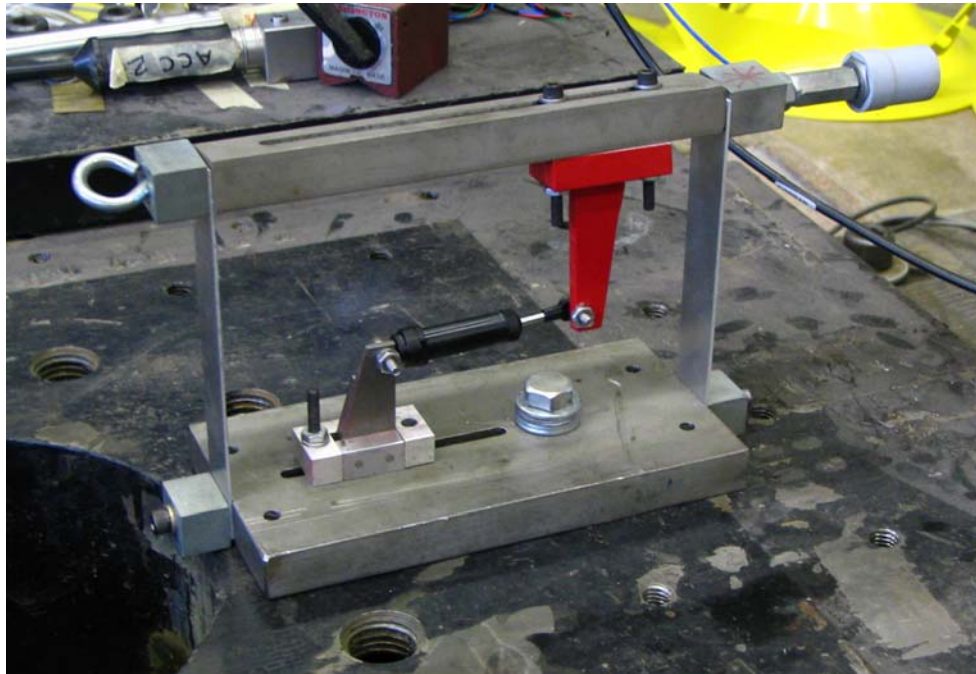


Figure A28 – SDOF shear structure with damper on displacement-controlled shake table

Table A5 – SDOF shear structure with damper, properties used for modeling

Storey mass ($lb \cdot s^2/in$)	0.00600
Storey stiffness (lb/in)	41.1
Damping ratio with damper	0.004763
Damping ratio without damper	0.001866

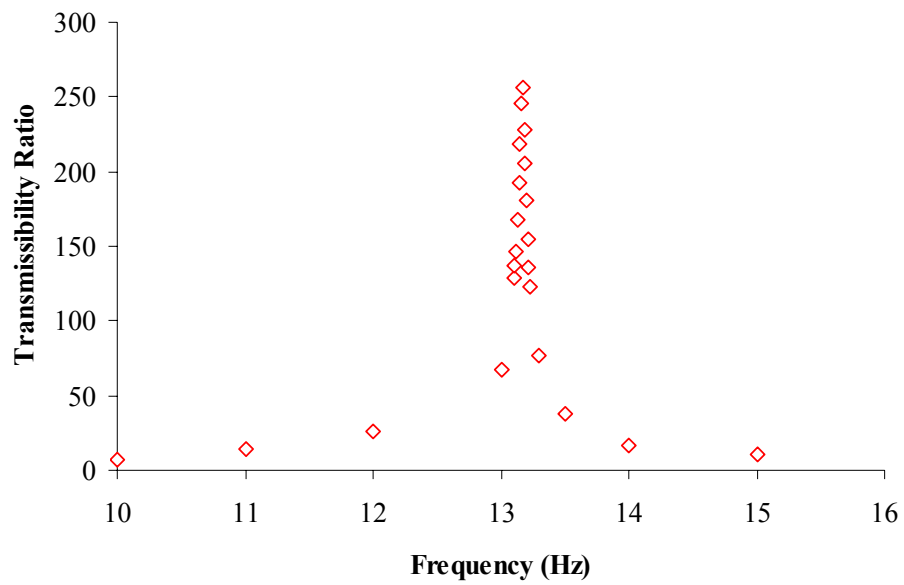


Figure A29 – SDOF shear structure, forced vibration response

A 2-DOF structure with the damper placed in the top floor was then tested in forced vibration. The setup of the structure was identical to previous testing and is shown in Figure A21. Due to the nature of the shake table, higher frequency testing was limited and therefore could not fully capture the second structural vibration mode. The plots of transmissibility ratio at each DOF are given in Figures A30 and A31.

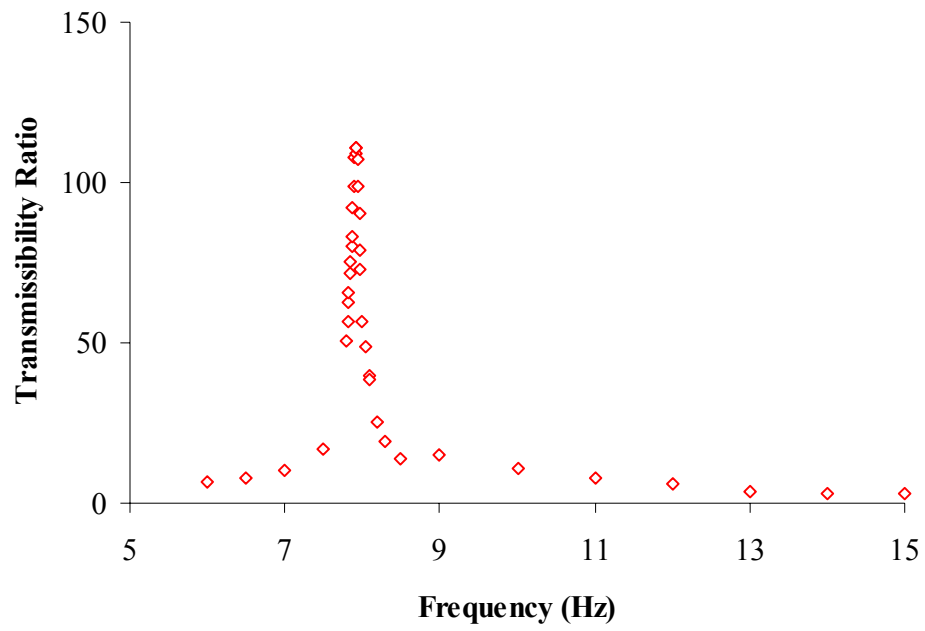


Figure A30 - Response at DOF 1, 2-DOF system with damper

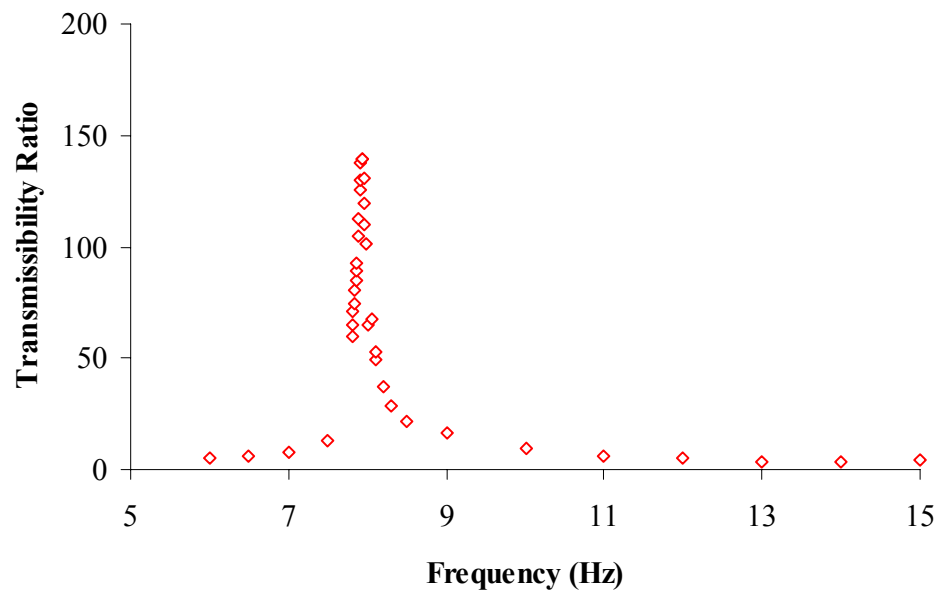


Figure A31 - Response at DOF 2, 2-DOF system with damper

A 3-DOF structure incorporating the damping device, shown in Figure A24, was constructed and tested in forced vibration. The transmissibility response of the structure at each DOF is shown in Figures A32 – A34. As with the 2-DOF system, higher structural modes were difficult to excite experimentally due to the presence of the damper. Therefore the plots of the frequency domain response of the system focus on the first mode response.

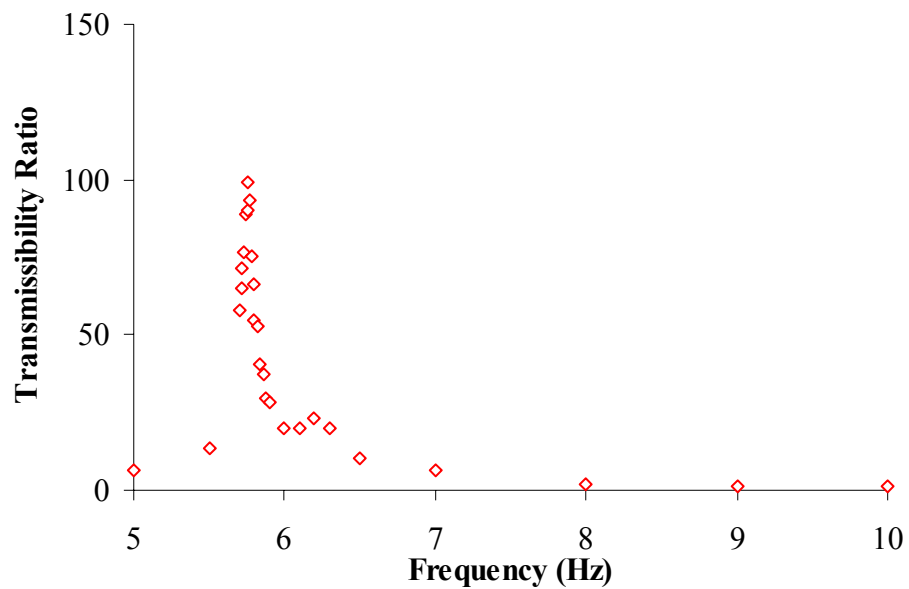


Figure A32 - Response at DOF 1, 3-DOF system with damper

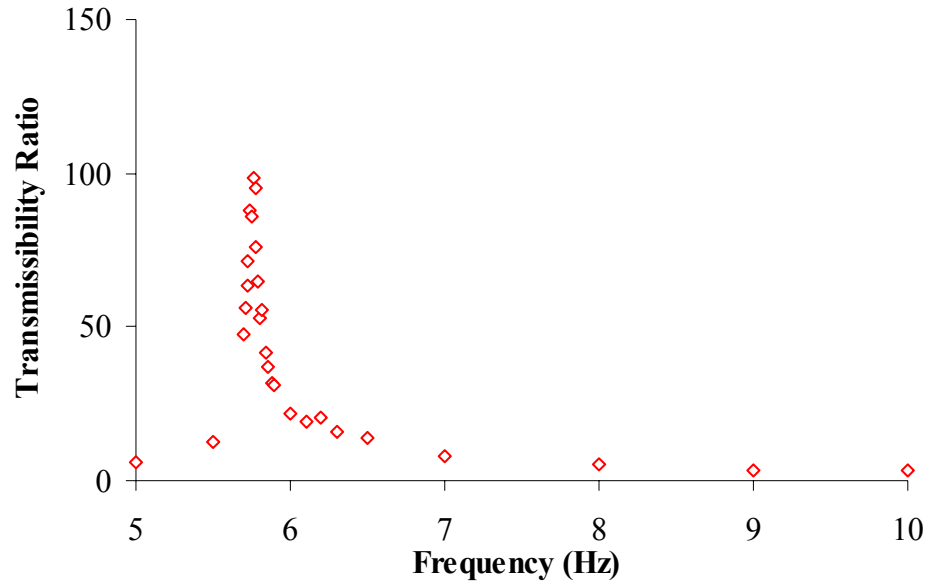


Figure A33 - Response at DOF 2, 3-DOF system with damper

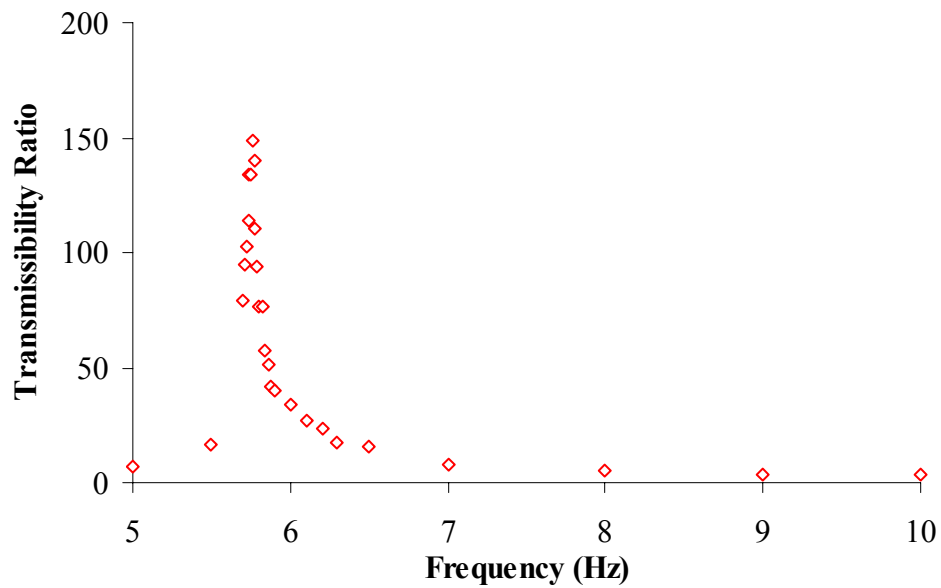


Figure A34 - Response at DOF 3, 3-DOF system with damper

A.5 Structure with Damper Experiments (II) – Displacement Controlled Shake Table

A second full set of tests for the structures with a damping device were performed on the displacement-controlled shake table to confirm the earlier results. As before, SDOF testing was performed both with and without the damper to determine the structural properties of the system. Forced vibration test data for the structure is provided in Figure A35, and Table A6 gives the system properties with the damper in place. Again, two forced vibration tests were performed with the damper to ensure consistent results.

Table A6 – SDOF shear structure with damper, properties used for modeling

Storey mass ($lb \cdot s^2/in$)	0.00600
Storey stiffness (lb/in)	44.5
Damping ratio with damper	0.005639
Damping ratio without damper	0.001187

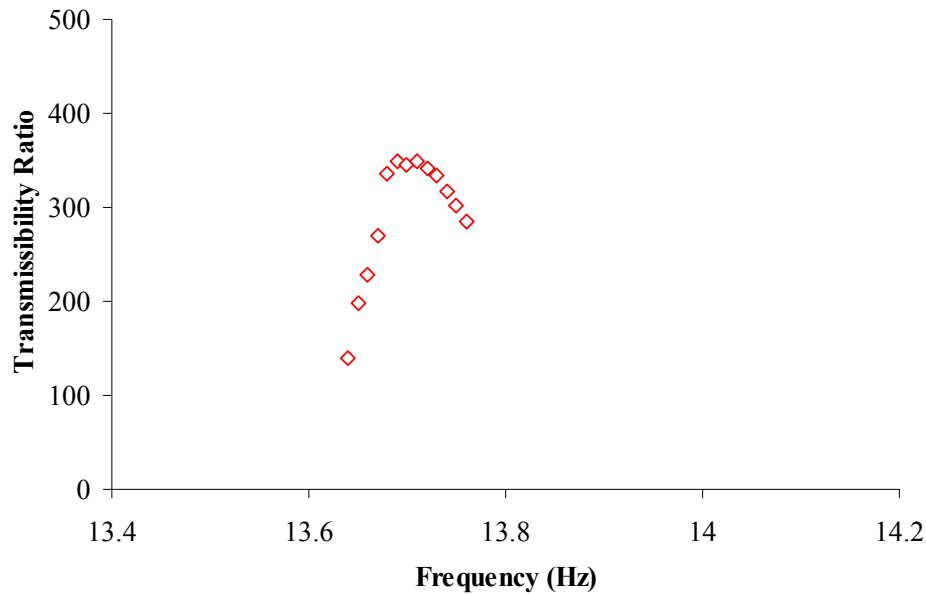


Figure A35 – SDOF shear structure with damper, forced vibration response

A 2-DOF structure with the damper placed in the top floor was then tested in forced vibration. The setup of the structure was identical to previous testing and is shown in Figure A21. Due to the nature of the shake table, higher frequency testing was limited and therefore could not fully capture the second structural vibration mode. The plots of transmissibility ratio at each DOF are given in Figures A36 and A37.

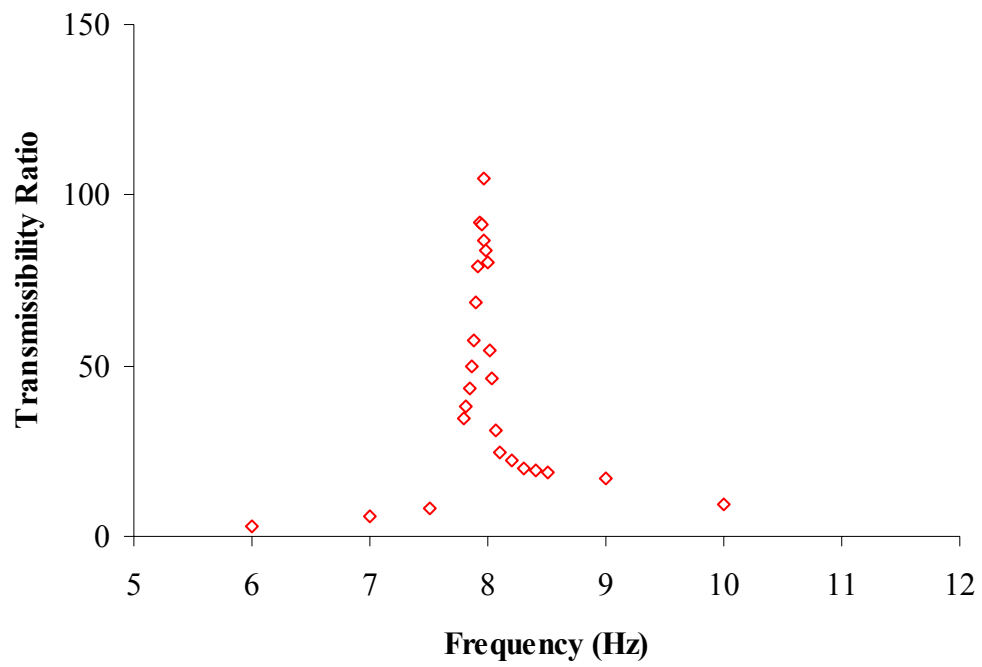


Figure A36 - Response at DOF 1, 2-DOF system with damper

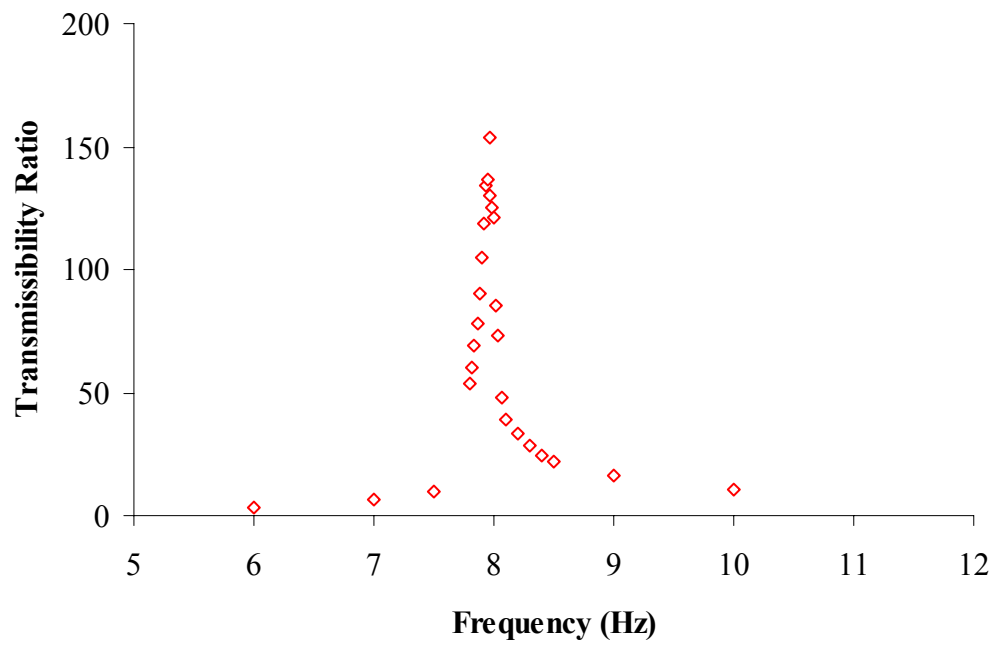


Figure A37 - Response at DOF 2, 2-DOF system with damper

A 3-DOF structure incorporating the damping device was also retested in force vibration.

The transmissibility response of the structure at each DOF is shown in Figures A38 – A40.

As with previous structures incorporating a damper, higher structural modes were difficult to excite experimentally due to the presence of the damper. Therefore the plots of the frequency domain response of the system focus on the first mode response.

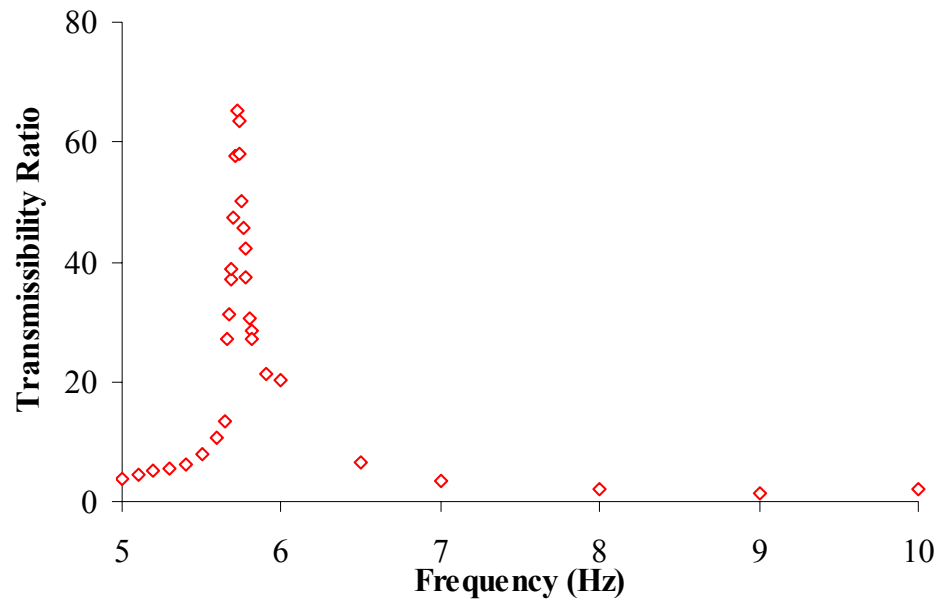


Figure A38 - Response at DOF 1, 3-DOF system with damper

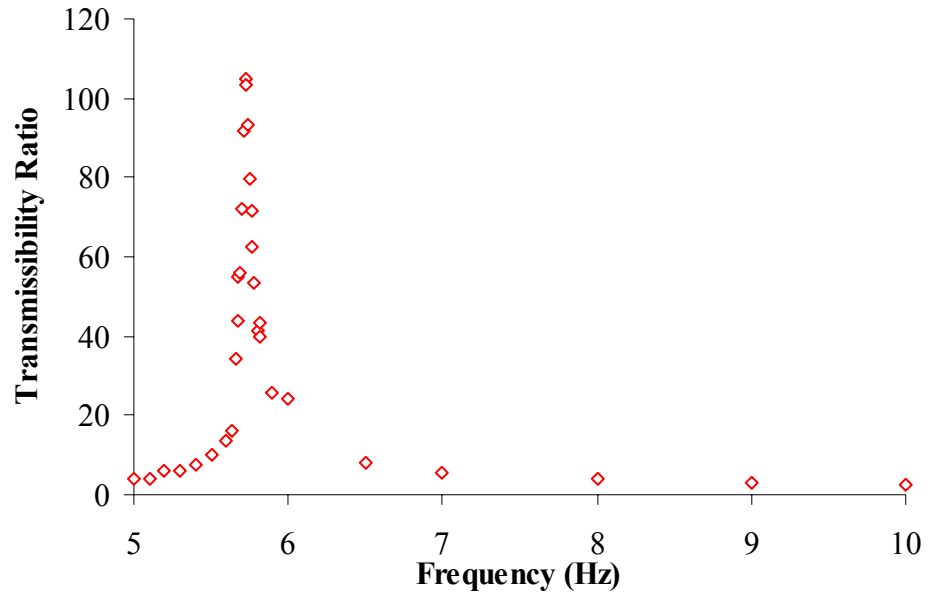


Figure A39 - Response at DOF 2, 3-DOF system with damper

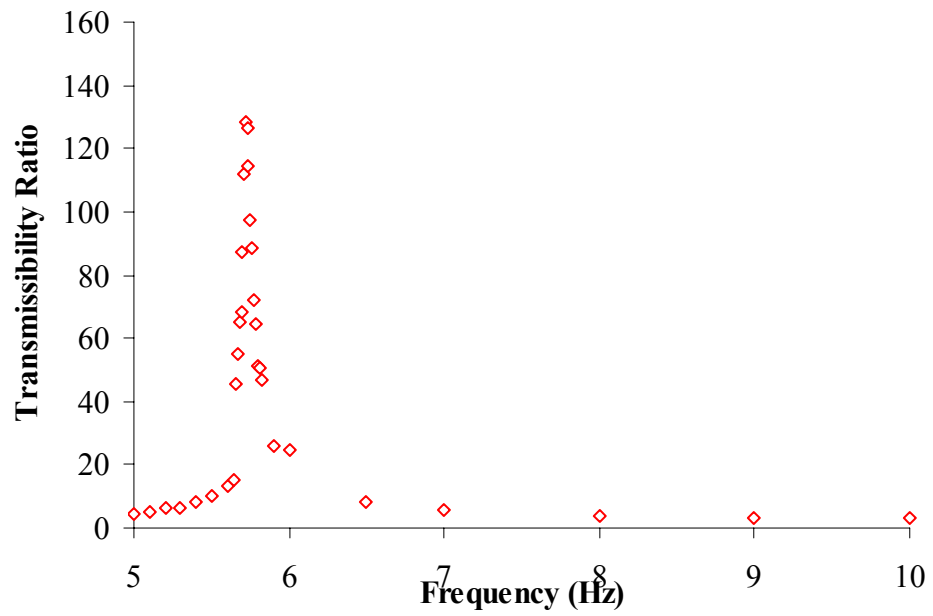


Figure A40 - Response at DOF 3, 3-DOF system with damper

The results from a second test of the structures incorporating a damping device are very similar to the original test. Because of the very light damping of the structure, the results for the SDOF structure without a damper are difficult to reproduce exactly. However, it is clear that the responses for the MDOF structures match very well with the previous tests of the structure.

A.6 Larger Structure– Displacement Controlled Shake Table

To further investigate the damping matrix for structures, a larger structure was tested on the displacement-controlled shake table. The structure was designed as a simple shear model, but on a larger scale. The steel girders were three times the width as previous girders. Thicker aluminum columns were used, and they were lengthened to retain a similar range of natural frequency. The steel end caps were attached to the structure with two large screws in order to generate enough capacity to prevent rotation of the columns.

Columns were 3” wide and 1/8” thick. The length of the columns considering the centerline to centerline distance between the girders was 12”. The clear distance of the columns between the girders was 11.25”. The storey stiffness could be calculated using both lengths and then averaged, yielding an estimated stiffness of 79.6 lb/in . Each column had a mass of $0.001176 \text{ lb} \cdot \text{s}^2/\text{in}$ and the mass of the girder was $0.02427 \text{ lb} \cdot \text{s}^2/\text{in}$. Based on the mass and stiffness, the single degree-of-freedom natural frequency was estimated to be 8.90 Hz.

The new structure is shown in Figure A41. SDOF testing was performed similarly to earlier structures to determine the properties of the structure. A plot of transmissibility ratio for forced vibration testing is shown in Figure A42, and free vibration response is plotted in Figure A43. The measured properties of the structure are compared in Table A7. Values used for subsequent analysis of the structure are given in Table A8.

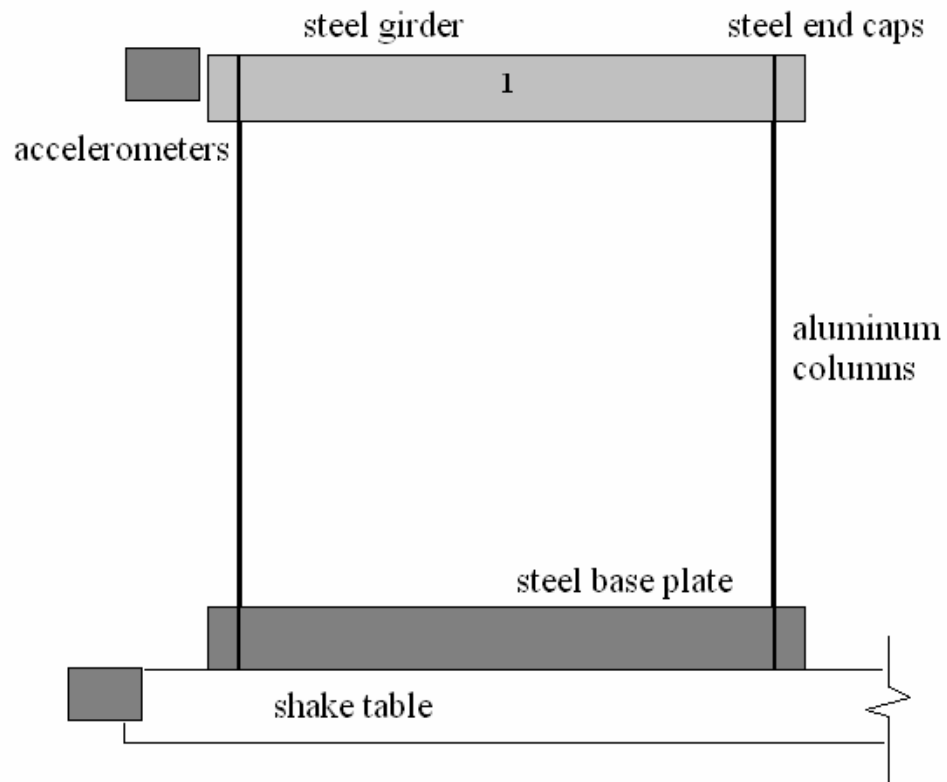


Figure A41 – Larger SDOF shear model structure

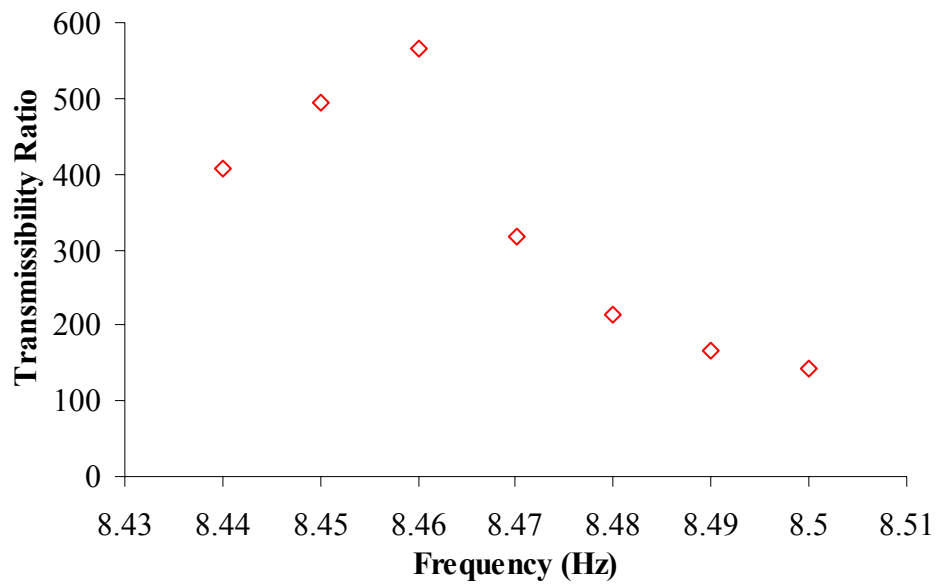


Figure A42 – Larger SDOF shear structure, forced vibration response

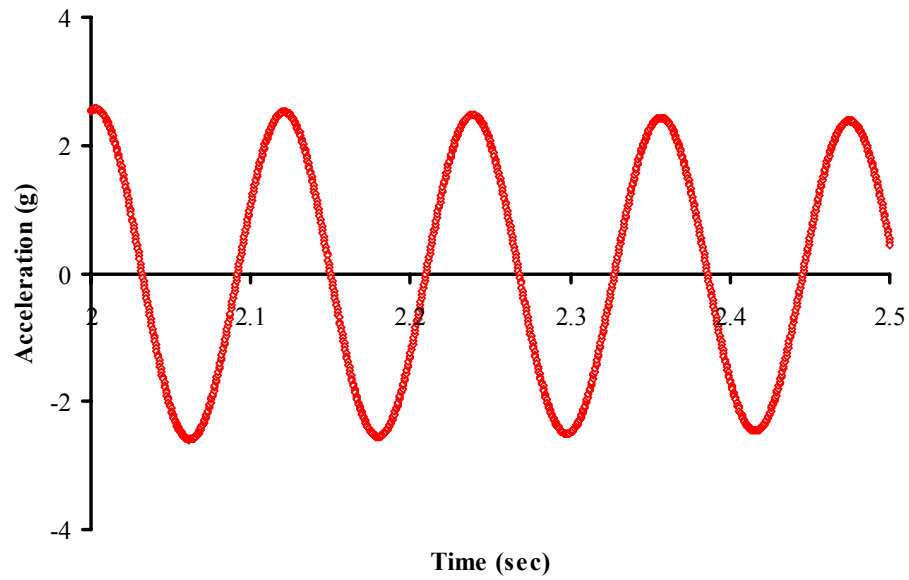


Figure A43 – Larger SDOF shear structure, free vibration response

Table A7 – Larger SDOF shear structure properties

	Free vibration	Forced vibration	Logarithmic decrement
Natural Frequency (Hz)	8.034	8.455	8.503
Damping Ratio	0.0005747	0.0007071	0.002743

Table A8 – Larger SDOF shear structure properties, used for modeling

Storey mass ($lb \cdot s^2/in$)	0.02544
Natural frequency (Hz)	8.455
Storey stiffness (lb/in)	71.8
Damping ratio	0.0007071

A 2-DOF structure consisting of identical stories, shown in Figures A44 – A45 was constructed to examine the multiple degree-of-freedom response for a larger structure. The

structure was tested in forced vibration at a suitable range of frequencies. Plots of measured transmissibility ratio at each DOF are shown in Figures A46 and A47.

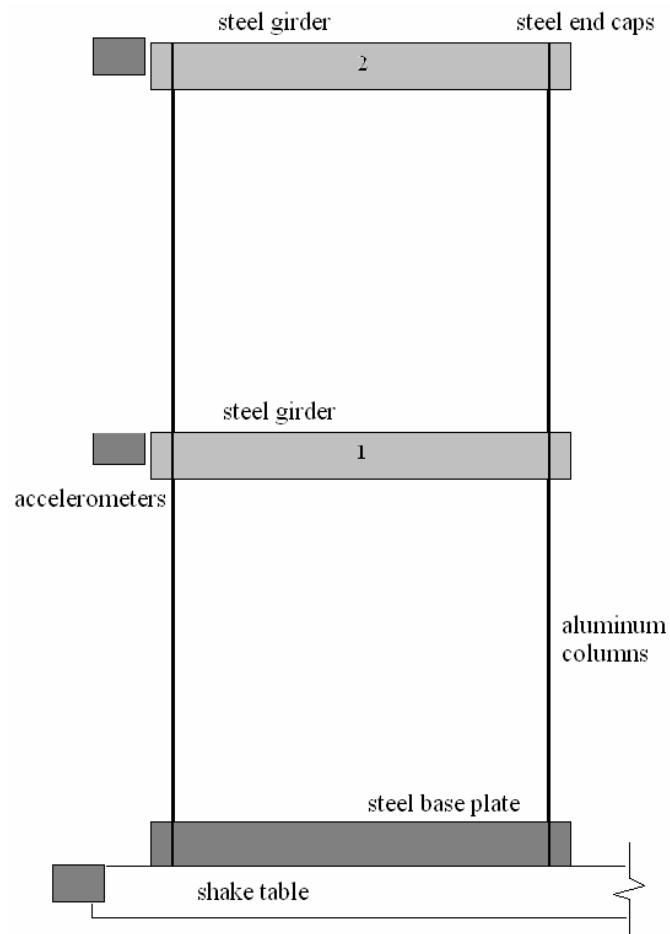


Figure A44 – Larger 2DOF shear model structure



Figure A45 – Larger 2DOF shear model structure

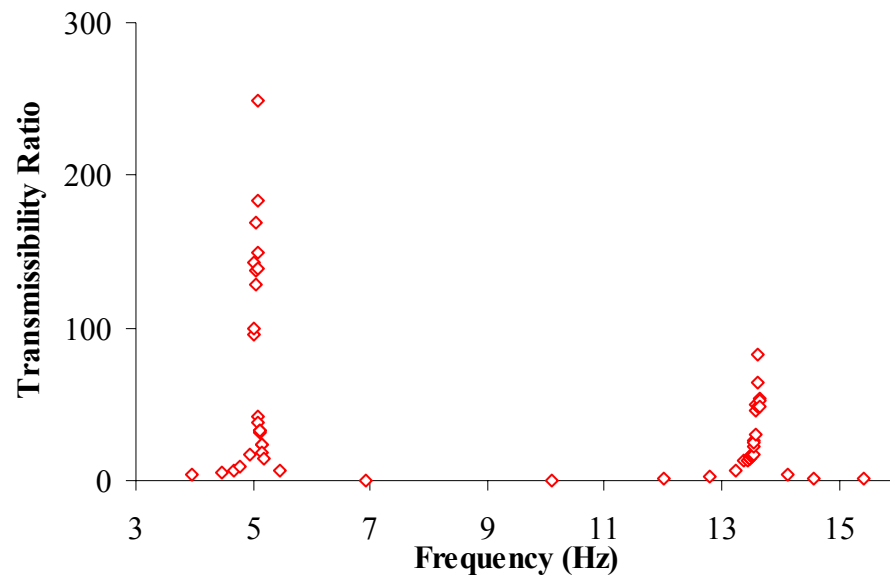


Figure A46 – Response at DOF 1, 2-DOF system

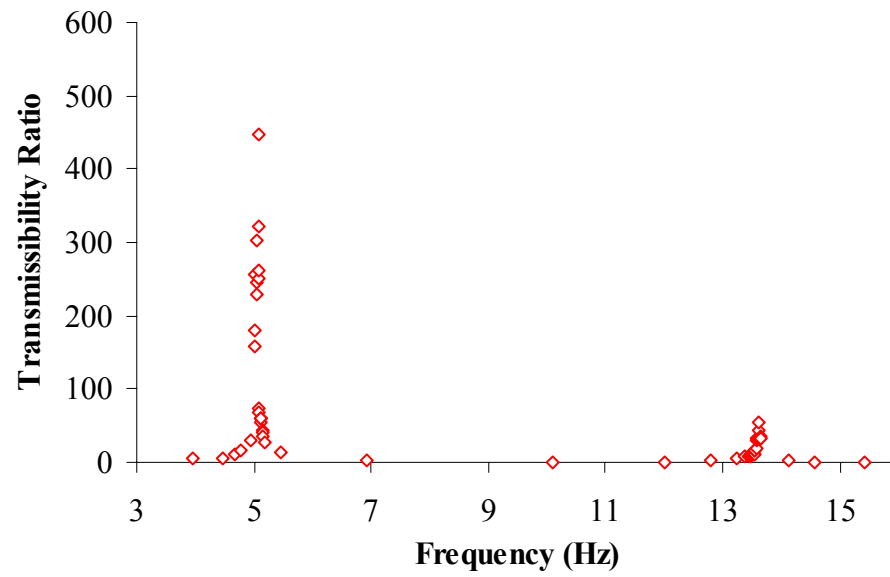


Figure A47 – Response at DOF 2, 2-DOF system

A.7 Direct Solution to the Equation of Motion

As described in Part II, the determination of transmissibility curves was performed analytically by a direct solution of the equation of motion. In this section we present the solution technique for a 2-DOF and 3-DOF structure.

A.7.1 Direct Solution for 2-DOF Structure

The equation of motion for harmonic excitation can be written alternatively as shown below.

By substituting in for the quantities $\{u\} = \{u_o\} \cdot e^{i\Omega t}$, $\{\dot{u}\} = i\Omega \cdot \{u_o\} \cdot e^{i\Omega t}$ and

$\{\ddot{u}\} = -\Omega^2 \cdot \{u_o\} \cdot e^{i\Omega t}$, the equation of motion can be transformed as follows:

$$[M]\{\ddot{u}\} + [C]\{\dot{u}\} + [K]\{u\} = -[M]\{u_b\}\ddot{u}_{g0} e^{i\Omega t} \quad (A5)$$

For a 2-DOF structure, in which $\{u_o\}^T = [u_{10} \quad u_{20}]$, the equation becomes:

$$[-m_1\Omega^2 + i\Omega c_{11} + k_{11}] \cdot u_{10} + [i\Omega c_{12} + k_{12}] \cdot u_{20} = -m_1 \ddot{u}_{g0} \quad (A6)$$

$$[i\Omega c_{21} + k_{21}] \cdot u_{10} + [-m_2\Omega^2 + i\Omega c_{22} + k_{22}] \cdot u_{20} = -m_2 \ddot{u}_{g0} \quad (A7)$$

Since acceleration records measured during experiments directly give \ddot{u}_{10} and \ddot{u}_{20} , we can write:

$$\frac{1}{\Omega^2 m_1} [-m_1\Omega^2 + i\Omega c_{11} + k_{11}] \cdot \ddot{u}_{10} + \frac{1}{\Omega^2 m_1} [i\Omega c_{12} + k_{12}] \cdot \ddot{u}_{20} = \ddot{u}_{g0} \quad (A8)$$

$$\frac{1}{\Omega^2 m_2} [i\Omega c_{21} + k_{21}] \cdot \ddot{u}_{10} + \frac{1}{\Omega^2 m_2} [-m_2\Omega^2 + i\Omega c_{22} + k_{22}] \cdot \ddot{u}_{20} = \ddot{u}_{g0} \quad (A9)$$

The expressions can be simplified using the following notation

$$\mathbf{A}_{11} \cdot \ddot{\mathbf{u}}_{10} + \mathbf{A}_{12} \cdot \ddot{\mathbf{u}}_{20} = \ddot{\mathbf{u}}_{g0} \quad (\text{A10})$$

$$\mathbf{A}_{21} \cdot \ddot{\mathbf{u}}_{10} + \mathbf{A}_{22} \cdot \ddot{\mathbf{u}}_{20} = \ddot{\mathbf{u}}_{g0} \quad (\text{A11})$$

$$[\mathbf{A}]\{\ddot{\mathbf{u}}_0\} = \{\ddot{\mathbf{u}}_{g0}\} \quad (\text{A12})$$

Solving the system of equations for $\ddot{\mathbf{u}}_{10}$ we have:

$$\ddot{\mathbf{u}}_{10} \cdot (\mathbf{A}_{22}\mathbf{A}_{11} - \mathbf{A}_{12}\mathbf{A}_{21}) = (\mathbf{A}_{22} - \mathbf{A}_{12}) \cdot \ddot{\mathbf{u}}_{g0} \quad (\text{A13})$$

Which can be simplified in the form of:

$$\ddot{\mathbf{u}}_{10} \cdot (\mathbf{A}_1 + i\mathbf{B}_1) = (\mathbf{C}_1 + i\mathbf{D}_1) \cdot \ddot{\mathbf{u}}_{g0} \quad (\text{A14})$$

In which the coefficients are expressed as:

$$\mathbf{A}_1 = \frac{1}{\Omega^4 \mathbf{m}_1 \mathbf{m}_2} \left[(-\mathbf{m}_2 \Omega^2 + \mathbf{k}_{22}) (-\mathbf{m}_1 \Omega^2 + \mathbf{k}_{11}) - \Omega^2 \cdot \mathbf{c}_{11} \cdot \mathbf{c}_{22} + \Omega^2 \cdot \mathbf{c}_{12} \cdot \mathbf{c}_{21} - \mathbf{k}_{12} \cdot \mathbf{k}_{21} \right] \quad (\text{A15})$$

$$\mathbf{B}_1 = \frac{1}{\Omega^4 \mathbf{m}_1 \mathbf{m}_2} \left[(\Omega \cdot \mathbf{c}_{22}) (-\mathbf{m}_1 \Omega^2 + \mathbf{k}_{11}) + (\Omega \cdot \mathbf{c}_{11}) (-\mathbf{m}_2 \Omega^2 + \mathbf{k}_{22}) - \Omega \cdot \mathbf{c}_{12} \cdot \mathbf{k}_{21} - \Omega \cdot \mathbf{c}_{21} \cdot \mathbf{k}_{12} \right] \quad (\text{A16})$$

$$\mathbf{C}_1 = \frac{1}{\Omega^2 \mathbf{m}_2} (-\mathbf{m}_2 \Omega^2 + \mathbf{k}_{22}) - \frac{1}{\Omega^2 \mathbf{m}_1} \mathbf{k}_{12} \quad (\text{A17})$$

$$\mathbf{D}_1 = \frac{1}{\Omega \cdot \mathbf{m}_2} \mathbf{c}_{22} - \frac{1}{\Omega^2 \mathbf{m}_1} \mathbf{c}_{12} \quad (\text{A18})$$

Therefore the transmissibility ratio at the first storey can be expressed as:

$$TR_1 = \frac{\ddot{u}_{10}}{\ddot{u}_{g0}} = \frac{\sqrt{C_1^2 + D_1^2}}{\sqrt{A_1^2 + B_1^2}} \quad (A19)$$

Similarly, solving the system of equations for \ddot{u}_{20} we have:

$$\ddot{u}_{20} \cdot (A_{21}A_{12} - A_{11}A_{22}) = (A_{21} - A_{11}) \cdot \ddot{u}_{g0} \quad (A20)$$

Which can be simplified in the form of:

$$\ddot{u}_{20} \cdot (A_2 + iB_2) = (C_2 + iD_2) \cdot \ddot{u}_{g0} \quad (A21)$$

In which the coefficients are expressed as:

$$A_2 = \frac{1}{\Omega^4 m_1 m_2} \left[-(-m_2 \Omega^2 + k_{22})(-m_1 \Omega^2 + k_{11}) + \Omega^2 \cdot c_{11} \cdot c_{22} - \Omega^2 \cdot c_{12} \cdot c_{21} + k_{12} \cdot k_{21} \right] \quad (A22)$$

$$B_2 = \frac{1}{\Omega^4 m_1 m_2} \left[-(\Omega \cdot c_{22})(-m_1 \Omega^2 + k_{11}) - (\Omega \cdot c_{11})(-m_2 \Omega^2 + k_{22}) + \Omega \cdot c_{12} \cdot k_{21} + \Omega \cdot c_{21} \cdot k_{12} \right] \quad (A23)$$

$$C_2 = -\frac{1}{\Omega^2 m_1} (-m_1 \Omega^2 + k_{11}) + \frac{1}{\Omega^2 m_2} k_{21} \quad (A24)$$

$$D_2 = \frac{1}{\Omega \cdot m_2} c_{21} - \frac{1}{\Omega^2 m_1} c_{11} \quad (A25)$$

Therefore the transmissibility ratio at the second storey can be expressed as:

$$\text{TR}_2 = \frac{\ddot{u}_{20}}{\ddot{u}_{g0}} = \frac{\sqrt{C_2^2 + D_2^2}}{\sqrt{A_2^2 + B_2^2}} \quad (\text{A26})$$

A.7.2 Direct Solution for 3DOF Structure

For a 3-DOF structure, we can show that

$$[A] = \begin{bmatrix} A_{11} & A_{12} & A_{13} \\ A_{21} & A_{22} & A_{23} \\ A_{31} & A_{32} & A_{33} \end{bmatrix} \quad (A27)$$

For $i, j = 1..n$ dofs, the coefficients of $[A]$ can be written as follows:

$$\text{For } i \neq j \quad A_{ij} = \frac{1}{\Omega^2 m_i} [k_{ij} + i\Omega c_{ij}] \quad (A28)$$

$$\text{For } i = j \quad A_{ii} = \frac{1}{\Omega^2 m_i} [-m_i \Omega^2 + k_{ii} + i\Omega c_{ii}] \quad \text{and} \quad A_{jj} = \frac{1}{\Omega^2 m_j} [-m_j \Omega^2 + k_{jj} + i\Omega c_{jj}] \quad (A29)$$

If we solve the system of equations to isolate the acceleration at each storey, we find that the equations can be written as

$$\ddot{u}_{10} \cdot (A_1 + iB_1) = (C_1 + iD_1) \cdot \ddot{u}_{g0} \quad (A30)$$

$$\ddot{u}_{20} \cdot (A_2 + iB_2) = (C_2 + iD_2) \cdot \ddot{u}_{g0} \quad (A31)$$

$$\ddot{u}_{30} \cdot (A_3 + iB_3) = (C_3 + iD_3) \cdot \ddot{u}_{g0} \quad (A32)$$

The resulting transmissibility at each storey can be written as before

$$TR_1 = \frac{\ddot{u}_{10}}{\ddot{u}_{g0}} = \frac{\sqrt{C_1^2 + D_1^2}}{\sqrt{A_1^2 + B_1^2}} \quad (A33)$$

$$TR_2 = \frac{\ddot{u}_{20}}{\ddot{u}_{g0}} = \frac{\sqrt{C_2^2 + D_2^2}}{\sqrt{A_2^2 + B_2^2}} \quad (A34)$$

$$TR_3 = \frac{\ddot{u}_{30}}{\ddot{u}_{g0}} = \frac{\sqrt{C_3^2 + D_3^2}}{\sqrt{A_3^2 + B_3^2}} \quad (A35)$$

A.7.3 MATLAB Code for 3-DOF Direct Solution

```
clc
clear

m1 = 0.006;
m2 = 0.006;
m3 = 0.006;

zeta1 = 0.001866;
zeta2 = 0.001866;
zeta3 = 0.001866;

k1 = 41.1;
k2 = 41.1;
k3 = 41.1;

c1 = 2*zeta1*m1*sqrt(k1/m1);
c2 = 2*zeta2*m2*sqrt(k2/m2);
c3 = 2*zeta3*m3*sqrt(k3/m3);

% DAMPER PROPERTIES

DB_zeta = 0.004763;
cdb = 2*sqrt(k1/m1)*DB_zeta*m1;
cd = cdb-c1;

C_d = [ 0 0 0 ; 0 cd -cd ; 0 -cd cd ]

k11 = k1+k2;
k12 = -k2;
k13 = 0;

k21 = -k2;
k22 = k2+k3;
k23 = -k3;

k31 = 0;
k32 = -k3;
k33 = k3;
```

$K = \begin{bmatrix} k_{11} & k_{12} & k_{13} \\ k_{21} & k_{22} & k_{23} \\ k_{31} & k_{32} & k_{33} \end{bmatrix}$

$c_{11} = c_1 + c_2;$

$c_{12} = -c_2;$

$c_{13} = 0;$

$c_{21} = -c_2;$

$c_{22} = c_2 + c_3;$

$c_{23} = -c_3;$

$c_{31} = 0;$

$c_{32} = -c_3;$

$c_{33} = c_3;$

$C_bare = \begin{bmatrix} c_{11} & c_{12} & c_{13} \\ c_{21} & c_{22} & c_{23} \\ c_{31} & c_{32} & c_{33} \end{bmatrix}$

$C = C_bare + C_d$

$data = \text{zeros}(2000, 4);$

for $k=1:2500;$

$freq = k/100;$

$om = 2 * \pi * freq;$

$A_{11} = 1/om^2/m_1 * (-m_1 * om^2 + i * om * c_{11} + k_{11});$

$A_{12} = 1/om^2/m_1 * (i * om * c_{12} + k_{12});$

$A_{13} = 1/om^2/m_1 * (i * om * c_{13} + k_{13});$

$A_{21} = 1/om^2/m_2 * (i * om * c_{21} + k_{21});$

$A_{22} = 1/om^2/m_2 * (-m_2 * om^2 + i * om * c_{22} + k_{22});$

$A_{23} = 1/om^2/m_2 * (i * om * c_{23} + k_{23});$

$A_{31} = 1/om^2/m_3 * (i * om * c_{31} + k_{31});$

$A_{32} = 1/om^2/m_3 * (i * om * c_{32} + k_{32});$

$A_{33} = 1/om^2/m_3 * (-m_3 * om^2 + i * om * c_{33} + k_{33});$

$LHS1 = (A_{32} * A_{23} - A_{22} * A_{33}) * (A_{22} * A_{11} - A_{12} * A_{21}) - (A_{22} * A_{13} - A_{12} * A_{23}) * (A_{32} * A_{21} - A_{22} * A_{31});$

$RHS1 = (A_{32} * A_{23} - A_{22} * A_{33}) * (A_{22} - A_{12}) - (A_{22} * A_{13} - A_{12} * A_{23}) * (A_{32} - A_{22});$

$A1 = \text{real}(LHS1);$

$B1 = (LHS1 - \text{real}(LHS1))/i;$

$C1 = \text{real}(RHS1);$

$D1 = (RHS1 - \text{real}(RHS1))/i;$

```

TR1 = sqrt(C1^2+D1^2)/sqrt(A1^2+B1^2);

LHS2 = (A31*A23-A21*A33)*(A21*A12-A11*A22)-(A21*A13-A11*A23)*(A31*A22-
A21*A32);
RHS2 = (A31*A23-A21*A33)*(A21-A11)-(A21*A13-A11*A23)*(A31-A21);

A2 = real(LHS2);
B2 = (LHS2-real(LHS2))/i;

C2 = real(RHS2);
D2 = (RHS2-real(RHS2))/i;

TR2 = sqrt(C2^2+D2^2)/sqrt(A2^2+B2^2);

LHS3 = (A32*A21-A22*A31)*(A22*A13-A12*A23)-(A22*A11-A12*A21)*(A32*A23-
A22*A33);
RHS3 = (A32*A21-A22*A31)*(A22-A12)-(A22*A11-A12*A21)*(A32-A22);

A3 = real(LHS3);
B3 = (LHS3-real(LHS3))/i;

C3 = real(RHS3);
D3 = (RHS3-real(RHS3))/i;

TR3 = sqrt(C3^2+D3^2)/sqrt(A3^2+B3^2);

data(k,1) = freq;
data(k,2) = TR1;
data(k,3) = TR2;
data(k,4) = TR3;

end

data

```